

Assessment Report
Concerning the 2004 Airborne Geophysical Survey
Of the
HOWELL PROPERTY
FORT STEELE MINING DIVISION, BRITISH COLUMBIA
NTS: 82G027

Latitude 49 degrees, 13 minutes N, Longitude 114 degrees, 38 minutes W
UTM 668000E, 5455000N
(NAD 83, Zone 11)

For

LA QUINTA RESOURCES CORP.
Suite 1400 – 400 Burrard St.
Vancouver, B.C.
V6C 3G2

And

EASTFIELD RESOURCES LTD.
Suite 110 – 325 Howe Street.
Vancouver, B.C.
V6C 1Z7

By

J.W. (Bill) Morton P.Geo.
Mincord Exploration Consultants Ltd.
Suite 110 – 325 Howe Street.
Vancouver, B.C.
V6C 1Z7

October 22, 2005

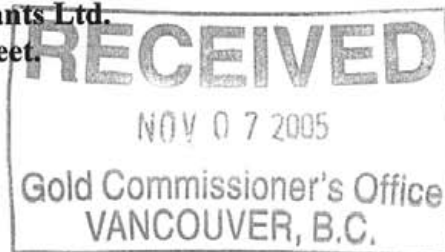


TABLE OF CONTENTS

	<i>Page</i>
SUMMARY	1
PROPERTY DESCRIPTION AND LOCATION	2
ACCESSIBILITY, CLIMATE, LOCAL RESOURCES, INFRASTRUCTURE AND PHYSIOGRAPHY	2
CLAIM MAP	3
GEOLOGICAL SETTING	4
DEPOSIT TYPES	4
INTERPRETATION AND CONCLUSIONS	4
COST STATEMENT	5
AUTHOR QUALIFICATIONS	6
FUGRO REPORT	Appendix

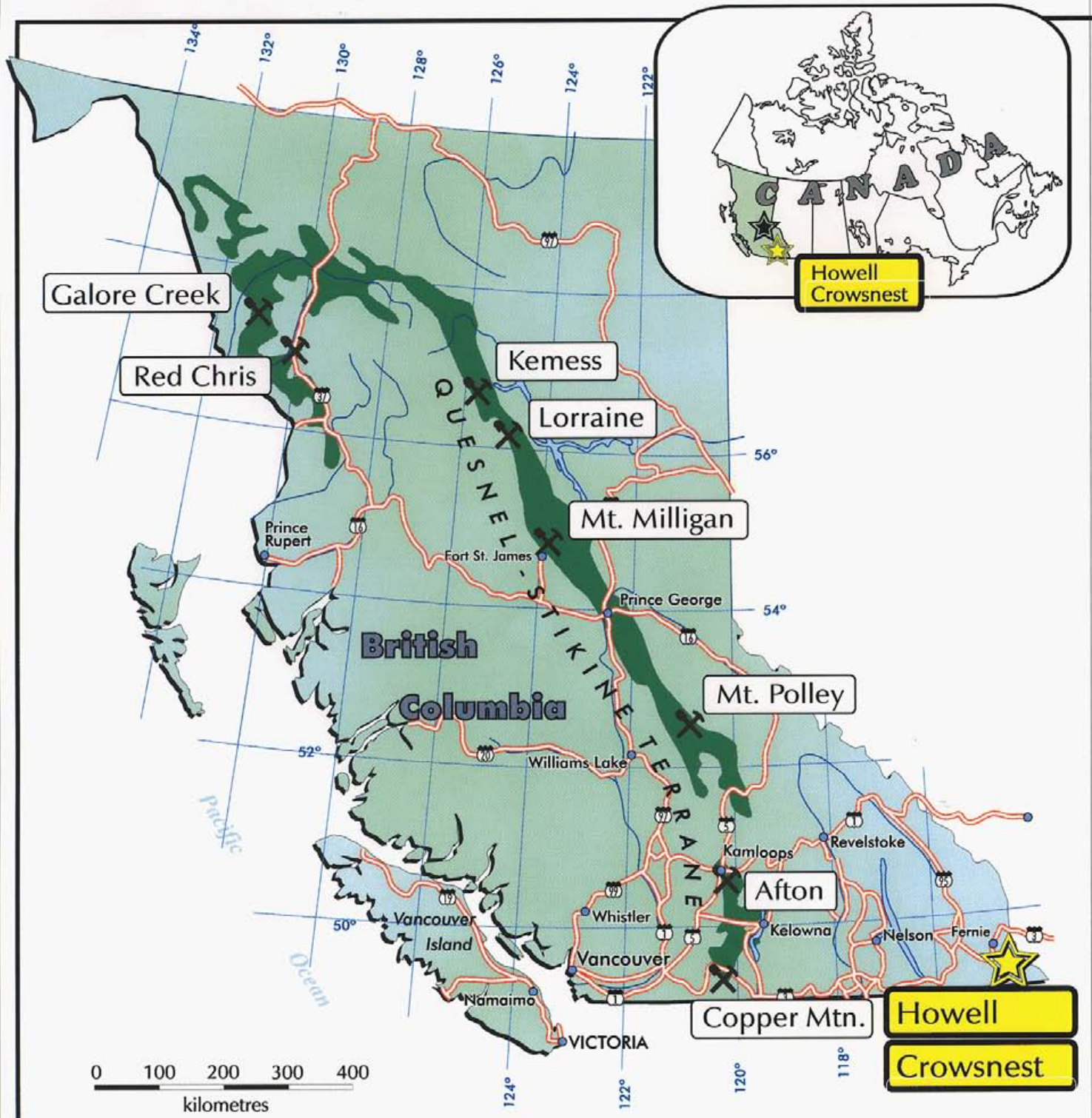
SUMMARY

Fugro Airborne Surveys Corp. completed 217 line kilometers of airborne survey on the Howell property with the flying being completed between October 26 and October 27, 2004 and the data processing and interpretation being completed in December 2004 and January 2005. The report provided by Fugro Airborne Surveys is dated January 19, 2005.

The area of the Howell claims was flown by Fugro in 2002 with a system that lacked an electromagnetic component. In 2004 it was decided to re-fly the area with a system that included an EM component to provide real resistivity data that could be used to interpret important stratigraphic contacts that control gold mineralization.

The Howell claims have an additional potential for base metal mineralization with several previously taken samples of Cambrian aged Elko limestone returning analysis greater than 0.5% copper and 10.0% zinc. It was hoped that by including an electromagnetic component in the survey that previously unrecognized massive sulphide occurrences might be located. In this regard the 2004 survey was somewhat successful in locating a number of indistinct or weak EM anomalies.

The 2004 Fugro survey employed a DIGHEM multi-coil, multi-frequency electromagnetic system mounted in an AS350B3 turbine helicopter flying at an average speed of 72 kilometres per hour and maintaining an average EM sensor height of 30 metres.



LA QUINTA RESOURCES LTD.

Howell Property

Fort Steele Mining Division, B.C., Canada

Location Map

Scale	as shown	N.T.S.	82G027	Figure	1
Date	July 2005	U.T.M. Zone	11		

Mincord Exploration Consultants

PROPERTY DESCRIPTION AND LOCATION

Claim Name	Record #	Size (hectares)	Expiry Date
Howell 1	209981	500	November 1, 07
Howell 2	209982	500	November 1, 07
Howell 3	209983	500	November 1, 07
Howell 4	210011	500	November 1, 07
Howell 5	210012	200	November 1, 07
Ysoo	366755	<u>450</u>	November 1, 07
Total Area		2,650	

All claims are located in the Fort Steele Mining Division and are registered in the name of Eastfield Resources Ltd.

ACCESSIBILITY, CLIMATE, LOCAL RESOURCES, INFRASTRUCTURE and PHYSIOGRAPHY

The Howell Claim block is located in southeastern British Columbia, approximately 50 kilometres south of the city of Fernie. The claim block encompasses 2,650 hectares and lies within the MacDonald Range of the Rocky Mountains at an elevations ranging from 1670 to 2200 metres. The lowermost vegetation consists of moderately dense growth of Lodgepole pine and balsam fir, while at slightly higher elevations economic stands of mature spruce, and lesser larch exist. Alpine vegetation exists on the very highest topography with the majority of the claim block located below tree line. Deciduous growth is limited, marked by occasional thickets of alder, aspen and birch, which typically occur along the creeks. Extensive areas of the claim block have been clear-cut logged and are in a healthy state of reforestation.

Access to the claims is south from Fernie along the highway for fifteen kilometres to the Morrissey secondary road junction. From the south side of the Elk River bridge the Lodgepole Forest Service road connects to the Howell Creek road junction thirty two kilometres distant at the 47 kilometre sign. From the Howell Creek Road junction the centre of the property is approximately six kilometres. Access is restricted from May through to October owing to persistent snowfall during the winter months.

CLAIM MAP



MINISTRY OF ENERGY AND MINES

MINISTRY OF SUSTAINABLE
RESOURCE MANAGEMENT

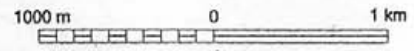
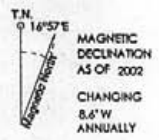
MINERAL TITLES REFERENCE MAP

M082G027

North American Datum - 1983
U.T.M. Coordinate System - Zone 11
Compilation Date: 2002 NOV 22

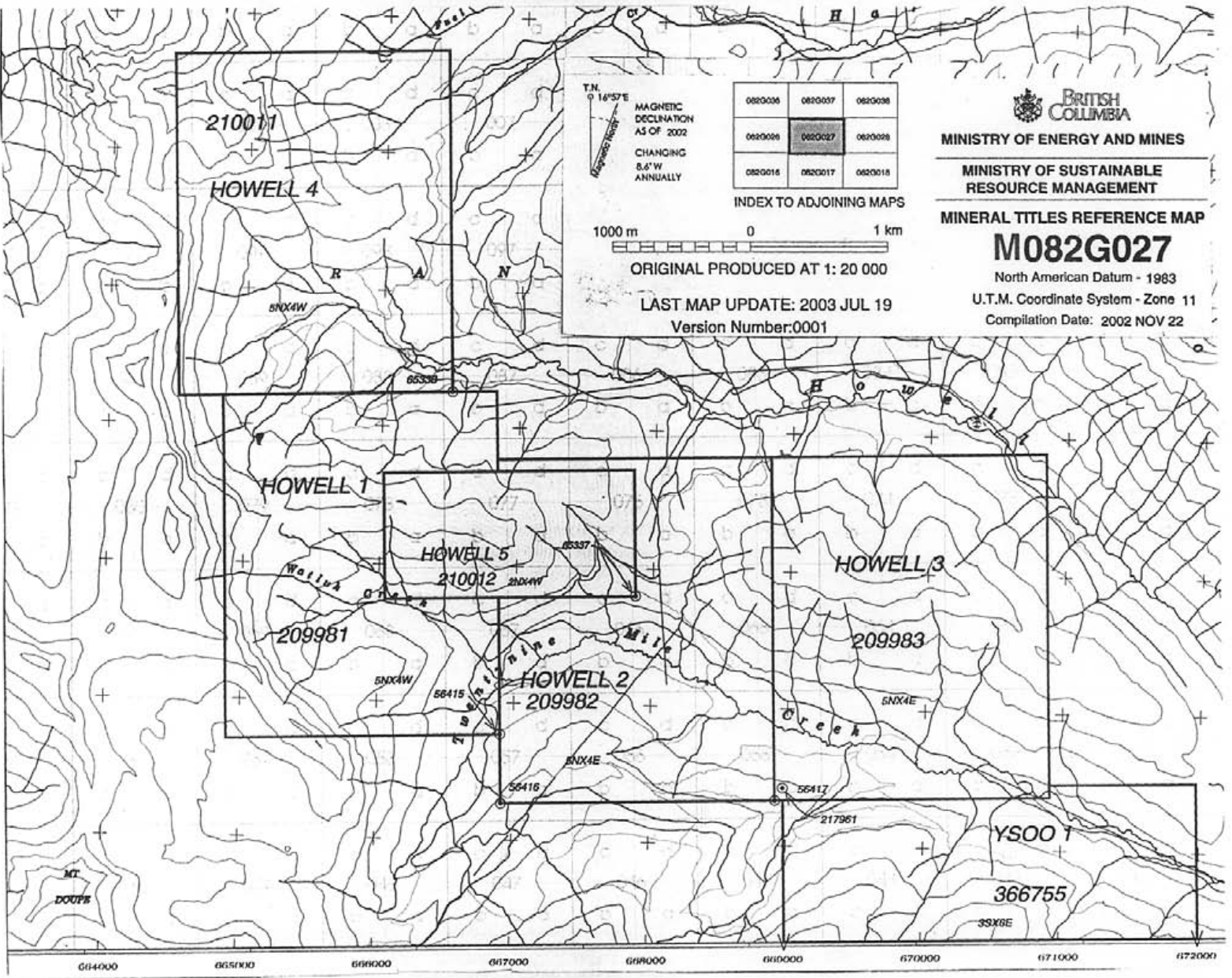
0820036	0820037	0820038
0820026	0820027	0820028
0820016	0820017	0820018

INDEX TO ADJOINING MAPS



ORIGINAL PRODUCED AT 1: 20 000

LAST MAP UPDATE: 2003 JUL 19
Version Number:0001



664000 665000 666000 667000 668000 669000 670000 671000 672000

GEOLOGICAL SETTING

The MacDonald Range lies within the Rocky Mountain Foreland and Thrust Belt. In this region, this tectono-stratigraphic assemblage consists of Proterozoic to Cretaceous clastics and carbonates and upper Cretaceous syenite intrusive phases.

The Howell claims are underlain by the Proterozoic Kintla, Cambrian Flathead, Elko, and Devonian Fairholme formations. These lie in juxtaposition with the upper Cretaceous Alberta Group via the regional scale Twenty-Nine Mile creek fault. Immediately north of the fault, two “assumed” klippe lie within the Alberta Group. These thrust blocks, known as the Eastern and Western Outliers, individually consist of the Kintla formation, and the Kintla through to the Fairholme assemblage, respectively. The Alberta Group is bound to the north by the Harvey Creek normal fault and on the west by the Northern Thrust fault. This fault block encompasses an area of at least ten square kilometres. Beyond these faults the Mississippian Rundle Group of carbonates form the base of the regional geological setting. These are overlain by a transitional sequence of carbonaceous shales, siltstones, sandstones and Triassic age coal measures.

DEPOSIT TYPES

Intrusive related gold linked to Cretaceous syenite and diatreme breccias is an obvious correlation and was one of the predominant reasons for completing the recent airborne survey. In addition to the link to intrusive activity limestone hosted gold such as is typified by drill hole HRC-25 with an intercept of 1.23 g/t gold over 58 metres complicates modeling. Previous authors have noted that the association of Paleozoic carbonate and shale stratigraphy affected by major thrusting is essentially the model for the gold deposits of Carlin Nevada. This remains a potential model for gold mineralization on Howell. A final style of sediment hosted base metal mineralization also exists. Samples of Cambrian aged Elko limestone have returned analysis greater than 0.5% copper and 10.0% zinc.

INTERPRETATION and CONCLUSIONS

Previous efforts to construct a working geological map and model for the Howell property have been only partially successful. One of the significant opportunities that now exists is to modify the historical perspective using new information provided by the 2004 magnetic and electromagnetic airborne survey.

A preliminary review of these surveys suggests that some previously rigorously inferred bounding structures are tenuous and mineralization may extend for some distance into areas that were previously interpreted to be sterile. Some observations of this survey are as follows:

"A" Grid: The disseminated and carbonate hosted gold mineralization such as is typified by RCH-25 is probably linked to small dykes and diatremes of alkalic intrusive hosted in limestone sediments. Minor to moderate levels of silicification and pyritization accompany gold mineralization. Hole RCH-25 occurs in an area of the 2004 airborne survey where a moderate increase in the total magnetic field response is accompanied by a higher resistivity response. This feature can be followed eastward more or less to the claim boundary approximately 1000 metres distant and for a like distance to the west. A similar, and in fact better defined, cohesive magnetic high with a corresponding resistivity high occurs on the south side of Howell ridge trending southerly to the access road. It likewise constitutes a high priority drill target.

"E" Grid Mineralization identified in the "E" Grid such as is typified by HE-2 is associated with a syenite dyke swarm in clastic sediments. A moderate to strong quartz stockwork accompanies gold mineralization here that is also accompanied with some lead zinc mineralization. The 2004 survey indicates that a large cohesive total field magnetic response extends at least 2500 meters to the south from HE-2. This area warrants further drill testing.

"Ysso" Area The 2004 survey indicates that a very strong total field magnetic anomaly occurs in this area near the creek crossing immediately south of the old "Fox" (Cominco) camp. Given that gold mineralization on the Howell property is probably linked to alkalic intrusive activity drilling should target this feature, which occurs in the very bottom of the valley and is blind.

COST STATEMENT

Fugro Airborne Surveys charges	\$68,000
Reporting	<u>\$1,000</u>
Total	\$69,000

* \$20,000 of this amount, estimated to be the costs accrued in December 2004 and January 2005, are applied to the current filing.

AUTHOR QUALIFICATIONS

I, J.W. Morton am a graduate of Carleton University Ottawa with a B.Sc. (1972) in Geology and a graduate of the University of British Columbia with a M. Sc. (1976) in Graduate Studies.

I, J.W Morton have been a member of the Association of Professional Engineers and Geoscientists of the Province of BC (P.Geol.) since 1991.

I, J.W. Morton have practiced my profession since graduation throughout Western Canada, the Western USA and Mexico.

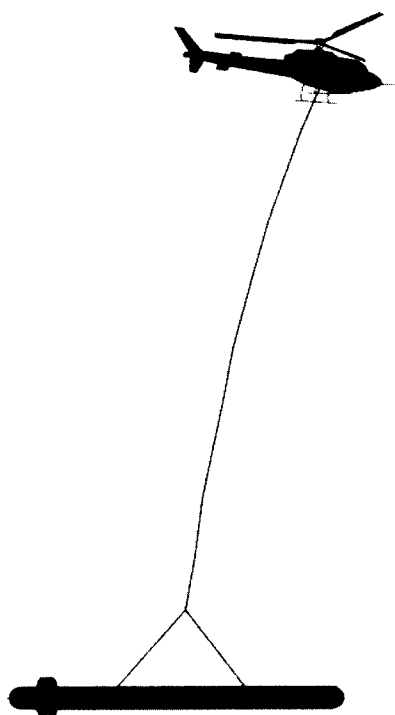
I, J.W Morton supervised the work outlined in this report.

Signed this 22 day of September, 2005

J.W Morton P.Geol

**DIGHEM^{V-DSP} SURVEY
FOR
LA QUINTA RESOURCE CORP.
HOWELL PROPERTY
BRITISH COLUMBIA**

NTS: 82G/2



Fugro Airborne Surveys Corp.
Mississauga, Ontario

Douglas G. Garrie
Geophysicist

January 19, 2005

SUMMARY

This report describes the logistics, data acquisition, processing and presentation of results of a DIGHEM^{V-DSP} airborne geophysical survey carried out for La Quinta Resource Corp., over a property located near Fernie, British Columbia. Total coverage of the survey block amounted to 217 km. The survey was flown from October 26 to October 27, 2004.

The purpose of the survey was to detect zones of conductive mineralization and to provide information that could be used to map the geology and structure of the survey area. This was accomplished by using a DIGHEM^{V-DSP} multi-coil, multi-frequency electromagnetic system, supplemented by a high sensitivity cesium magnetometer. The information from these sensors was processed to produce maps that display the magnetic and conductive properties of the survey area. A GPS electronic navigation system ensured accurate positioning of the geophysical data with respect to the base maps.

The survey data were processed and compiled in the Fugro Airborne Surveys Toronto office. Map products and digital data were provided in accordance with the scales and formats specified in the Survey Agreement.

The survey property contains several anomalous features, many of which are considered to be of moderate to high priority as exploration targets. Most of these anomalous features appear to warrant further investigation using appropriate surface exploration techniques. Areas of interest may be assigned priorities on the basis of supporting geophysical, geochemical and/or geological information. After initial investigations have been carried

out, it may be necessary to re-evaluate the remaining anomalies based on information acquired from the follow-up program.

CONTENTS

1.	INTRODUCTION.....	1.1
2.	SURVEY OPERATIONS	2.1
3.	SURVEY EQUIPMENT	3.1
	Electromagnetic System.....	3.1
	In-Flight EM System Calibration	3.2
	Airborne Magnetometer.....	3.4
	Magnetic Base Station	3.4
	Navigation (Global Positioning System).....	3.6
	Radar Altimeter	3.8
	Barometric Pressure and Temperature Sensors.....	3.8
	Analog Recorder	3.9
	Digital Data Acquisition System	3.9
	Video Flight Path Recording System.....	3.11
4.	QUALITY CONTROL AND IN-FIELD PROCESSING	4.1
5.	DATA PROCESSING	5.1
	Flight Path Recovery	5.1
	Electromagnetic Data	5.1
	Apparent Resistivity.....	5.2
	Total Magnetic Field	5.4
	Calculated Vertical Magnetic Gradient.....	5.5
	Contour, Colour and Shadow Map Displays	5.6
	Multi-channel Stacked Profiles	5.7
6.	PRODUCTS	6.1
	Base Maps	6.1
	Final Products	6.2
7.	SURVEY RESULTS	7.1
	General Discussion	7.1
	Magnetics	7.3
	Apparent Resistivity.....	7.5
	Electromagnetic Anomalies.....	7.5
	Howell Property Survey.....	7.7

8.	CONCLUSIONS AND RECOMMENDATIONS	8.1
----	---------------------------------------	-----

APPENDICES

- A. List of Personnel
- B. Optional Products
- C. Background Information
- D. Data Archive Description
- E. EM Anomaly List
- F. Data Processing Flowcharts
- G. Glossary

1. INTRODUCTION

A DIGHEM^{V-DSP} electromagnetic/resistivity/magnetic survey was flown for La Quinta Resource Corp., from October 26 to October 27, 2004, over a survey block located near Fernie, British Columbia. The survey area can be located on NTS map sheet 82G/2 (Figure 2).

Survey coverage consisted of approximately 217 line-km, including 9 line-km of tie lines. Flight lines were flown in an azimuthal direction of 105°/285° with a line separation of 150 metres. Two tie lines were flown orthogonal to the traverse lines with a line separation of 4800 metres.

The survey employed the DIGHEM^{V-DSP} electromagnetic system. Ancillary equipment consisted of a magnetometer, radar and barometric altimeter, video camera, analog and digital recorders, and an electronic navigation system. The instrumentation was installed in an AS350B2 turbine helicopter (Registration C-GBHP) that was provided by Big Horn Helicopters Ltd. The helicopter flew at an average airspeed of 72 km/h with an EM sensor height of approximately 30 metres.

In some portions of the survey area, the steep topography forced the pilot to exceed normal terrain clearance for reasons of safety. It is possible that some weak conductors may have escaped detection in areas where the bird height exceeded 120 m. In difficult areas where near-vertical climbs were necessary, the forward speed of the helicopter was reduced to a

level that permitted excessive bird swinging. This problem, combined with the severe stresses to which the bird was subjected, gave rise to aerodynamic noise levels that are slightly higher than normal on some lines. Where warranted, reflights were carried out to minimize these adverse effects.



Figure 1: Fugro Airborne Surveys RESOLVE EM bird with AS350-B3

2. SURVEY OPERATIONS

The base of operations for the survey was established at Fernie, British Columbia. The survey area can be located on NTS map sheet 82G/2 (Figure 2).

Table 2-1 lists the corner coordinates of the survey area in NAD83, UTM Zone 11, central meridian 117°W.

Table 2-1

Nad83 Utm Zone 11			
Block	Corners	X-UTM (E)	Y-UTM (N)
04086-1	1	666042	5457569
	2	671785	5455832
	3	671553	5455066
	4	673468	5454487
	5	672744	5452094
	6	671428	5452492
	7	671196	5451727
	8	665931	5453319
	9	666163	5454085
	10	665086	5454410

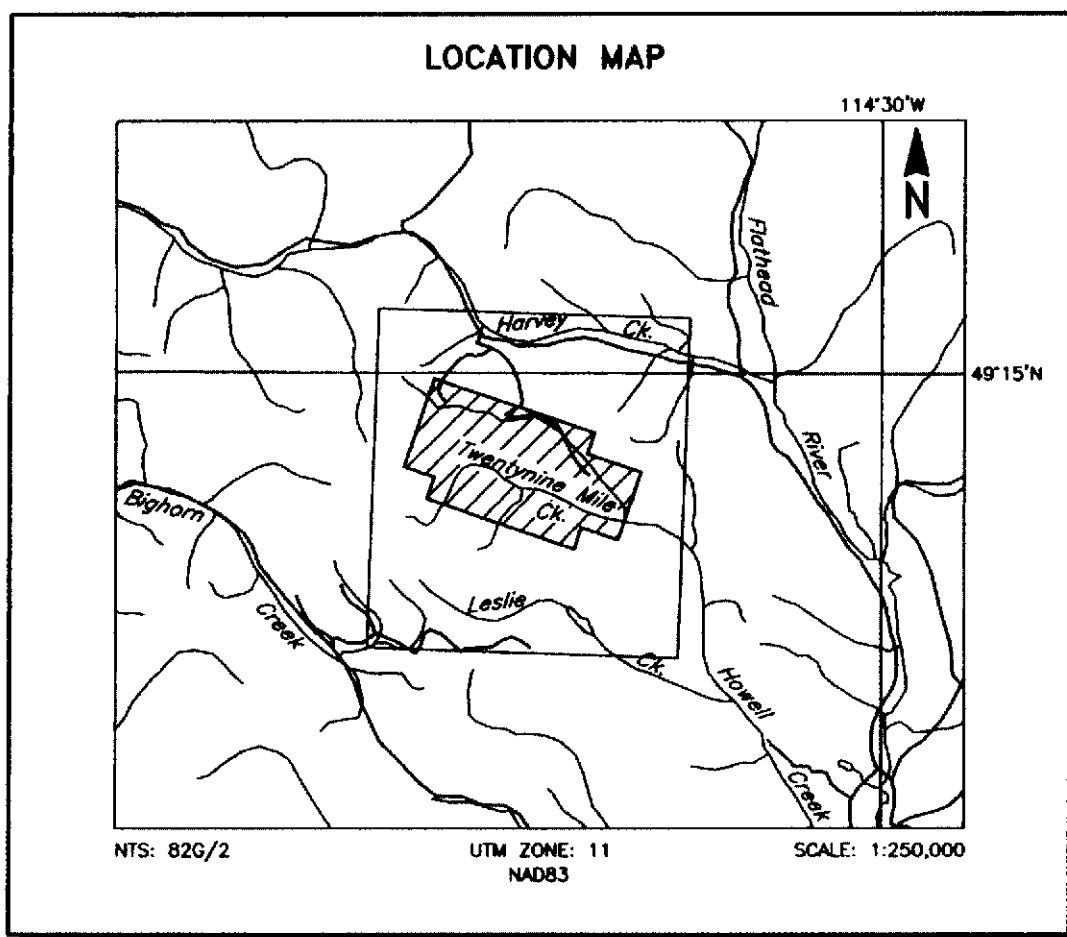


Figure 2
Location Map and Sheet Layout
Howell Property Survey Area
Job # 04086

The survey specifications were as follows:

Parameter	Specifications
Traverse line direction	105°/285°
Traverse line spacing	150 m
Tie line direction	15°/195°
Tie line spacing	4800 m
Sample interval	10 Hz, 3.3 m @ 120 km/h
Aircraft mean terrain clearance	58 m
EM sensor mean terrain clearance	30 m
Mag sensor mean terrain clearance	30 m
Average speed	120 km/h
Navigation (guidance)	±5 m, Real-time GPS
Post-survey flight path	±2 m, Differential GPS

3. SURVEY EQUIPMENT

This section provides a brief description of the geophysical instruments used to acquire the survey data and the calibration procedures employed. The geophysical equipment was installed in an AS350B2 helicopter. This aircraft provides a safe and efficient platform for surveys of this type.

Electromagnetic System

Model: DIGHEM^{V-DSP}

Type: Towed bird, symmetric dipole configuration operated at a nominal survey altitude of 30 metres. Coil separation is 8 metres for 900 Hz, 1000 Hz, 5500 Hz and 7200 Hz, and 6.3 metres for the 56,000 Hz coil-pair.

Coil orientations, frequencies and dipole moments	<u>Atm²</u>	<u>orientation</u>	<u>nominal</u>	<u>actual</u>
	211	coaxial /	1000 Hz	1113 Hz
	211	coplanar /	900 Hz	871 Hz
	67	coaxial /	5500 Hz	5655 Hz
	56	coplanar /	7200 Hz	7225 Hz
	15	coplanar /	56,000 Hz	56000 Hz

Channels recorded: 5 in-phase channels
5 quadrature channels
2 monitor channels

Sensitivity: 0.06 ppm at 1000 Hz Cx
0.12 ppm at 900 Hz Cp
0.12 ppm at 5,500 Hz Cx
0.24 ppm at 7,200 Hz Cp
0.60 ppm at 56,000 Hz Cp

Sample rate: 10 per second, equivalent to 1 sample every 3.3 m, at a survey speed of 120 km/h.

The electromagnetic system utilizes a multi-coil coaxial/coplanar technique to energize conductors in different directions. The coaxial coils are vertical with their axes in the flight direction. The coplanar coils are horizontal. The secondary fields are sensed simultaneously by means of receiver coils that are maximum coupled to their respective transmitter coils. The system yields an in-phase and a quadrature channel from each transmitter-receiver coil-pair.

In-Flight EM System Calibration

Calibration of the system during the survey uses the Fugro AutoCal automatic, internal calibration process. At the beginning and end of each flight, and at intervals during the flight, the system is flown up to high altitude to remove it from any “ground effect” (response from the earth). Any remaining signal from the receiver coils (base level) is measured as the zero level, and is removed from the data collected until the time of the next calibration. Following the zero level setting, internal calibration coils, for which the response phase and amplitude have been determined at the factory, are automatically triggered – one for each frequency. The on-time of the coils is sufficient to determine an accurate response through any ambient noise. The receiver response to each calibration coil “event” is compared to the expected response (from the factory calibration) for both phase angle and amplitude, and any phase and gain corrections are automatically applied to bring the data to the correct value.

In addition, the outputs of the transmitter coils are continuously monitored during the survey, and the gains are adjusted to correct for any change in transmitter output.

Because the internal calibration coils are calibrated at the factory (on a resistive halfspace) ground calibrations using external calibration coils on-site are not necessary for system calibration. A check calibration may be carried out on-site to ensure all systems are working correctly. All system calibrations will be carried out in the air, at sufficient altitude that there will be no measurable response from the ground.

The internal calibration coils are rigidly positioned and mounted in the system relative to the transmitter and receiver coils. In addition, when the internal calibration coils are calibrated at the factory, a rigid jig is employed to ensure accurate response from the external coils.

Using real time Fast Fourier Transforms and the calibration procedures outlined above, the data are processed in real time, from measured total field at a high sampling rate, to in-phase and quadrature values at 10 samples per second.

Airborne Magnetometer

Model:	Fugro AM102 processor with Scintrex CS2 sensor
Type:	Optically pumped cesium vapour
Sensitivity:	0.01 nT
Sample rate:	10 per second

The magnetometer sensor is housed in the EM bird, 28 m below the helicopter.

Magnetic Base Station

Primary

Model:	Fugro CF1 base station with timing provided by integrated GPS		
Sensor type:	Geometrics G822		
Counter specifications:	Accuracy:	± 0.1 nT	
	Resolution:	0.01 nT	
	Sample rate	1 Hz	
GPS specifications:	Model:	Marconi Allstar	
	Type:	Code and carrier tracking of L1 band, 12-channel, C/A code at 1575.42 MHz	
	Sensitivity:	-90 dBm, 1.0 second update	
	Accuracy:	Manufacturer's stated accuracy for differential corrected GPS is 2 metres	

Environmental

Monitor specifications:	Temperature:	
	• Accuracy:	$\pm 1.5^{\circ}\text{C}$ max
	• Resolution:	0.0305°C
	• Sample rate:	1 Hz
	• Range:	-40°C to $+75^{\circ}\text{C}$

Barometric pressure:

- Model: Motorola MPXA4115A
- Accuracy: $\pm 3.0^{\circ}$ kPa max (-20°C to 105°C temp. ranges)
- Resolution: 0.013 kPa
- Sample rate: 1 Hz
- Range: 55 kPa to 108 kPa

Backup

Model: GEM Systems GSM-19T
Type: Digital recording proton precession
Sensitivity: 0.10 nT
Sample rate: 3 second intervals

A digital recorder is operated in conjunction with the base station magnetometer to record the diurnal variations of the earth's magnetic field. The clock of the base station is synchronized with that of the airborne system, using GPS time, to permit subsequent removal of diurnal drift. The Fugro CF1 was the primary magnetic base station. It was located at latitude 49.3783989° N, longitude 114.9971924° W.

Navigation (Global Positioning System)

Airborne Receiver for Real-time Navigation & Guidance

Model:	Ashtech Glonass GG24 with PNAV 2100 interface
Type:	SPS (L1 band), 24-channel, C/A code at 1575.42 MHz, S code at 0.5625 MHz, Real-time differential.
Sensitivity:	-132 dBm, 0.5 second update
Accuracy:	Manufacturer's stated accuracy is better than 5 metres real-time
Antenna:	Mounted on tail of aircraft

Airborne Receiver for Flight Path Recovery

Model:	Ashtech Z-Surveyor
Type:	Code and carrier tracking of L1 band, 24-channel, dual frequency C/A code at 1575.2 MHz, and L2 P-code 1227 MHz.
Sample rate:	0.5 second update.
Accuracy:	Manufacturer's stated accuracy for differential corrected GPS is better than 1 metre.
Antenna:	Mounted on nose of EM bird.

Primary Base Station for Post-Survey Differential Correction

Model:	Novatel Millennium.
Type:	Code and carrier tracking of L1-C/A code at 1575.42 MHz and L2-P code at 1227.0 MHz. Dual frequency, 24-channel.
Sample rate:	10 Hz update.
Accuracy:	Better than 1 metre in differential mode.

Secondary GPS Base Station

Model:	Marconi Allstar OEM, CMT-1200
Type:	Code and carrier tracking of L1 band, 12-channel, C/A code at 1575.42 MHz
Sensitivity:	-90 dBm, 1.0 second update
Accuracy:	Manufacturer's stated accuracy for differential corrected GPS is 2 metres.

The Ashtech GG24 is a line of sight, satellite navigation system that utilizes time-coded signals from at least four of forty-eight available satellites. Both Russian GLONASS and American NAVSTAR satellite constellations are used to calculate the position and to provide real time guidance to the helicopter. For flight path processing an Ashtech Z-surveyor was used as the mobile receiver. A similar system was used as the primary base station receiver. The mobile and base station raw XYZ data were recorded, thereby permitting post-survey differential corrections for theoretical accuracies of better than 2 metres. A Marconi Allstar GPS unit, part of the CF-1, was used as a secondary (back-up) base station.

Each base station receiver is able to calculate its own latitude and longitude. For this survey, the primary GPS station was located at latitude 49° 23' 45.05825" N, longitude 115° 01' 01.73804" W at an elevation of 970.0312 metres above the ellipsoid. The secondary GPS unit was located at latitude 49.3783989° N, longitude 114.9971924° W. The GPS records data relative to the WGS84 ellipsoid, which is the basis of the revised North American Datum (NAD83).

Radar Altimeter

Manufacturer: Sperry
Model: RT330
Type: Short pulse modulation, 4.3 GHz
Sensitivity: 0.3 m
Sample rate: 2 per second

The radar altimeter measures the vertical distance between the helicopter and the ground. This information is used in the processing algorithm that determines conductor depth.

Barometric Pressure and Temperature Sensors

Model: DIGHEM D 1300
Type: Motorola MPX4115AP analog pressure sensor
AD592AN high-impedance remote temperature sensors
Sensitivity: Pressure: 150 mV/kPa
Temperature: 100 mV/°C or 10 mV/°C (selectable)
Sample rate: 10 per second

The D1300 circuit is used in conjunction with one barometric sensor and up to three temperature sensors. Two sensors (baro and temp) are installed in the EM console in the aircraft, to monitor pressure (1KPA) and internal operating temperatures (2TDC).

Analog Recorder

Manufacturer:	RMS Instruments
Type:	DGR33 dot-matrix graphics recorder
Resolution:	4x4 dots/mm
Speed:	1.5 mm/sec

The analog profiles are recorded on chart paper in the aircraft during the survey. Table 3-1 lists the geophysical data channels and the vertical scale of each profile.

Digital Data Acquisition System

Manufacturer:	RMS Instruments
Model:	DGR 33
Recorder:	San Disk compact flash card (PCMCIA)

The stored data are downloaded to the field workstation PC at the survey base, for verification, backup and preparation of in-field products.

Table 3-1. The Analog Profiles

Channel Name	Parameter	Scale units/mm
1X9I	coaxial in-phase (1000 Hz)	2.5 ppm
1X9Q	coaxial quad (1000 Hz)	2.5 ppm
3P9I	coplanar in-phase (900 Hz)	2.5 ppm
3P9Q	coplanar quad (900 Hz)	2.5 ppm
2P7I	coplanar in-phase (7200 Hz)	5 ppm
2P7Q	coplanar quad (7200 Hz)	5 ppm
4X7I	coaxial in-phase (5500 Hz)	5 ppm
4X7Q	coaxial quad (5500 Hz)	5 ppm
5P5I	coplanar in-phase (56000 Hz)	10 ppm
5P5Q	coplanar quad (56000 Hz)	10 ppm
ALTR	altimeter (radar)	3 m
MAGC	magnetics, coarse	20 nT
MAGF	magnetics, fine	2.0 nT
CXSP	coaxial spherics monitor	
CPSP	coplanar spherics monitor	
CXPL	coaxial powerline monitor	
CPPL	coplanar powerline monitor	
1KPA	altimeter (barometric)	30 m
2TDC	internal (console) temperature	1° C
3TDC	external temperature	1° C

Video Flight Path Recording System

Type: Panasonic WVCL322 Colour Video Camera
Recorder: Sanyo VWP-800
Format: NTSC (VHS)

Fiducial numbers are recorded continuously and are displayed on the margin of each image. This procedure ensures accurate correlation of data with respect to visible features on the ground.

4. QUALITY CONTROL AND IN-FIELD PROCESSING

Digital data for each flight were transferred to the field workstation, in order to verify data quality and completeness. A database was created and updated using Geosoft Oasis Montaj and proprietary Fugro Atlas software. This allowed the field personnel to calculate, display and verify both the positional (flight path) and geophysical data on a screen or printer. Records were examined as a preliminary assessment of the data acquired for each flight.

In-field processing of Fugro survey data consists of differential corrections to the airborne GPS data, verification of EM calibrations, drift correction of the raw airborne EM data, spike rejection and filtering of all geophysical and ancillary data, verification of flight videos, calculation of preliminary resistivity data, diurnal correction, and preliminary leveling of magnetic data.

All data, including base station records, were checked on a daily basis, to ensure compliance with the survey contract specifications. Reflights were required if any of the following specifications were not met.

Navigation - Positional (x,y) accuracy of better than 10 m, with a CEP (circular error of probability) of 95%.

- Flight Path - No lines to exceed $\pm 25\%$ departure from nominal line spacing over a continuous distance of more than 1 km, except for reasons of safety.

- Clearance - Mean terrain sensor clearance of 30 m, ± 10 m, except where precluded by safety considerations, e.g., restricted or populated areas, severe topography, obstructions, tree canopy, aerodynamic limitations, etc.

- Airborne Mag - The non-normalized 4th difference will not exceed 1.6 nT over a continuous distance of 1 kilometre excluding areas where this specification is exceeded due to natural anomalies.

- Base Mag - Non-linear variations not to exceed 10 nT per minute.

- EM - Spheric pulses may occur having strong peaks but narrow widths. The EM data area considered acceptable when their occurrence is less than 10 spheric events exceeding the stated noise specification for a given frequency per 100 samples continuously over a distance of 2,000 metres.

Frequency	Coil Orientation	Peak to Peak Noise Envelope (ppm)
1000 Hz	vertical coplanar	5.0
900 Hz	horizontal coplanar	10.0
5500 Hz	vertical coaxial	10.0
7200 Hz	horizontal coplanar	20.0
56,000 Hz	horizontal coplanar	40.0

5. DATA PROCESSING

Flight Path Recovery

The raw range data from at least four satellites are simultaneously recorded by both the base and mobile GPS units. The geographic positions of both units, relative to the model ellipsoid, are calculated from this information. Differential corrections, which are obtained from the base station, are applied to the mobile unit data to provide a post-flight track of the aircraft, accurate to within 2 m. Speed checks of the flight path are also carried out to determine if there are any spikes or gaps in the data.

The corrected WGS84 latitude/longitude coordinates are transformed to the coordinate system used on the final maps. Images or plots are then created to provide a visual check of the flight path.

Electromagnetic Data

EM data are processed at the recorded sample rate of 10 samples/second. Spheric rejection median and Hanning filters are then applied to reduce noise to acceptable levels.

EM test profiles are then created to allow the interpreter to select the most appropriate EM anomaly picking controls for a given survey area. The EM picking parameters depend on several factors but are primarily based on the dynamic range of the resistivities within the

The accuracy of the elevation calculation is directly dependent on the accuracy of the two input parameters, ALTBIRD and GPS-Z. The GPS-Z value is primarily dependent on the number of available satellites. Although post-processing of GPS data will yield X and Y accuracies in the order of 1-2 metres, the accuracy of the Z value is usually much less, sometimes in the ± 10 metre range. Further inaccuracies may be introduced during the interpolation and gridding process.

Because of the inherent inaccuracies of this method, no guarantee is made or implied that the information displayed is a true representation of the height above sea level. Although this product may be of some use as a general reference, THIS PRODUCT MUST NOT BE USED FOR NAVIGATION PURPOSES.

Contour, Colour and Shadow Map Displays

The geophysical data are interpolated onto a regular grid using a modified Akima spline technique. The resulting grid is suitable for image processing and generation of contour maps. The grid cell size was 30 metres or 20% of the line interval.

Colour maps are produced by interpolating the grid down to the pixel size. The parameter is then incremented with respect to specific amplitude ranges to provide colour "contour" maps.

Monochromatic shadow maps or images are generated by employing an artificial sun to cast shadows on a surface defined by the geophysical grid. There are many variations in

the shadowing technique. These techniques can be applied to total field or enhanced magnetic data, magnetic derivatives, resistivity, etc. The shadowing technique is also used as a quality control method to detect subtle changes between lines.

Multi-channel Stacked Profiles

Distance-based profiles of the digitally recorded geophysical data are generated and plotted at an appropriate scale. These profiles also contain the calculated parameters that are used in the interpretation process. These are produced as worksheets prior to interpretation, and are also presented in the final corrected form after interpretation. The profiles display electromagnetic anomalies with their respective interpretive symbols. Table 5-1 shows the parameters and scales for the multi-channel stacked profiles.

In Table 5-1, the log resistivity scale of 0.06 decade/mm means that the resistivity changes by an order of magnitude in 16.6 mm. The resistivities at 0, 33 and 67 mm up from the bottom of the digital profile are respectively 1, 100 and 10,000 ohm-m.

Table 5-1. Multi-channel Stacked Profiles

Channel Name (Freq)	Observed Parameters	Scale Units/mm
MAGFINAL	total magnetic field (fine)	5 nT
ALTBIRD	EM sensor height above ground	6 m
CXI1000	vertical coaxial coil-pair in-phase (1000 Hz)	2 ppm
CXQ1000	vertical coaxial coil-pair quadrature (1000 Hz)	2 ppm
CPI900	horizontal coplanar coil-pair in-phase (900 Hz)	4 ppm
CPQ900	horizontal coplanar coil-pair quadrature (900 Hz)	4 ppm
CXI5500	vertical coaxial coil-pair in-phase (5500 Hz)	5 ppm
CXQ5500	vertical coaxial coil-pair quadrature (5500 Hz)	5 ppm
CPI7200	horizontal coplanar coil-pair in-phase (7200 Hz)	10 ppm
CPQ7200	horizontal coplanar coil-pair quadrature (7200 Hz)	10 ppm
CPI56K	horizontal coplanar coil-pair in-phase (56,000 Hz)	10 ppm
CPQ56K	horizontal coplanar coil-pair quadrature (56,000 Hz)	10 ppm
	Computed Parameters	
DIFI (mid freq.)	difference function in-phase from CXI and CPI	4 ppm
DIFQ (mid freq.)	difference function quadrature from CXQ and CPQ	4 ppm
RES900	log resistivity	.06 decade
RES7200	log resistivity	.06 decade
RES56K	log resistivity	.06 decade
DEP900	apparent depth	6 m
DEP7200	apparent depth	6 m
DEP56K	apparent depth	6 m
CDT	conductance	1 grade

6. PRODUCTS

This section lists the final maps and products that have been provided under the terms of the survey agreement. Other products can be prepared from the existing dataset, if requested. These include magnetic enhancements or derivatives, percent magnetite, resistivities corrected for magnetic permeability and/or dielectric permittivity, digital terrain, resistivity-depth sections, inversions, and overburden thickness. Most parameters can be displayed as contours, profiles, or in colour.

Base Maps

Base maps of the survey area were produced from digital topography files supplied by La Quinta Resource Corp. This process provides a relatively accurate, distortion-free base that facilitates correlation of the navigation data to the map coordinate system. The topographic files were combined with geophysical data for plotting the final maps. All maps were created using the following parameters:

Projection Description:

Datum:	NAD83
Ellipsoid:	GRS80
Projection:	UTM (Zone: 11)
Central Meridian:	117° W
False Northing:	0
False Easting:	500000
Scale Factor:	0.9996
WGS84 to Local Conversion:	Molodensky
Datum Shifts:	DX: 0 DY: 0 DZ: 0

The following parameters are presented on one map sheet, at a scale of 1:20,000. All maps include flight lines and topography, unless otherwise indicated. Preliminary products are not listed.

Final Products

	No. of Map Sets		
	Mylar	Blackline	Colour
EM Anomalies		2	
Total Magnetic Field			2
Calculated Vertical Magnetic Gradient			2
Apparent Resistivity 900 Hz			2
Apparent Resistivity 7200 Hz			2
Apparent Resistivity 56,000 Hz			2

Additional Products

Digital Archive (see Archive Description)	1 CD-ROM
Survey Report	2 copies
Multi-channel Stacked Profiles	All lines
Analog Chart Records	All lines
Flight Path Video (VHS)	1 cassette

7. SURVEY RESULTS

General Discussion

Table 7-1 summarizes the EM responses in the survey area, with respect to conductance grade and interpretation.

The anomalies shown on the electromagnetic anomaly maps are based on a near-vertical, half plane model. This model best reflects "discrete" bedrock conductors. Wide bedrock conductors or flat-lying conductive units, whether from surficial or bedrock sources, may give rise to very broad anomalous responses on the EM profiles. These may not appear on the electromagnetic anomaly map if they have a regional character rather than a locally anomalous character.

These broad conductors, which more closely approximate a half-space model, will be maximum coupled to the horizontal (coplanar) coil-pair and should be more evident on the resistivity parameter. Resistivity maps, therefore, may be more valuable than the electromagnetic anomaly maps, in areas where broad or flat-lying conductors are considered to be of importance. Contoured resistivity maps, based on the 7200 Hz and 56000 Hz coplanar data are included with this report.

**TABLE 7-1 EM ANOMALY STATISTICS
HOWELL PROPERTY, B.C.**

CONDUCTOR GRADE	CONDUCTANCE RANGE SIEMENS (MHOS)	NUMBER OF RESPONSES
7	>100	0
6	50 - 100	0
5	20 - 50	0
4	10 - 20	0
3	5 - 10	0
2	1 - 5	1
1	<1	0
*	INDETERMINATE	148
TOTAL		149

CONDUCTOR MODEL	MOST LIKELY SOURCE	NUMBER OF RESPONSES
S	CONDUCTIVE COVER	148
H	ROCK UNIT OR THICK COVER	1
TOTAL		149

(SEE EM MAP LEGEND FOR EXPLANATIONS)

Excellent resolution and discrimination of conductors was accomplished by using a fast sampling rate of 0.1 sec and by employing a "common" frequency (5500/7200 Hz) on two orthogonal coil-pairs (coaxial and coplanar). The resulting difference channel parameters often permit differentiation of bedrock and surficial conductors, even though they may exhibit similar conductance values.

Anomalies that occur near the ends of the survey lines (i.e., outside the survey area), should be viewed with caution. Some of the weaker anomalies could be due to aerodynamic noise, i.e., bird bending, which is created by abnormal stresses to which the bird is subjected during the climb and turn of the aircraft between lines. Such aerodynamic noise is usually manifested by an anomaly on the coaxial in-phase channel only, although severe stresses can affect the coplanar in-phase channels as well.

Magnetics

A Fugro CF-1 cesium vapour magnetometer was operated at the survey base to record diurnal variations of the earth's magnetic field. The clock of the base station was synchronized with that of the airborne system to permit subsequent removal of diurnal drift. A GEM Systems GSM-19T proton precession magnetometer was also operated as a backup unit.

The total magnetic field data have been presented as contours on the base map using a contour interval of 2 nT where gradients permit. The map shows the magnetic properties of the rock units underlying the survey area.

The total magnetic field data have been subjected to a processing algorithm to produce maps of the calculated vertical gradient. This procedure enhances near-surface magnetic units and suppresses regional gradients. It also provides better definition and resolution of magnetic units and displays weak magnetic features that may not be clearly evident on the total field maps.

There is some evidence on the magnetic maps that suggests that the survey area has been subjected to deformation and/or alteration. These structural complexities are evident on the contour maps as variations in magnetic intensity, irregular patterns, and as offsets or changes in strike direction.

If a specific magnetic intensity can be assigned to the rock type that is believed to host the target mineralization, it may be possible to select areas of higher priority on the basis of the total field magnetic data. This is based on the assumption that the magnetite content of the host rocks will give rise to a limited range of contour values that will permit differentiation of various lithological units.

The magnetic results, in conjunction with the other geophysical parameters, have provided valuable information that can be used to effectively map the geology and structure in the survey area.

Apparent Resistivity

Apparent resistivity maps, which display the conductive properties of the survey area, were produced from the 900 Hz, 7200 Hz and 56,000 Hz coplanar data. The maximum resistivity values, which are calculated for each frequency, are 1,000 8,000 and 20,000 ohm-m respectively. These cutoffs eliminate the erratic higher resistivities that would result from unstable ratios of very small EM amplitudes.

Electromagnetic Anomalies

The EM anomalies resulting from this survey appear to fall within one general category. This type of anomaly comprises moderately broad responses that exhibit the characteristics of a half-space and do not yield well-defined inflections on the difference channels. Anomalies in this category are given an "S" or "H" interpretive symbol. The lack of a difference channel response usually implies a broad or flat-lying conductive source such as overburden. Some of these anomalies could reflect conductive rock units, zones of deep weathering, or the weathered tops of kimberlite pipes, all of which can yield "non-discrete" signatures.

The effects of conductive overburden are evident over portions of the survey area. Although the difference channels (DIFI and DIFQ) are extremely valuable in detecting bedrock conductors that are partially masked by conductive overburden, sharp undulations in the

survey area, and the types and expected geophysical responses of the targets being sought.

Anomalous electromagnetic responses are selected and analysed by computer to provide a preliminary electromagnetic anomaly map. The automatic selection algorithm is intentionally oversensitive to assure that no meaningful responses are missed. Using the preliminary map in conjunction with the multi-parameter stacked profiles, the interpreter then classifies the anomalies according to their source and eliminates those that are not substantiated by the data. The final interpreted EM anomaly map includes bedrock, surficial and cultural conductors. A map containing only bedrock conductors can be generated, if desired.

Apparent Resistivity

The apparent resistivities in ohm-m are generated from the in-phase and quadrature EM components for all of the coplanar frequencies, using a pseudo-layer half-space model. The inputs to the resistivity algorithm are the in-phase and quadrature amplitudes of the secondary field. The algorithm calculates the apparent resistivity in ohm-m, and the apparent height of the bird above the conductive source. Any difference between the apparent height and the true height, as measured by the radar altimeter, is called the pseudo-layer and reflects the difference between the real geology and a homogeneous halfspace. This difference is often attributed to the presence of a highly resistive upper layer. Any errors in the altimeter reading, caused by heavy tree cover, are included in the pseudo-layer and do not affect the resistivity calculation. The apparent depth estimates,

however, will reflect the altimeter errors. Apparent resistivities calculated in this manner may differ from those calculated using other models.

In areas where the effects of magnetic permeability or dielectric permittivity have suppressed the in-phase responses, the calculated resistivities will be erroneously high. Various algorithms and inversion techniques can be used to partially correct for the effects of permeability and permittivity.

Apparent resistivity maps portray all of the information for a given frequency over the entire survey area. This full coverage contrasts with the electromagnetic anomaly map, which provides information only over interpreted conductors. The large dynamic range afforded by the multiple frequencies makes the apparent resistivity parameter an excellent mapping tool.

The preliminary apparent resistivity maps and images are carefully inspected to identify any lines or line segments that might require base level adjustments. Subtle changes between in-flight calibrations of the system can result in line-to-line differences that are more recognizable in resistive (low signal amplitude) areas. If required, manual level adjustments are carried out to eliminate or minimize resistivity differences that can be attributed, in part, to changes in operating temperatures. These leveling adjustments are usually very subtle, and do not result in the degradation of discrete anomalies.

After the manual leveling process is complete, revised resistivity grids are created. The resulting grids can be subjected to a microleveling technique in order to smooth the data for contouring.

The calculated resistivities for all coplanar frequencies are included in the XYZ and grid archives. Values are in ohm-metres on all final products.

Total Magnetic Field

The aeromagnetic data were inspected in grid and profile format. Spikes were removed manually with the aid of a fourth difference calculation. Lag corrections were then applied to the magnetic data. A consistent lag of 0.5 seconds was applied to the entire survey dataset. A Geometrics G822 cesium vapour magnetometer was operated at the survey base to record diurnal variations of the earth's magnetic field. The clock of the base station was synchronized with that of the airborne system to permit subsequent removal of diurnal drift. The diurnal data were inspected for spikes and filtered to retain the longer wavelength diurnal variations. The filtered diurnal data were subtracted from the total magnetic field data after removal of a base value of 56769 nT. The resulting diurnally corrected survey data were then leveled using tie and traverse line intercepts. Manual adjustments were applied to any lines that required additional leveling, as indicated by shadowed images of both the total field magnetic data and the calculated vertical gradient data. A microlevelling filter was then applied to the manually adjusted leveled total field data to provide a grid suitable for image processing presentation. Microrolevelling errors were limited to +/- 1.0 nT.

The final magnetic field data were gridded using the bi-directional akima spline algorithm.

Calculated Vertical Magnetic Gradient

The total magnetic field data was subjected to a processing algorithm that enhances the response of magnetic bodies in the upper 500 m and attenuates the response of deeper bodies. This processing algorithm includes a frequency domain filter combination of the vertical derivative operator and a Butterworth filter to suppress the amplification of high-frequencies. The resulting vertical gradient map provides better definition and resolution of near-surface magnetic units. It also identifies weak magnetic features that may not be evident on the total field map. However, regional magnetic variations and changes in lithology may be better defined on the total magnetic field map.

Digital Terrain (digital product only)

The radar altimeter values (ALTBIRD : bird to ground clearance) were subtracted from the differentially corrected and de-spiked GPS-Z values to produce profiles of the height above the ellipsoid along the survey lines. These values were gridded to produce contour maps showing approximate elevations within the survey area. The calculated digital terrain data did not require any further levelling. The digital terrain data were then DC shifted to match the published topography as closely as possible.

bedrock/overburden interface can yield anomalies in the difference channels which may be interpreted as possible bedrock conductors.

The "?" symbol does not question the validity of an anomaly, but instead indicates some degree of uncertainty as to which is the most appropriate EM source model. This ambiguity results from the combination of effects from two or more conductive sources, such as overburden and bedrock, gradational changes, or moderately shallow dips. The presence of a conductive upper layer has a tendency to mask or alter the characteristics of bedrock conductors, making interpretation difficult. This problem is further exacerbated in the presence of magnetite.

In areas where EM responses are evident primarily on the quadrature components, zones of poor conductivity are indicated. Where these responses are coincident with magnetic anomalies, it is possible that the in-phase component amplitudes have been suppressed by the effects of magnetite. Poorly-conductive magnetic features can give rise to resistivity anomalies that are only slightly below or slightly above background. If it is expected that poorly-conductive economic mineralization could be associated with magnetite-rich units, most of these weakly anomalous features will be of interest. In areas where magnetite causes the in-phase components to become negative, the apparent conductance and depth of EM anomalies will be unreliable. Magnetite effects usually give rise to overstated (higher) resistivity values and understated (shallow) depth calculations.

It is impractical to assess the relative merits of EM anomalies on the basis of conductance. It is recommended that an attempt be made to compile a suite of geophysical "signatures"

over any known areas of interest. Anomaly characteristics are clearly defined on the multi-parameter geophysical data profiles that are supplied as one of the survey products.

Howell Property Survey

The resistivity data, as calculated from all three coplanar coil-pairs, display similar patterns throughout the survey area. There is a general increase in conductivity from the southeast, northward across the survey area. Within the northern region of the survey block, resistivities of less than 200 ohm-m are not uncommon, as displayed by the 56,000 Hz resistivity map. Towards the south, the background resistivities increase to over 1,000 ohm-m. The eastern limits of the survey area generally yield the highest background calculated resistivities, with values over 10,000 ohm-m commonly displayed.

A narrow magnetic high, extending from line 10270, fiducial 4705 eastwards to line 10220, fiducial 2725 is clearly evident on the calculated vertical magnetic gradient map. It displays excellent correlation with a resistivity low that is best defined on the 56,000 Hz resistivity map. As the 56,000 Hz resistivity data is most influenced by surficial features, this indicates that the conductivity may be surficial in nature. However, the good correlation with the magnetic data indicates that the conductivity may be related to a bedrock feature.

There is limited correlation between the resistivity patterns and the topographic features. Many of the topographic highs correlate well with zones of higher resistivities. This is apparent on all of the resistivity maps. However, there are also regions where the rivers

valleys are coincident with highly resistive material. There is poor correlation between the location of Twentynine Mile Creek on the topographic map and the resistivity patterns. Although there is a general increase in conductivity near the creek, the creek itself does not appear to have strongly influenced the resistivity data.

The calculated resistivities are slightly lower on the 7200 Hz resistivity maps, as compared to the 56,000 Hz maps. This is particularly evident within the northern conductive portions of the survey area. It may indicate that there is a slight increase in conductivity with depth. However, this pattern is not consistent with the 900 Hz resistivity data, as the 900 Hz resistivity maps display a slight decrease in conductivity. This could be due to the very low measured secondary EM fields by the 900 Hz coil-pair, resulting in slightly overstated resistivities.

The measured EM signals on all frequencies can be characterized as broad responses as opposed to discrete responses. This suggests that the source of the conductivity is generally horizontal or layered as opposed to vertical or steeply dipping.

The magnetic data displays a dynamic range of over 480 nT across the entire survey area. Most of this dynamic range is contained within one magnetic feature centered near line 10190, fiducial 1690. There is little evidence of this anomaly within the resistivity data. The magnetic display generally reveals little relief near the northern edge of the survey property. Along the western and southern edges, several high amplitude, short wavelength magnetic features have been mapped. Most of these features are better defined on the calculated vertical magnetic gradient map.

8. CONCLUSIONS AND RECOMMENDATIONS

This report provides a very brief description of the survey results and describes the equipment, data processing procedures and logistics of the survey.

The survey was successful in locating a few moderately weak or broad conductors that may warrant additional work. The various maps included with this report display the magnetic and conductive properties of the survey area. It is recommended that a complete assessment and detailed evaluation of the survey results be carried out, in conjunction with all available geophysical, geological and geochemical information. Particular reference should be made to the multi-parameter data profiles that clearly define the characteristics of the individual anomalies.

Most anomalies in the area are moderately weak and poorly-defined. Many have been attributed to conductive overburden or deep weathering, although a few appear to be associated with magnetite-rich rock units. Others coincide with magnetic gradients that may reflect contacts, faults or shears. Such structural breaks are considered to be of particular interest as they may have influenced mineral deposition within the survey area.

The interpreted bedrock conductors and anomalous targets defined by the survey should be subjected to further investigation, using appropriate surface exploration techniques. Anomalies that are currently considered to be of moderately low priority may require upgrading if follow-up results are favourable.

It is also recommended that image processing of existing geophysical data be considered, in order to extract the maximum amount of information from the survey results. Current software and imaging techniques often provide valuable information on structure and lithology, which may not be clearly evident on the contour and colour maps. These techniques can yield images that define subtle, but significant, structural details.

Respectfully submitted,

FUGRO AIRBORNE SURVEYS CORP.

Douglas G. Garrie
Geophysicist

DGG/sdp

R04086JAN.05

APPENDIX A

LIST OF PERSONNEL

The following personnel were involved in the acquisition, processing, interpretation and presentation of data, relating to a DIGHEM^{V-DSP} airborne geophysical survey carried out for La Quinta Resource Corp., near Fernie, British Columbia.

David Miles	Manager, Helicopter Operations
Emily Farquhar	Manager, Data Processing and Interpretation
John Douglas	Geophysical Operator
Jeffrey Fleming	Field Geophysicist
Greg Goodison	Pilot (Big Horn Helicopters Ltd.)
Gordon Smith	Data Processing Supervisor
Emily Farquhar	Geophysical Data Processor
Douglas Garrie	Interpretation Geophysicist
Lyn Vanderstarren	Drafting Supervisor
Susan Pothiah	Word Processing Operator
Albina Tonello	Secretary/Expeditor

The survey consisted of 217 km of coverage, flown from October 26 to October 27, 2004.

All personnel are employees of Fugro Airborne Surveys, except for the pilot who is an employee of Big Horn Helicopters Ltd.

APPENDIX B

OPTIONAL PRODUCTS

APPENDIX B

OPTIONAL PRODUCTS

Dielectric Permittivity and Magnetic Permeability Corrections¹

In resistive areas having magnetic rocks, the magnetic and dielectric effects will both generally be present in high-frequency EM data, whereas only the magnetic effect will exist in low-frequency data.

The magnetic permeability is first obtained from the EM data at the lowest frequency, because the ratio of the magnetic response to conductive response is maximized and because displacement currents are negligible. The homogeneous half-space model is used. The computed magnetic permeability is then used along with the in-phase and quadrature response at the highest frequency to obtain the relative dielectric permittivity, again using the homogeneous half-space model. The highest frequency is used because the ratio of dielectric response to conductive response is maximized. The resistivity can then be determined from the measured in-phase and quadrature components of each frequency, given the relative magnetic permeability and relative dielectric permittivity.

¹ Huang, H. and Fraser, D.C., 2001 Mapping of the Resistivity, Susceptibility, and Permittivity of the Earth Using a Helicopter-borne Electromagnetic System: Geophysics 106 pg 148-157.

Resistivity-depth Sections

The apparent resistivities for all frequencies can be displayed simultaneously as coloured resistivity-depth sections. Usually, only the coplanar data are displayed as the close frequency separation between the coplanar and adjacent coaxial data tends to distort the section. The sections can be plotted using the topographic elevation profile as the surface. The digital terrain values, in metres a.m.s.l., can be calculated from the GPS Z-value or barometric altimeter, minus the aircraft radar altimeter.

Resistivity-depth sections can be generated in three formats:

- (1) Sengpiel resistivity sections, where the apparent resistivity for each frequency is plotted at the depth of the centroid of the in-phase current flow²; and,
- (2) Differential resistivity sections, where the differential resistivity is plotted at the differential depth³.

² Sengpiel, K.P., 1988, Approximate Inversion of Airborne EM Data from Multilayered Ground: *Geophysical Prospecting* 36, 446-459.

³ Huang, H. and Fraser, D.C., 1993, Differential Resistivity Method for Multi-frequency Airborne EM Sounding: presented at Intern. Airb. EM Workshop, Tucson, Ariz.

- Appendix B.7 -

(3) Occam⁴ or Multi-layer⁵ inversion.

Both the Sengpiel and differential methods are derived from the pseudo-layer half-space model. Both yield a coloured resistivity-depth section that attempts to portray a smoothed approximation of the true resistivity distribution with depth. Resistivity-depth sections are most useful in conductive layered situations, but may be unreliable in areas of moderate to high resistivity where signal amplitudes are weak. In areas where in-phase responses have been suppressed by the effects of magnetite, or adversely affected by cultural features, the computed resistivities shown on the sections may be unreliable.

Both the Occam and multi-layer inversions compute the layered earth resistivity model that would best match the measured EM data. The Occam inversion uses a series of thin, fixed layers (usually 20 x 5m and 10 x 10m layers) and computes resistivities to fit the EM data. The multi-layer inversion computes the resistivity and thickness for each of a defined number of layers (typically 3-5 layers) to best fit the data.

⁴ Constable et al, 1987, Occam's inversion: a practical algorithm for generating smooth models from electromagnetic sounding data: *Geophysics*, 52, 289-300.

⁵ Huang H., and Palacky, G.J., 1991, Damped least-squares inversion of time domain airborne EM data based on singular value decomposition: *Geophysical Prospecting*, 39, 827-844.

EM Magnetite

The apparent percent magnetite by weight is computed wherever magnetite produces a negative in-phase EM response. This calculation is more meaningful in resistive areas.

Residual Magnetic Intensity

The residual magnetic intensity (RMI) is derived from the total magnetic field (TMF), the diurnal, and the regional magnetic field. The total magnetic intensity is measured in the aircraft, the diurnal is measured from the ground station, and the regional magnetic field is calculated from the international geo-referenced magnetic field (IGRF). The low frequency component of the diurnal is extracted from the filtered ground station data and removed from the TMF. The average of the diurnal is then added back in to obtain the resultant total magnetic intensity. The regional magnetic field, calculated for the specific survey location and the time of the survey, is then removed from the resultant total magnetic intensity to yield the residual magnetic intensity.

Magnetic Derivatives

The total magnetic field data can be subjected to a variety of filtering techniques to yield maps or images of the following:

- Appendix B.9 -

enhanced magnetics

second vertical derivative

reduction to the pole/equator

magnetic susceptibility with reduction to the pole

upward/downward continuations

analytic signal

All of these filtering techniques improve the recognition of near-surface magnetic bodies, with the exception of upward continuation. Any of these parameters can be produced on request.

APPENDIX C

BACKGROUND INFORMATION

BACKGROUND INFORMATION

Electromagnetics

Fugro electromagnetic responses fall into two general classes, discrete and broad. The discrete class consists of sharp, well-defined anomalies from discrete conductors such as sulphide lenses and steeply dipping sheets of graphite and sulphides. The broad class consists of wide anomalies from conductors having a large horizontal surface such as flatly dipping graphite or sulphide sheets, saline water-saturated sedimentary formations, conductive overburden and rock, kimberlite pipes and geothermal zones. A vertical conductive slab with a width of 200 m would straddle these two classes.

The vertical sheet (half plane) is the most common model used for the analysis of discrete conductors. All anomalies plotted on the geophysical maps are analyzed according to this model. The following section entitled **Discrete Conductor Analysis** describes this model in detail, including the effect of using it on anomalies caused by broad conductors such as conductive overburden.

The conductive earth (half-space) model is suitable for broad conductors. Resistivity contour maps result from the use of this model. A later section entitled **Resistivity Mapping** describes the method further, including the effect of using it on anomalies caused by discrete conductors such as sulphide bodies.

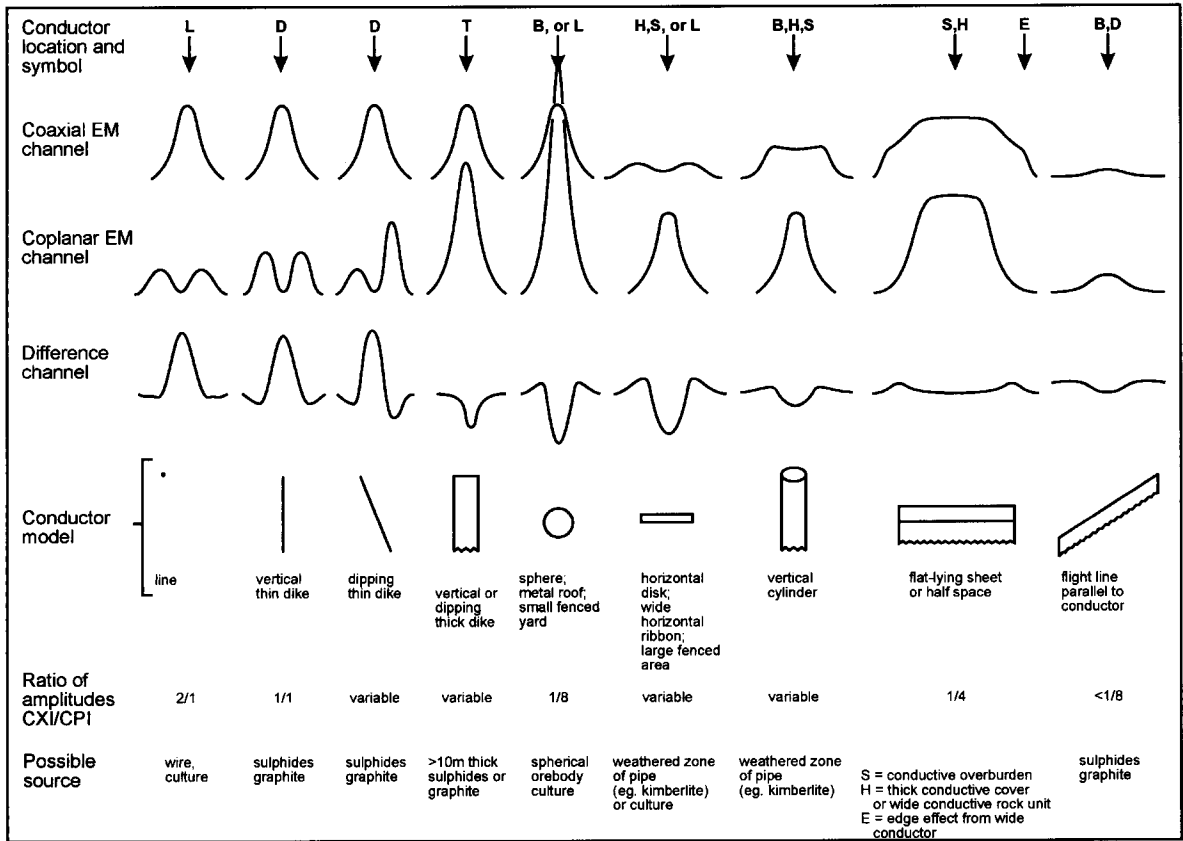
Geometric Interpretation

The geophysical interpreter attempts to determine the geometric shape and dip of the conductor. Figure C-1 shows typical HEM anomaly shapes which are used to guide the geometric interpretation.

Discrete Conductor Analysis

The EM anomalies appearing on the electromagnetic map are analyzed by computer to give the conductance (i.e., conductivity-thickness product) in siemens (mhos) of a vertical sheet model. This is done regardless of the interpreted geometric shape of the conductor. This is not an unreasonable procedure, because the computed conductance increases as the electrical quality of the conductor increases, regardless of its true shape. DIGHEM anomalies are divided into seven grades of conductance, as shown in Table C-1. The conductance in siemens (mhos) is the reciprocal of resistance in ohms.

- Appendix C.2 -



Typical HEM anomaly shapes
Figure C-1

- Appendix C.3 -

The conductance value is a geological parameter because it is a characteristic of the conductor alone. It generally is independent of frequency, flying height or depth of burial, apart from the averaging over a greater portion of the conductor as height increases. Small anomalies from deeply buried strong conductors are not confused with small anomalies from shallow weak conductors because the former will have larger conductance values.

Table C-1. EM Anomaly Grades

Anomaly Grade	Siemens
7	> 100
6	50 - 100
5	20 - 50
4	10 - 20
3	5 - 10
2	1 - 5
1	< 1

Conductive overburden generally produces broad EM responses which may not be shown as anomalies on the geophysical maps. However, patchy conductive overburden in otherwise resistive areas can yield discrete anomalies with a conductance grade (cf. Table C-1) of 1, 2 or even 3 for conducting clays which have resistivities as low as 50 ohm-m. In areas where ground resistivities are below 10 ohm-m, anomalies caused by weathering variations and similar causes can have any conductance grade. The anomaly shapes from the multiple coils often allow such conductors to be recognized, and these are indicated by the letters S, H, and sometimes E on the geophysical maps (see EM legend on maps).

For bedrock conductors, the higher anomaly grades indicate increasingly higher conductances. Examples: the New Inco copper discovery (Noranda, Canada) yielded a grade 5 anomaly, as did the neighbouring copper-zinc Magusi River ore body; Mattabi (copper-zinc, Sturgeon Lake, Canada) and Whistle (nickel, Sudbury, Canada) gave grade 6; and the Montcalm nickel-copper discovery (Timmins, Canada) yielded a grade 7 anomaly. Graphite and sulphides can span all grades but, in any particular survey area, field work may show that the different grades indicate different types of conductors.

Strong conductors (i.e., grades 6 and 7) are characteristic of massive sulphides or graphite. Moderate conductors (grades 4 and 5) typically reflect graphite or sulphides of a less massive character, while weak bedrock conductors (grades 1 to 3) can signify poorly connected graphite or heavily disseminated sulphides. Grades 1 and 2 conductors may not respond to ground EM equipment using frequencies less than 2000 Hz.

The presence of sphalerite or gangue can result in ore deposits having weak to moderate conductances. As an example, the three million ton lead-zinc deposit of Restigouche Mining Corporation near Bathurst, Canada, yielded a well-defined grade 2 conductor. The 10 percent by volume of sphalerite occurs as a coating around the fine grained massive pyrite, thereby inhibiting electrical conduction. Faults, fractures and shear zones may produce anomalies that typically have low conductances (e.g., grades 1 to 3). Conductive rock formations can yield anomalies of any conductance grade. The conductive materials in

- Appendix C.4 -

such rock formations can be salt water, weathered products such as clays, original depositional clays, and carbonaceous material.

For each interpreted electromagnetic anomaly on the geophysical maps, a letter identifier and an interpretive symbol are plotted beside the EM grade symbol. The horizontal rows of dots, under the interpretive symbol, indicate the anomaly amplitude on the flight record. The vertical column of dots, under the anomaly letter, gives the estimated depth. In areas where anomalies are crowded, the letter identifiers, interpretive symbols and dots may be obliterated. The EM grade symbols, however, will always be discernible, and the obliterated information can be obtained from the anomaly listing appended to this report.

The purpose of indicating the anomaly amplitude by dots is to provide an estimate of the reliability of the conductance calculation. Thus, a conductance value obtained from a large ppm anomaly (3 or 4 dots) will tend to be accurate whereas one obtained from a small ppm anomaly (no dots) could be quite inaccurate. The absence of amplitude dots indicates that the anomaly from the coaxial coil-pair is 5 ppm or less on both the in-phase and quadrature channels. Such small anomalies could reflect a weak conductor at the surface or a stronger conductor at depth. The conductance grade and depth estimate illustrates which of these possibilities fits the recorded data best.

The conductance measurement is considered more reliable than the depth estimate. There are a number of factors that can produce an error in the depth estimate, including the averaging of topographic variations by the altimeter, overlying conductive overburden, and the location and attitude of the conductor relative to the flight line. Conductor location and attitude can provide an erroneous depth estimate because the stronger part of the conductor may be deeper or to one side of the flight line, or because it has a shallow dip. A heavy tree cover can also produce errors in depth estimates. This is because the depth estimate is computed as the distance of bird from conductor, minus the altimeter reading. The altimeter can lock onto the top of a dense forest canopy. This situation yields an erroneously large depth estimate but does not affect the conductance estimate.

Dip symbols are used to indicate the direction of dip of conductors. These symbols are used only when the anomaly shapes are unambiguous, which usually requires a fairly resistive environment.

A further interpretation is presented on the EM map by means of the line-to-line correlation of bedrock anomalies, which is based on a comparison of anomaly shapes on adjacent lines. This provides conductor axes that may define the geological structure over portions of the survey area. The absence of conductor axes in an area implies that anomalies could not be correlated from line to line with reasonable confidence.

The electromagnetic anomalies are designed to provide a correct impression of conductor quality by means of the conductance grade symbols. The symbols can stand alone with geology when planning a follow-up program. The actual conductance values are printed in the attached anomaly list for those who wish quantitative data. The anomaly ppm and depth are indicated by inconspicuous dots which should not distract from the conductor patterns, while being helpful to those who wish this information. The map provides an

- Appendix C.5 -

interpretation of conductors in terms of length, strike and dip, geometric shape, conductance, depth, and thickness. The accuracy is comparable to an interpretation from a high quality ground EM survey having the same line spacing.

The appended EM anomaly list provides a tabulation of anomalies in ppm, conductance, and depth for the vertical sheet model. No conductance or depth estimates are shown for weak anomalous responses that are not of sufficient amplitude to yield reliable calculations.

Since discrete bodies normally are the targets of EM surveys, local base (or zero) levels are used to compute local anomaly amplitudes. This contrasts with the use of true zero levels which are used to compute true EM amplitudes. Local anomaly amplitudes are shown in the EM anomaly list and these are used to compute the vertical sheet parameters of conductance and depth.

Questionable Anomalies

The EM maps may contain anomalous responses that are displayed as asterisks (*). These responses denote weak anomalies of indeterminate conductance, which may reflect one of the following: a weak conductor near the surface, a strong conductor at depth (e.g., 100 to 120 m below surface) or to one side of the flight line, or aerodynamic noise. Those responses that have the appearance of valid bedrock anomalies on the flight profiles are indicated by appropriate interpretive symbols (see EM legend on maps). The others probably do not warrant further investigation unless their locations are of considerable geological interest.

The Thickness Parameter

A comparison of coaxial and coplanar shapes can provide an indication of the thickness of a steeply dipping conductor. The amplitude of the coplanar anomaly (e.g., CPI channel) increases relative to the coaxial anomaly (e.g., CXI) as the apparent thickness increases, i.e., the thickness in the horizontal plane. (The thickness is equal to the conductor width if the conductor dips at 90 degrees and strikes at right angles to the flight line.) This report refers to a conductor as thin when the thickness is likely to be less than 3 m, and thick when in excess of 10 m. Thick conductors are indicated on the EM map by parentheses "()". For base metal exploration in steeply dipping geology, thick conductors can be high priority targets because many massive sulphide ore bodies are thick. The system cannot sense the thickness when the strike of the conductor is subparallel to the flight line, when the conductor has a shallow dip, when the anomaly amplitudes are small, or when the resistivity of the environment is below 100 ohm-m.

Resistivity Mapping

Resistivity mapping is useful in areas where broad or flat lying conductive units are of interest. One example of this is the clay alteration which is associated with Carlin-type

- Appendix C.6 -

deposits in the south west United States. The resistivity parameter was able to identify the clay alteration zone over the Cove deposit. The alteration zone appeared as a strong resistivity low on the 900 Hz resistivity parameter. The 7,200 Hz and 56,000 Hz resistivities showed more detail in the covering sediments, and delineated a range front fault. This is typical in many areas of the south west United States, where conductive near surface sediments, which may sometimes be alkalic, attenuate the higher frequencies.

Resistivity mapping has proven successful for locating diatremes in diamond exploration. Weathering products from relatively soft kimberlite pipes produce a resistivity contrast with the unaltered host rock. In many cases weathered kimberlite pipes were associated with thick conductive layers that contrasted with overlying or adjacent relatively thin layers of lake bottom sediments or overburden.

Areas of widespread conductivity are commonly encountered during surveys. These conductive zones may reflect alteration zones, shallow-dipping sulphide or graphite-rich units, saline ground water, or conductive overburden. In such areas, EM amplitude changes can be generated by decreases of only 5 m in survey altitude, as well as by increases in conductivity. The typical flight record in conductive areas is characterized by in-phase and quadrature channels that are continuously active. Local EM peaks reflect either increases in conductivity of the earth or decreases in survey altitude. For such conductive areas, apparent resistivity profiles and contour maps are necessary for the correct interpretation of the airborne data. The advantage of the resistivity parameter is that anomalies caused by altitude changes are virtually eliminated, so the resistivity data reflect only those anomalies caused by conductivity changes. The resistivity analysis also helps the interpreter to differentiate between conductive bedrock and conductive overburden. For example, discrete conductors will generally appear as narrow lows on the contour map and broad conductors (e.g., overburden) will appear as wide lows.

The apparent resistivity is calculated using the pseudo-layer (or buried) half-space model defined by Fraser (1978)⁶. This model consists of a resistive layer overlying a conductive half-space. The depth channels give the apparent depth below surface of the conductive material. The apparent depth is simply the apparent thickness of the overlying resistive layer. The apparent depth (or thickness) parameter will be positive when the upper layer is more resistive than the underlying material, in which case the apparent depth may be quite close to the true depth.

The apparent depth will be negative when the upper layer is more conductive than the underlying material, and will be zero when a homogeneous half-space exists. The apparent depth parameter must be interpreted cautiously because it will contain any errors that might exist in the measured altitude of the EM bird (e.g., as caused by a dense tree cover). The inputs to the resistivity algorithm are the in-phase and quadrature components of the coplanar coil-pair. The outputs are the apparent resistivity of the conductive half-space (the

⁶ Resistivity mapping with an airborne multicoil electromagnetic system: Geophysics, v. 43, p.144-172

- Appendix C.7 -

source) and the sensor-source distance. The flying height is not an input variable, and the output resistivity and sensor-source distance are independent of the flying height when the conductivity of the measured material is sufficient to yield significant in-phase as well as quadrature responses. The apparent depth, discussed above, is simply the sensor-source distance minus the measured altitude or flying height. Consequently, errors in the measured altitude will affect the apparent depth parameter but not the apparent resistivity parameter.

The apparent depth parameter is a useful indicator of simple layering in areas lacking a heavy tree cover. Depth information has been used for permafrost mapping, where positive apparent depths were used as a measure of permafrost thickness. However, little quantitative use has been made of negative apparent depths because the absolute value of the negative depth is not a measure of the thickness of the conductive upper layer and, therefore, is not meaningful physically. Qualitatively, a negative apparent depth estimate usually shows that the EM anomaly is caused by conductive overburden. Consequently, the apparent depth channel can be of significant help in distinguishing between overburden and bedrock conductors.

Interpretation in Conductive Environments

Environments having low background resistivities (e.g., below 30 ohm-m for a 900 Hz system) yield very large responses from the conductive ground. This usually prohibits the recognition of discrete bedrock conductors. However, Fugro data processing techniques produce three parameters that contribute significantly to the recognition of bedrock conductors in conductive environments. These are the in-phase and quadrature difference channels (DIFI and DIFQ, which are available only on systems with "common" frequencies on orthogonal coil pairs), and the resistivity and depth channels (RES and DEP) for each coplanar frequency.

The EM difference channels (DIFI and DIFQ) eliminate most of the responses from conductive ground, leaving responses from bedrock conductors, cultural features (e.g., telephone lines, fences, etc.) and edge effects. Edge effects often occur near the perimeter of broad conductive zones. This can be a source of geologic noise. While edge effects yield anomalies on the EM difference channels, they do not produce resistivity anomalies. Consequently, the resistivity channel aids in eliminating anomalies due to edge effects. On the other hand, resistivity anomalies will coincide with the most highly conductive sections of conductive ground, and this is another source of geologic noise. The recognition of a bedrock conductor in a conductive environment therefore is based on the anomalous responses of the two difference channels (DIFI and DIFQ) and the resistivity channels (RES). The most favourable situation is where anomalies coincide on all channels.

The DEP channels, which give the apparent depth to the conductive material, also help to determine whether a conductive response arises from surficial material or from a conductive zone in the bedrock. When these channels ride above the zero level on the depth profiles (i.e., depth is negative), it implies that the EM and resistivity profiles are responding primarily to a conductive upper layer, i.e., conductive overburden. If the DEP channels are below the zero level, it indicates that a resistive upper layer exists, and this usually implies the

existence of a bedrock conductor. If the low frequency DEP channel is below the zero level and the high frequency DEP is above, this suggests that a bedrock conductor occurs beneath conductive cover.

Reduction of Geologic Noise

Geologic noise refers to unwanted geophysical responses. For purposes of airborne EM surveying, geologic noise refers to EM responses caused by conductive overburden and magnetic permeability. It was mentioned previously that the EM difference channels (i.e., channel DIFI for in-phase and DIFQ for quadrature) tend to eliminate the response of conductive overburden.

Magnetite produces a form of geological noise on the in-phase channels. Rocks containing less than 1% magnetite can yield negative in-phase anomalies caused by magnetic permeability. When magnetite is widely distributed throughout a survey area, the in-phase EM channels may continuously rise and fall, reflecting variations in the magnetite percentage, flying height, and overburden thickness. This can lead to difficulties in recognizing deeply buried bedrock conductors, particularly if conductive overburden also exists. However, the response of broadly distributed magnetite generally vanishes on the in-phase difference channel DIFI. This feature can be a significant aid in the recognition of conductors that occur in rocks containing accessory magnetite.

EM Magnetite Mapping

The information content of HEM data consists of a combination of conductive eddy current responses and magnetic permeability responses. The secondary field resulting from conductive eddy current flow is frequency-dependent and consists of both in-phase and quadrature components, which are positive in sign. On the other hand, the secondary field resulting from magnetic permeability is independent of frequency and consists of only an in-phase component which is negative in sign. When magnetic permeability manifests itself by decreasing the measured amount of positive in-phase, its presence may be difficult to recognize. However, when it manifests itself by yielding a negative in-phase anomaly (e.g., in the absence of eddy current flow), its presence is assured. In this latter case, the negative component can be used to estimate the percent magnetite content.

A magnetite mapping technique, based on the low frequency coplanar data, can be complementary to magnetometer mapping in certain cases. Compared to magnetometry, it is far less sensitive but is more able to resolve closely spaced magnetite zones, as well as providing an estimate of the amount of magnetite in the rock. The method is sensitive to 1/4% magnetite by weight when the EM sensor is at a height of 30 m above a magnetitic half-space. It can individually resolve steep dipping narrow magnetite-rich bands which are separated by 60 m. Unlike magnetometry, the EM magnetite method is unaffected by remanent magnetism or magnetic latitude.

The EM magnetite mapping technique provides estimates of magnetite content which are usually correct within a factor of 2 when the magnetite is fairly uniformly distributed. EM

magnetite maps can be generated when magnetic permeability is evident as negative in-phase responses on the data profiles.

Like magnetometry, the EM magnetite method maps only bedrock features, provided that the overburden is characterized by a general lack of magnetite. This contrasts with resistivity mapping which portrays the combined effect of bedrock and overburden.

The Susceptibility Effect

When the host rock is conductive, the positive conductivity response will usually dominate the secondary field, and the susceptibility effect⁷ will appear as a reduction in the in-phase, rather than as a negative value. The in-phase response will be lower than would be predicted by a model using zero susceptibility. At higher frequencies the in-phase conductivity response also gets larger, so a negative magnetite effect observed on the low frequency might not be observable on the higher frequencies, over the same body. The susceptibility effect is most obvious over discrete magnetite-rich zones, but also occurs over uniform geology such as a homogeneous half-space.

High magnetic susceptibility will affect the calculated apparent resistivity, if only conductivity is considered. Standard apparent resistivity algorithms use a homogeneous half-space model, with zero susceptibility. For these algorithms, the reduced in-phase response will, in most cases, make the apparent resistivity higher than it should be. It is important to note that there is nothing wrong with the data, nor is there anything wrong with the processing algorithms. The apparent difference results from the fact that the simple geological model used in processing does not match the complex geology.

Measuring and Correcting the Magnetite Effect

Theoretically, it is possible to calculate (forward model) the combined effect of electrical conductivity and magnetic susceptibility on an EM response in all environments. The difficulty lies, however, in separating out the susceptibility effect from other geological effects when deriving resistivity and susceptibility from EM data.

Over a homogeneous half-space, there is a precise relationship between in-phase, quadrature, and altitude. These are often resolved as phase angle, amplitude, and altitude. Within a reasonable range, any two of these three parameters can be used to calculate the half space resistivity. If the rock has a positive magnetic susceptibility, the in-phase component will be reduced and this departure can be recognized by comparison to the other parameters.

⁷ Magnetic susceptibility and permeability are two measures of the same physical property. Permeability is generally given as relative permeability, μ_r , which is the permeability of the substance divided by the permeability of free space ($4 \pi \times 10^{-7}$). Magnetic susceptibility k is related to permeability by $k = \mu_r - 1$. Susceptibility is a unitless measurement, and is usually reported in units of 10^{-6} . The typical range of susceptibilities is -1 for quartz, 130 for pyrite, and up to 5×10^5 for magnetite, in 10^{-6} units (Telford et al, 1986).

The algorithm used to calculate apparent susceptibility and apparent resistivity from HEM data, uses a homogeneous half-space geological model. Non half-space geology, such as horizontal layers or dipping sources, can also distort the perfect half-space relationship of the three data parameters. While it may be possible to use more complex models to calculate both rock parameters, this procedure becomes very complex and time-consuming. For basic HEM data processing, it is most practical to stick to the simplest geological model.

Magnetite reversals (reversed in-phase anomalies) have been used for many years to calculate an "FeO" or magnetite response from HEM data (Fraser, 1981). However, this technique could only be applied to data where the in-phase was observed to be negative, which happens when susceptibility is high and conductivity is low.

Applying Susceptibility Corrections

Resistivity calculations done with susceptibility correction may change the apparent resistivity. High-susceptibility conductors, that were previously masked by the susceptibility effect in standard resistivity algorithms, may become evident. In this case the susceptibility corrected apparent resistivity is a better measure of the actual resistivity of the earth. However, other geological variations, such as a deep resistive layer, can also reduce the in-phase by the same amount. In this case, susceptibility correction would not be the best method. Different geological models can apply in different areas of the same data set. The effects of susceptibility, and other effects that can create a similar response, must be considered when selecting the resistivity algorithm.

Susceptibility from EM vs Magnetic Field Data

The response of the EM system to magnetite may not match that from a magnetometer survey. First, HEM-derived susceptibility is a rock property measurement, like resistivity. Magnetic data show the total magnetic field, a measure of the potential field, not the rock property. Secondly, the shape of an anomaly depends on the shape and direction of the source magnetic field. The electromagnetic field of HEM is much different in shape from the earth's magnetic field. Total field magnetic anomalies are different at different magnetic latitudes; HEM susceptibility anomalies have the same shape regardless of their location on the earth.

In far northern latitudes, where the magnetic field is nearly vertical, the total magnetic field measurement over a thin vertical dike is very similar in shape to the anomaly from the HEM-derived susceptibility (a sharp peak over the body). The same vertical dike at the magnetic equator would yield a negative magnetic anomaly, but the HEM susceptibility anomaly would show a positive susceptibility peak.

Effects of Permeability and Dielectric Permittivity

Resistivity algorithms that assume free-space magnetic permeability and dielectric permittivity, do not yield reliable values in highly magnetic or highly resistive areas. Both magnetic polarization and displacement currents cause a decrease in the in-phase component, often resulting in negative values that yield erroneously high apparent resistivities. The effects of magnetite occur at all frequencies, but are most evident at the lowest frequency. Conversely, the negative effects of dielectric permittivity are most evident at the higher frequencies, in resistive areas.

The table below shows the effects of varying permittivity over a resistive (10,000 ohm-m) half space, at frequencies of 56,000 Hz (DIGHEM^V) and 102,000 Hz (RESOLVE).

Apparent Resistivity Calculations Effects of Permittivity on In-phase/Quadrature/Resistivity

Freq (Hz)	Coil	Sep (m)	Thres (ppm)	Alt (m)	In Phase	Quad Phase	App Res	App Depth (m)	Permittivity
56,000	CP	6.3	0.1	30	7.3	35.3	10118	-1.0	1 Air
56,000	CP	6.3	0.1	30	3.6	36.6	19838	-13.2	5 Quartz
56,000	CP	6.3	0.1	30	-1.1	38.3	81832	-25.7	10 Epidote
56,000	CP	6.3	0.1	30	-10.4	42.3	76620	-25.8	20 Granite
56,000	CP	6.3	0.1	30	-19.7	46.9	71550	-26.0	30 Diabase
56,000	CP	6.3	0.1	30	-28.7	52.0	66787	-26.1	40 Gabbro
102,000	CP	7.86	0.1	30	32.5	117.2	9409	-0.3	1 Air
102,000	CP	7.86	0.1	30	11.7	127.2	25956	-16.8	5 Quartz
102,000	CP	7.86	0.1	30	-14.0	141.6	97064	-26.5	10 Epidote
102,000	CP	7.86	0.1	30	-62.9	176.0	83995	-26.8	20 Granite
102,000	CP	7.86	0.1	30	-107.5	215.8	73320	-27.0	30 Diabase
102,000	CP	7.86	0.1	30	-147.1	259.2	64875	-27.2	40 Gabbro

Methods have been developed (Huang and Fraser, 2000, 2001) to correct apparent resistivities for the effects of permittivity and permeability. The corrected resistivities yield more credible values than if the effects of permittivity and permeability are disregarded.

Recognition of Culture

Cultural responses include all EM anomalies caused by man-made metallic objects. Such anomalies may be caused by inductive coupling or current gathering. The concern of the interpreter is to recognize when an EM response is due to culture. Points of consideration used by the interpreter, when coaxial and coplanar coil-pairs are operated at a common frequency, are as follows:

- Appendix C.12 -

1. Channels CXPL and CPPL monitor 60 Hz radiation. An anomaly on these channels shows that the conductor is radiating power. Such an indication is normally a guarantee that the conductor is cultural. However, care must be taken to ensure that the conductor is not a geologic body that strikes across a power line, carrying leakage currents.
2. A flight that crosses a "line" (e.g., fence, telephone line, etc.) yields a centre-peaked coaxial anomaly and an m-shaped coplanar anomaly.⁸ When the flight crosses the cultural line at a high angle of intersection, the amplitude ratio of coaxial/coplanar response is 2. Such an EM anomaly can only be caused by a line. The geologic body that yields anomalies most closely resembling a line is the vertically dipping thin dike. Such a body, however, yields an amplitude ratio of 1 rather than 2. Consequently, an m-shaped coplanar anomaly with a CXI/CPI amplitude ratio of 2 is virtually a guarantee that the source is a cultural line.
3. A flight that crosses a sphere or horizontal disk yields centre-peaked coaxial and coplanar anomalies with a CXI/CPI amplitude ratio (i.e., coaxial/coplanar) of 1/8. In the absence of geologic bodies of this geometry, the most likely conductor is a metal roof or small fenced yard.⁹ Anomalies of this type are virtually certain to be cultural if they occur in an area of culture.
4. A flight that crosses a horizontal rectangular body or wide ribbon yields an m-shaped coaxial anomaly and a centre-peaked coplanar anomaly. In the absence of geologic bodies of this geometry, the most likely conductor is a large fenced area.⁵ Anomalies of this type are virtually certain to be cultural if they occur in an area of culture.
5. EM anomalies that coincide with culture, as seen on the camera film or video display, are usually caused by culture. However, care is taken with such coincidences because a geologic conductor could occur beneath a fence, for example. In this example, the fence would be expected to yield an m-shaped coplanar anomaly as in case #2 above. If, instead, a centre-peaked coplanar anomaly occurred, there would be concern that a thick geologic conductor coincided with the cultural line.
6. The above description of anomaly shapes is valid when the culture is not conductively coupled to the environment. In this case, the anomalies arise from inductive coupling to the EM transmitter. However, when the environment is quite conductive (e.g., less than 100 ohm-m at 900 Hz), the cultural conductor may be conductively coupled to the environment. In this latter case, the anomaly shapes tend to be governed by current gathering. Current gathering can completely distort

⁸ See Figure C-1 presented earlier.

⁹ It is a characteristic of EM that geometrically similar anomalies are obtained from: (1) a planar conductor, and (2) a wire which forms a loop having dimensions identical to the perimeter of the equivalent planar conductor.

the anomaly shapes, thereby complicating the identification of cultural anomalies. In such circumstances, the interpreter can only rely on the radiation channels and on the camera film or video records.

Magnetic Responses

The measured total magnetic field provides information on the magnetic properties of the earth materials in the survey area. The information can be used to locate magnetic bodies of direct interest for exploration, and for structural and lithological mapping.

The total magnetic field response reflects the abundance of magnetic material in the source. Magnetite is the most common magnetic mineral. Other minerals such as ilmenite, pyrrhotite, franklinite, chromite, hematite, arsenopyrite, limonite and pyrite are also magnetic, but to a lesser extent than magnetite on average.

In some geological environments, an EM anomaly with magnetic correlation has a greater likelihood of being produced by sulphides than one which is non-magnetic. However, sulphide ore bodies may be non-magnetic (e.g., the Kidd Creek deposit near Timmins, Canada) as well as magnetic (e.g., the Mattabi deposit near Sturgeon Lake, Canada).

Iron ore deposits will be anomalously magnetic in comparison to surrounding rock due to the concentration of iron minerals such as magnetite, ilmenite and hematite.

Changes in magnetic susceptibility often allow rock units to be differentiated based on the total field magnetic response. Geophysical classifications may differ from geological classifications if various magnetite levels exist within one general geological classification. Geometric considerations of the source such as shape, dip and depth, inclination of the earth's field and remanent magnetization will complicate such an analysis.

In general, mafic lithologies contain more magnetite and are therefore more magnetic than many sediments which tend to be weakly magnetic. Metamorphism and alteration can also increase or decrease the magnetization of a rock unit.

Textural differences on a total field magnetic contour, colour or shadow map due to the frequency of activity of the magnetic parameter resulting from inhomogeneities in the distribution of magnetite within the rock, may define certain lithologies. For example, near surface volcanics may display highly complex contour patterns with little line-to-line correlation.

Rock units may be differentiated based on the plan shapes of their total field magnetic responses. Mafic intrusive plugs can appear as isolated "bulls-eye" anomalies. Granitic intrusives appear as sub-circular zones, and may have contrasting rings due to contact metamorphism. Generally, granitic terrain will lack a pronounced strike direction, although granite gneiss may display strike.

Linear north-south units are theoretically not well-defined on total field magnetic maps in equatorial regions due to the low inclination of the earth's magnetic field. However, most stratigraphic units will have variations in composition along strike that will cause the units to appear as a series of alternating magnetic highs and lows.

Faults and shear zones may be characterized by alteration that causes destruction of magnetite (e.g., weathering) that produces a contrast with surrounding rock. Structural breaks may be filled by magnetite-rich, fracture filling material as is the case with diabase dikes, or by non-magnetic felsic material.

Faulting can also be identified by patterns in the magnetic total field contours or colours. Faults and dikes tend to appear as lineaments and often have strike lengths of several kilometres. Offsets in narrow, magnetic, stratigraphic trends also delineate structure. Sharp contrasts in magnetic lithologies may arise due to large displacements along strike-slip or dip-slip faults.

Gamma Ray Spectrometry

Radioelement concentrations are measures of the abundance of radioactive elements in the rock. The original abundance of the radioelements in any rock can be altered by the subsequent processes of metamorphism and weathering.

Gamma radiation in the range that is measured in the thorium, potassium, uranium and total count windows is strongly attenuated by rock, overburden and water. Almost all of the total radiation measured from rock and overburden originates in the upper .5 metres. Moisture in soil and bodies of water will mask the radioactivity from underlying rock. Weathered rock materials that have been displaced by glacial, water or wind action will not reflect the general composition of the underlying bedrock. Where residual soils exist, they may reflect the composition of underlying rock except where equilibrium does not exist between the original radioelement and the products in its decay series.

Radioelement counts (expressed as counts per second) are the rates of detection of the gamma radiation from specific decaying particles corresponding to products in each radioelements decay series. The radiation source for uranium is bismuth (Bi-214), for thorium it is thallium (Tl-208) and for potassium it is potassium (K-40).

The uranium and thorium radioelement concentrations are dependent on a state of equilibrium between the parent and daughter products in the decay series. Some daughter products in the uranium decay are long lived and could be removed by processes such as leaching. One product in the series, radon (Rn-222), is a gas which can easily escape. Both of these factors can affect the degree to which the calculated uranium concentrations reflect the actual composition of the source rock. Because the daughter products of thorium are relatively short lived, there is more likelihood that the thorium decay series is in equilibrium.

Lithological discrimination can be based on the measured relative concentrations and total, combined, radioactivity of the radioelements. Feldspar and mica contain potassium.

- Appendix C.15 -

Zircon, sphene and apatite are accessory minerals in igneous rocks that are sources of uranium and thorium. Monazite, thorianite, thorite, uraninite and uranothorite are also sources of uranium and thorium which are found in granites and pegmatites.

In general, the abundance of uranium, thorium and potassium in igneous rock increases with acidity. Pegmatites commonly have elevated concentrations of uranium relative to thorium. Sedimentary rocks derived from igneous rocks may have characteristic signatures that are influenced by their parent rocks, but these will have been altered by subsequent weathering and alteration.

Metamorphism and alteration will cause variations in the abundance of certain radioelements relative to each other. For example, alterative processes may cause uranium enrichment to the extent that a rock will be of economic interest. Uranium anomalies are more likely to be economically significant if they consist of an increase in the uranium relative to thorium and potassium, rather than a sympathetic increase in all three radioelements.

Faults can exhibit radioactive highs due to increased permeability which allows radon migration, or as lows due to structural control of drainage and fluvial sediments which attenuate gamma radiation from the underlying rocks. Faults can also be recognized by sharp contrasts in radiometric lithologies due to large strike-slip or dip-slip displacements. Changes in relative radioelement concentrations due to alteration will also define faults.

Similar to magnetics, certain rock types can be identified by their plan shapes if they also produce a radiometric contrast with surrounding rock. For example, granite intrusions will appear as sub-circular bodies, and may display concentric zonations. They will tend to lack a prominent strike direction. Offsets of narrow, continuous, stratigraphic units with contrasting radiometric signatures can identify faulting, and folding of stratigraphic trends will also be apparent.

APPENDIX D

DATA ARCHIVE DESCRIPTION

APPENDIX D

ARCHIVE DESCRIPTION

Reference: CCD02275

Disc 1 of 1

Archive Date: 2005-January-27

This archive contains the FINAL ARCHIVE of an airborne geophysical survey conducted by FUGRO AIRBORNE SURVEYS CORP. over the Howell Property, Fernie Area, B.C., on behalf of La Quinta Resource Corp. in November, 2005.

Job # 04086

Disc 1 of 1

\ ARCHIVE DESCRIPTION.DOC - This file

GRIDS\

Grids in Geosoft (V2.0) IEEE format

04086_CVG	- Vertical gradient calculated from TMI grid (nT/m)
04086_TMI	- Total Magnetic Field (nT)
04086_RES56k	- Apparent Resistivity 56000 Hz coplanar (ohm*m)
04086_RES900	- Apparent Resistivity 900 Hz coplanar (ohm*m)
04086_RES7200	- Apparent Resistivity 7200 Hz coplanar (ohm*m)
04086_DTM	- Pseudotopography (m)

NOTE: Coil orientations and frequencies

orientation	nominal	Actual
coaxial	1000 Hz	1113 Hz
coplanar	900 Hz	871 Hz
coaxial	5500 Hz	5655 Hz
coplanar	7200 Hz	7225 Hz
coplanar	56,000 Hz	56,000 Hz

REPORT\

R04086.PDF - Logistics and interpretation report in Adobe Acrobat PDF format

PROFILE\

04086_LaQuinta.XYZ	- Final Geosoft format ASCII archive
04086_LaQuinta.GDB	- Final Geosoft GDB archive
anomaly_04086.XYZ	- Geosoft format ASCII archive of EM anomalies
04086_XYZ.DOC	- Word document file describing XYZ file format

Channel Descriptions for .XYZ files

X - UTM Easting NAD83 (zone 11N)
Y - UTM Northing NAD83 (zone 11N)
FID - Fiducial (Synchronization Counter)
ALTBIRDM - Radar Altimeter Height of bird above terrain (m)
Z - GPS height of bird (m)
BALT - Barometric height of helicopter (m)
DTM - Digital Terrain calculated from (GPSZ-ALTBIRD)
DIURNAL - Diurnal magnetic variation (nT)
MAGRAW - Despiked Raw Total Magnetic Intensity (nT)
MAGLD - Despiked Total Magnetic Intensity, diurnal and lag corrected (nT)
MAGFINAL - Final Levelled Total Magnetic Intensity (nT)
CPIR900 - Raw 900 Hz coplanar inphase (ppm)
CPQR900 - Raw 900 Hz coplanar quadrature (ppm)
CXIR1000 - Raw 1000 Hz coaxial inphase (ppm)
CXQR1000 - Raw 1000 Hz coaxial quadrature (ppm)
CXIR5500 - Raw 5500 Hz coaxial inphase (ppm)
CXQR5500 - Raw 5500 Hz coaxial quadrature (ppm)
CPIR7200 - Raw 7200 Hz coplanar inphase (ppm)
CPQR7200 - Raw 7200 Hz coplanar quadrature (ppm)
CPIR56K - Raw 56000 Hz coplanar inphase (ppm)
CPQR56K - Raw 56000 Hz coplanar quadrature (ppm)
CPI900 - Levelled 900 Hz coplanar inphase (ppm)
CPQ900 - Levelled 900 Hz coplanar quadrature (ppm)
CXI1000 - Levelled 1000 Hz coaxial inphase (ppm)
CXQ1000 - Levelled 1000 Hz coaxial quadrature (ppm)
CXI5500 - Levelled 5500 Hz coaxial inphase (ppm)
CXQ5500 - Levelled 5500 Hz coaxial quadrature (ppm)
CPI7200 - Levelled 7200 Hz coplanar inphase (ppm)
CPQ7200 - Levelled 7200 Hz coplanar quadrature (ppm)
CPI56K - Levelled 56000 Hz coplanar inphase (ppm)
CPQ56K - Levelled 56000 Hz coplanar quadrature (ppm)
RES900 - 900 Hz coplanar apparent resistivity (ohmm)
RES7200 - 7200 Hz coplanar apparent resistivity (ohmm)
RES56K - 56000 Hz coplanar apparent resistivity (ohmm)
DEP900 - 900 Hz coplanar apparent depth (m)
DEP7200 - 7200 Hz coplanar apparent depth (m)
DEP56K - 56000 Hz coplanar apparent depth (m)
CXSPR - Coaxial spherics monitor
DIFI - Midfrequency coax/coplan inphase difference
DIFQ - Midfrequency coax/coplan quad difference
FLT - Flight
DATE - Date of survey flight

Channel descriptions for ANOMALY_04086.XYZ files:

#	CHANNAME	TIME	UNITS	DESCRIPTION
1	EASTING	0.10	m	UTME-NAD83 (zone 11N)
2	NORTHING	0.10	m	UTMN-NAD83 (zone 11N)
3	FID	1.00	n/a	Synchronization Counter
4	FLT	0.10	n/a	Flight
5	MHOS	0.10	siemens	Conductance based on Vertical Dike Model

6 DEPTH	0.10	m	Depth based on Vertical Dike Model
7 MAG	0.10	nT	Mag Correlation, local amplitude
8 CXI1	0.10	ppm	Inphase Coaxial 5500 Hz, local amplitude
9 CXQ1	0.10	ppm	Quadrature Coaxial 5500 Hz, local amplitude
10 CPI1	0.10	ppm	Inphase Coplanar 7200 Hz, absolute amplitude
11 CPQ1	0.10	ppm	Quadrature Coplanar 7200 Hz, absolute amplitude
12 CPI2	0.10	ppm	Inphase Coplanar 900 Hz, absolute amplitude
13 CPQ2	0.10	ppm	Quadrature Coplanar 900 Hz, absolute amplitude
14 LET	0.10	n/a	Anomaly Identifier
15 SYM	0.10	n/a	Anomaly Interpretation Symbol

All EM data in the archive is presented in the standard normalization convention for the coplanar coils. The ratio of coplanar to coaxial amplitudes for the same frequency is 4:1 over a layered earth.

Resistivity is calculated using a proprietary pseudo-layer half-space algorithm.

The coordinate system for all grids and XY is projected as follows

Datum	NAD83
Spheroid	GRS80
Projection	UTM (Zone 11N)
Central meridian	117 West
False easting	500000
False northing	0
Scale factor	0.9996
WGS84 to local conversion method	Molodensky
Delta X shift	0
Delta Y shift	0
Delta Z shift	0

If you have any problems with this archive please contact

Processing Manager
FUGRO AIRBORNE SURVEYS CORP.
2270 Argentia Road
Mississauga, Ontario
Canada L5N 6A6
Tel (905) 812-0212
Fax (905) 812-1504
E-mail toronto@fugroairborne.com

APPENDIX E

EM ANOMALY LIST

EM Anomaly List

Label	Fid	Interp	XUTM m	YUTM m	CX 900 HZ		CP 900 HZ		CP 7200 HZ		Vertical Dike		Mag. Corr NT
					Real ppm	Quad ppm	Real ppm	Quad ppm	Real ppm	Quad ppm	COND siemens	DEPTH* m	

LINE	10010		FLIGHT 4										
A	8397.0	S	666487	5457413	0.0	0.0	0.0	0.0	0.3	0.3	---	---	0
B	8369.0	S	667266	5457187	0.0	0.1	0.0	0.1	0.4	1.1	---	---	0
C	8315.6	S	668647	5456763	0.1	0.1	0.1	0.1	0.4	0.1	---	---	0
D	8273.0	S	669885	5456396	0.0	0.0	0.1	0.2	0.3	0.7	---	---	0
E	8229.1	S	671057	5456032	0.0	0.0	0.0	0.0	0.1	0.3	---	---	0

LINE	10020		FLIGHT 1										
A	2655.0	S	666659	5457192	1.5	6.5	3.2	29.0	87.1	165.8	---	---	0
B	2540.5	S	668852	5456511	0.4	1.1	2.6	2.9	13.5	31.4	---	---	0
C	2491.4	S	669748	5456232	0.1	1.9	3.0	12.7	43.5	70.3	---	---	0
D	2448.2	S	670643	5455995	0.7	1.4	1.0	13.1	47.5	81.6	---	---	0

LINE	10030		FLIGHT 4										
A	7770.4	S	665943	5457273	0.9	2.9	6.4	16.6	58.7	47.6	---	---	0
B	7800.1	S	666550	5457102	0.4	12.9	4.8	63.4	176.2	418.0	---	---	0
C	7832.9	S	667434	5456812	0.7	1.6	1.7	5.1	14.8	31.7	---	---	0
D	7865.8	S	668445	5456497	2.2	8.3	7.3	40.8	152.0	207.0	---	---	0
E	7972.0	S	671233	5455659	0.7	2.4	0.9	18.5	69.7	109.4	---	---	0

LINE	10040		FLIGHT 1										
A	3655.7	S	666000	5457088	0.8	2.4	4.4	18.1	56.9	68.4	---	---	0
B	3600.0	S	667296	5456694	0.6	2.5	0.6	20.0	74.4	129.8	---	---	0
C	3568.4	S	668045	5456472	0.7	2.2	2.8	15.9	49.5	79.5	---	---	0
D	3542.2	S	668567	5456286	0.5	4.3	4.2	34.9	133.0	176.8	---	---	0
E	3433.9	S	670742	5455628	0.1	2.0	1.3	15.6	32.0	129.4	---	---	0
F	3394.5	S	671457	5455420	0.4	1.0	0.8	9.1	28.5	67.7	---	---	0

LINE	10050		FLIGHT 1										
A	3744.8	S	666144	5456885	0.6	2.8	4.0	29.4	101.8	146.8	---	---	0
B	3797.6	S	667431	5456504	0.5	3.8	0.6	32.8	75.5	257.9	---	---	0
C	3833.5	S	668303	5456235	1.7	10.7	8.0	59.9	172.0	355.8	---	---	0
D	3849.8	S	668692	5456129	1.1	4.5	6.4	38.4	144.3	195.4	---	---	0
E	3899.7	S	669568	5455841	1.6	11.6	6.2	43.9	162.0	231.1	---	---	0

LINE	10060		FLIGHT 1										
A	4358.7	S	666751	5456538	0.2	1.8	2.0	9.1	36.1	37.9	---	---	0
B	4279.0	S	668616	5455983	0.9	1.9	5.5	22.8	91.7	77.7	---	---	0

CX = COAXIAL
CP = COPLANAR

Note: EM values shown above
are local amplitudes

*Estimated Depth may be unreliable because the
stronger part of the conductor may be deeper or
to one side of the flight line, or because of a
shallow dip or magnetite/overburden effects

EM Anomaly List

LINE	Fid	Interp	XUTM m	YUTM m	CX Real ppm	900 HZ Quad ppm	CP Real ppm	900 HZ Quad ppm	CP Real ppm	7200 HZ Quad ppm	Vertical Dike COND siemens	Dike DEPTH* m	Mag. Corr NT
LINE 10060			FLIGHT 1										
IC	4259.2	S	669020	5455849	2.4	9.7	5.8	49.3	149.4	325.9	---	---	0
ID	4230.0	S?	669484	5455698	1.3	7.8	0.3	16.4	51.6	93.4	---	---	0
IE	4143.2	S	670644	5455350	0.4	11.2	1.1	38.9	91.0	275.1	---	---	0
LINE 10070			FLIGHT 1										
IA	4700.0	S	666044	5456612	0.2	2.3	3.0	11.5	62.4	68.6	---	---	0
IB	4731.1	S	666801	5456383	1.2	2.0	2.0	10.4	39.9	53.8	---	---	0
IC	4795.9	S	668315	5455917	1.7	8.3	4.6	38.8	117.3	198.2	---	---	0
ID	4820.0	S?	668857	5455765	0.3	5.2	0.0	19.4	50.2	126.8	---	---	0
IE	4835.1	S	669127	5455689	0.4	1.5	3.7	12.6	45.4	52.8	---	---	0
IF	4871.6	S	669589	5455531	0.2	1.0	1.9	11.1	35.2	75.2	---	---	0
IG	4945.7	S	670731	5455187	1.3	5.4	0.0	21.4	53.7	182.7	---	---	0
LINE 10080			FLIGHT 1										
IA	5594.3	S	666234	5456388	1.3	3.9	2.8	13.4	62.6	32.1	---	---	0
IB	5565.1	S?	666887	5456181	1.0	5.5	2.6	28.7	77.3	186.7	---	---	0
IC	5475.6	S	668430	5455704	1.2	5.9	5.6	39.2	116.8	209.7	---	---	0
ID	5338.6	S	670646	5455049	0.2	2.2	1.9	12.3	41.2	87.5	---	---	0
IE	5329.0	S	670883	5454975	0.1	8.3	0.8	18.3	41.6	150.3	---	---	0
IF	5289.2	S	671603	5454752	0.1	1.8	0.4	7.6	9.1	64.6	---	---	0
LINE 10090			FLIGHT 4										
IA	6939.3	S	667176	5455938	0.7	4.2	3.2	16.2	46.8	101.1	---	---	0
IB	6995.6	S	668305	5455606	1.5	7.6	5.2	51.4	160.2	291.9	---	---	0
IC	7100.8	S	669947	5455109	0.4	1.4	0.5	8.1	26.8	57.7	---	---	0
ID	7156.0	S?	670973	5454785	0.3	13.7	1.3	31.2	67.5	254.0	---	---	0
LINE 10100			FLIGHT 4										
IA	6767.7	S	666942	5455859	0.9	0.9	4.5	9.4	55.7	113.2	---	---	0
IB	6713.3	S	667827	5455600	0.9	2.9	1.9	15.2	49.7	104.4	---	---	0
IC	6694.3	S	668287	5455458	1.2	3.5	6.1	27.2	103.2	102.4	---	---	0
ID	6622.7	S	669576	5455068	1.4	1.1	1.7	3.6	14.0	14.6	---	---	0
IE	6603.4	S	670010	5454933	0.2	1.3	0.3	6.9	17.1	39.7	---	---	0
IF	6565.3	S	670786	5454703	0.6	0.1	1.3	8.7	28.7	56.2	---	---	0
IG	6514.0	S	671935	5454356	0.7	2.0	0.6	6.9	10.8	60.9	---	---	0
LINE 10110			FLIGHT 1										
IA	6693.3	S	666916	5455683	0.9	2.1	3.6	18.2	96.4	54.5	---	---	0

CX = COAXIAL
CP = COPLANAR

Note: EM values shown above
are local amplitudes

*Estimated Depth may be unreliable because the
stronger part of the conductor may be deeper or
to one side of the flight line, or because of a
shallow dip or magnetite/overburden effects

EM Anomaly List

LINE	Fid	Interp	XUTM m	YUTM m	CX Real ppm	900 HZ Quad ppm	CP Real ppm	900 HZ Quad ppm	CP Real ppm	7200 HZ Quad ppm	Vertical COND siemens	Dike DEPTH* m	Mag. Corr NT

LINE	10110		FLIGHT 1										
IB	6628.2	S	667945	5455394	0.6	1.3	2.1	14.8	51.4	85.4	---	---	0
IC	6611.4	S	668317	5455290	2.3	1.6	4.1	34.5	115.0	182.2	---	---	0
ID	6496.0	S?	670179	5454712	0.6	1.4	1.2	5.9	18.9	47.5	---	---	0
IE	6488.0	S?	670366	5454661	0.5	1.6	0.9	4.1	20.2	19.3	---	---	0
IF	6457.2	S	671087	5454431	0.2	4.3	1.0	16.9	41.2	137.6	---	---	0
IG	6402.9	S	672039	5454146	0.6	1.9	0.7	6.4	9.4	60.6	---	---	0

LINE	10120		FLIGHT 4										
IA	5933.0	S	666563	5455663	0.3	2.2	1.9	10.4	22.5	76.8	---	---	0
IB	5967.8	S	667336	5455422	1.4	3.1	2.4	17.2	64.6	81.1	---	---	0
IC	5996.0	S	667954	5455240	0.9	2.2	1.3	21.3	71.2	140.2	---	---	0
ID	6018.0	S	668404	5455100	0.1	2.3	4.6	26.8	102.9	36.0	---	---	0
IE	6126.7	S	669927	5454641	0.0	0.6	0.2	8.1	17.9	49.6	---	---	12
IF	6149.4	S?	670367	5454507	0.2	2.5	3.7	5.3	15.5	35.1	---	---	0

LINE	10130		FLIGHT 1										
IA	7819.2	S	666484	5455522	1.2	0.9	1.0	6.0	14.8	41.0	---	---	0
IB	7748.7	S	667440	5455261	1.5	4.9	2.1	23.5	86.6	156.5	---	---	0
IC	7705.0	S?	668446	5454952	1.9	6.1	3.2	25.3	74.6	131.1	---	---	0
ID	7663.6	S	669174	5454714	0.4	2.0	1.0	5.3	11.2	41.3	---	---	14
IE	7594.7	S	670507	5454305	0.1	3.6	1.2	6.7	18.7	64.4	---	---	0

LINE	10140		FLIGHT 2										
IA	676.1	S	667269	5455126	0.3	0.9	0.4	11.5	32.0	69.8	---	---	0
IB	653.4	S	667567	5455042	0.7	2.0	0.4	13.8	45.7	98.2	---	---	0
IC	615.9	S	668403	5454807	1.2	4.5	1.9	17.0	53.9	96.5	---	---	0
ID	572.8	S	669353	5454486	0.9	4.7	0.6	10.9	24.3	93.1	---	---	0
IE	524.8	S	670343	5454200	0.6	3.0	1.0	13.5	36.2	100.5	---	---	0
IF	450.6	S	672142	5453669	0.3	0.7	0.4	4.4	7.2	34.3	---	---	0

LINE	10150		FLIGHT 4										
IA	5675.5	S?	667637	5454861	2.2	1.7	2.5	15.8	64.0	76.4	---	---	0
IB	5644.2	S	668525	5454624	0.9	1.4	1.7	12.4	38.7	75.1	---	---	0
IC	5612.2	S	669323	5454356	0.3	1.8	1.5	8.9	26.7	61.4	---	---	0
ID	5579.1	S	670176	5454100	1.3	5.2	1.0	20.6	51.1	160.3	---	---	0

LINE	10160		FLIGHT 2										
IA	1658.0	S?	667794	5454641	1.6	5.7	0.6	13.2	68.5	86.1	---	---	0

CX = COAXIAL
CP = COPLANAR

Note: EM values shown above
are local amplitudes

*Estimated Depth may be unreliable because the
stronger part of the conductor may be deeper or
to one side of the flight line, or because of a
shallow dip or magnetite/overburden effects

EM Anomaly List

LINE	Fid	Interp	XUTM m	YUTM m	CX Real ppm	900 HZ Quad ppm	CP Real ppm	900 HZ Quad ppm	CP Real ppm	7200 HZ Quad ppm	Vertical COND siemens	Dike DEPTH* m	Mag. Corr NT
LINE 10160			FLIGHT 2										
IB	1641.3	S	668243	5454531	0.0	0.6	0.6	10.6	28.2	67.9	---	---	0
IC	1584.0	S	669741	5454042	1.0	2.5	4.1	15.0	53.9	120.7	---	---	0
ID	1569.7	S	670162	5453934	3.6	2.7	2.9	14.6	27.0	121.8	---	---	21
LINE 10170			FLIGHT 2										
IA	1867.8	S	665979	5455040	0.6	0.9	0.4	2.6	6.7	22.9	---	---	24
IB	1933.3	S?	667726	5454531	1.5	6.8	2.1	12.7	63.9	66.8	---	---	0
IC	1959.6	S	668518	5454274	0.1	2.5	0.6	17.5	40.3	138.9	---	---	0
ID	1987.6	S	669351	5454032	0.4	1.4	0.7	12.0	40.8	84.5	---	---	0
IE	2043.2	S	671034	5453516	0.7	0.8	1.8	6.4	10.8	49.2	---	---	0
LINE 10180			FLIGHT 2										
IA	2639.8	S	665382	5455095	0.0	1.8	1.0	15.0	42.7	116.1	---	---	0
IB	2588.3	S	666335	5454799	0.2	1.7	0.0	9.0	18.3	73.9	---	---	0
IC	2522.0	S	667764	5454348	0.5	6.6	1.2	27.2	103.2	188.1	---	---	0
ID	2504.2	S	668298	5454190	0.2	2.7	0.6	4.6	12.1	44.0	---	---	0
IE	2451.5	S	669836	5453733	1.0	1.4	2.1	7.9	25.7	72.0	---	---	0
IF	2415.4	S	670840	5453390	0.6	1.4	2.4	6.2	11.7	43.6	---	---	0
LINE 10190			FLIGHT 4										
IA	1507.0	S	665381	5454925	0.4	1.5	1.3	6.0	19.2	28.3	---	---	0
IB	1559.2	S	666583	5454565	0.7	0.6	5.2	2.6	10.1	18.4	---	---	0
IC	1610.6	S	667889	5454166	0.2	0.3	1.7	15.6	70.9	118.4	---	---	0
ID	1626.7	S	668343	5454033	0.5	3.7	0.5	9.7	22.0	81.4	---	---	0
IE	1666.0	S	669437	5453692	0.0	1.3	0.6	4.6	10.7	37.8	---	---	0
IF	1747.4	S	671675	5453005	0.4	1.4	0.7	8.7	17.9	71.0	---	---	0
LINE 10200			FLIGHT 2										
IA	3419.7	S	665331	5454777	0.5	0.8	1.5	12.7	31.8	96.3	---	---	0
IB	3372.1	S	666393	5454448	1.4	1.3	11.6	9.4	10.2	81.0	---	---	82
IC	3309.5	S	668019	5453959	0.5	4.0	0.7	13.2	37.8	102.6	---	---	0
ID	3280.0	S	668887	5453685	0.5	1.5	0.5	7.4	10.4	56.6	---	---	0
IE	3219.4	S	670549	5453188	0.3	1.7	0.4	7.8	21.1	61.1	---	---	0
IF	3172.3	S	671789	5452814	0.2	0.7	0.8	4.7	9.6	44.6	---	---	0
LINE 10210			FLIGHT 4										
IA	2228.1	S	665363	5454618	0.5	1.1	0.0	11.8	26.8	81.8	---	---	23
IB	2108.4	S	666828	5454165	0.8	0.9	3.2	8.1	20.1	64.3	---	---	0

CX = COAXIAL
CP = COPLANAR

Note: EM values shown above
are local amplitudes

*Estimated Depth may be unreliable because the
stronger part of the conductor may be deeper or
to one side of the flight line, or because of a
shallow dip or magnetite/overburden effects

EM Anomaly List

Label	Fid	Interp	XUTM m	YUTM m	CX Real ppm	900 HZ Quad ppm	CP Real ppm	900 HZ Quad ppm	CP Real ppm	7200 HZ Quad ppm	Vertical COND siemens	Dike DEPTH* m	Mag. Corr NT
LINE 10210			FLIGHT 4										
IC	2049.9	S	668163	5453764	0.4	3.5	0.6	17.6	45.5	145.2	---	---	0
ID	2010.1	S	669262	5453445	0.4	3.0	1.0	13.2	22.9	111.4	---	---	0
IE	1964.5	S	670492	5453056	0.4	1.7	0.1	7.3	23.7	46.1	---	---	0
IF	1916.1	S	671757	5452685	0.0	0.9	0.8	5.6	7.9	52.9	---	---	0
LINE 10220			FLIGHT 4										
IA	2576.6	S	666728	5454044	0.8	1.4	2.2	7.0	13.2	54.3	---	---	0
IB	2639.5	S	668194	5453608	1.1	2.4	1.2	11.4	35.1	86.0	---	---	0
IC	2666.9	S	668972	5453368	0.3	1.1	0.6	12.7	25.6	107.8	---	---	0
ID	2716.0	S	670143	5453006	0.3	0.2	0.7	1.5	7.1	12.6	---	---	13
LINE 10231			FLIGHT 4										
IA	3202.0	S	666667	5453905	0.6	0.7	1.9	8.5	13.7	58.7	---	---	0
IB	3132.7	S	668620	5453320	0.2	1.9	1.0	6.2	17.5	49.8	---	---	0
IC	3066.2	H	669932	5452918	0.6	0.9	0.8	11.7	46.7	71.2	---	---	0
LINE 10240			FLIGHT 4										
IA	3342.8	S	666927	5453672	0.4	1.5	0.5	8.9	19.6	74.9	---	---	0
IB	3380.5	S	667808	5453400	0.2	2.3	0.7	9.9	18.2	53.2	---	---	0
IC	3428.5	S	668901	5453068	0.4	2.3	0.7	14.0	35.4	99.0	---	---	0
ID	3463.2	S	669358	5452950	0.5	1.4	0.5	5.1	15.6	43.6	---	---	0
LINE 10250			FLIGHT 4										
IA	3861.9	S	666572	5453622	0.6	1.3	2.5	4.6	14.8	37.9	---	---	0
IB	3825.6	S	667720	5453283	0.2	1.0	0.4	11.2	25.6	96.5	---	---	0
IC	3783.3	S	668721	5452971	0.6	0.4	2.8	4.0	9.7	27.4	---	---	0
ID	3760.0	S	669230	5452820	0.7	1.3	0.5	6.0	25.1	43.7	---	---	0
LINE 10260			FLIGHT 4										
IA	3976.3	S	666578	5453487	0.6	1.2	5.9	6.3	17.0	56.8	---	---	0
IB	3995.6	S	667003	5453353	1.0	0.0	6.4	5.7	17.3	44.2	---	---	0
IC	4039.7	S	668007	5453030	0.6	1.6	3.5	6.5	19.6	52.9	---	---	0
ID	4089.8	S	669095	5452717	0.3	1.0	0.7	4.3	13.0	31.8	---	---	0
LINE 10270			FLIGHT 4										
IA	4764.3	S	666376	5453365	1.3	1.9	0.5	10.7	26.2	74.5	---	---	0
IB	4730.4	S	667461	5453044	1.0	2.0	7.8	9.2	10.6	78.1	---	---	0
IC	4712.0	S	667977	5452869	1.1	2.0	6.9	7.9	28.6	58.9	---	---	0

CX = COAXIAL
CP = COPLANAR

Note: EM values shown above
are local amplitudes

*Estimated Depth may be unreliable because the
stronger part of the conductor may be deeper or
to one side of the flight line, or because of a
shallow dip or magnetite/overburden effects

EM Anomaly List

Label	Fid	Interp	XUTM m	YUTM m	CX Real ppm	900 HZ Quad ppm	CP Real ppm	900 HZ Quad ppm	CP Real ppm	7200 HZ Quad ppm	Vertical COND siemens	Dike DEPTH* m	Mag. Corr NT

LINE	10270		FLIGHT 4										
D	4671.2	S	668872	5452591	0.3	1.2	1.3	8.0	27.7	48.7	---	---	0
E	4518.0	S	671110	5451946	0.2	0.0	0.8	1.9	2.3	14.9	---	---	0

LINE	10280		FLIGHT 4										
A	4916.7	S	667064	5453008	0.3	1.0	1.9	10.0	20.8	81.5	---	---	11
B	4960.4	S	668033	5452710	0.4	0.8	2.0	1.5	17.6	10.5	---	---	0
C	4986.3	S	668675	5452515	1.3	4.6	1.7	19.6	51.3	137.0	---	---	16

LINE	19010		FLIGHT 5										
A	1378.1	S	666121	5453786	0.7	1.5	1.3	9.8	33.8	57.9	---	---	0
B	1308.3	S	666403	5454700	0.7	4.5	2.0	13.9	29.6	109.9	---	---	0
C	1223.6	S	666746	5455868	1.8	9.5	4.0	48.8	142.6	295.6	---	---	0
D	1170.8	S	667030	5456863	2.7	9.7	6.7	49.3	151.9	341.1	---	---	0
E	1158.0	S?	667099	5457119	4.1	13.0	4.8	39.3	129.5	176.1	1.6	0	0

LINE	19020		FLIGHT 5										
A	1700.0	S	670945	5453193	0.9	0.8	0.0	9.6	19.0	72.8	---	---	0
B	1877.5	S?	671610	5455319	0.9	3.0	0.7	18.5	39.8	157.2	---	---	0

CX = COAXIAL
CP = COPLANAR

Note: EM values shown above
are local amplitudes

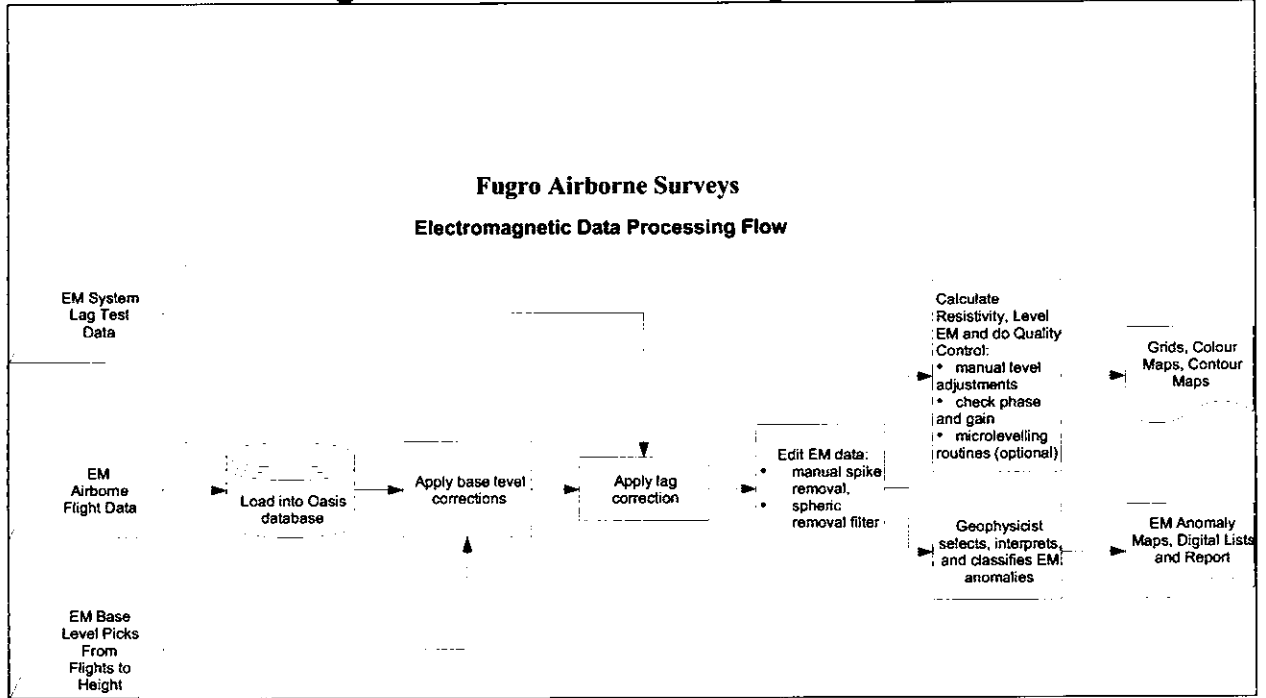
*Estimated Depth may be unreliable because the
stronger part of the conductor may be deeper or
to one side of the flight line, or because of a
shallow dip or magnetite/overburden effects

APPENDIX F

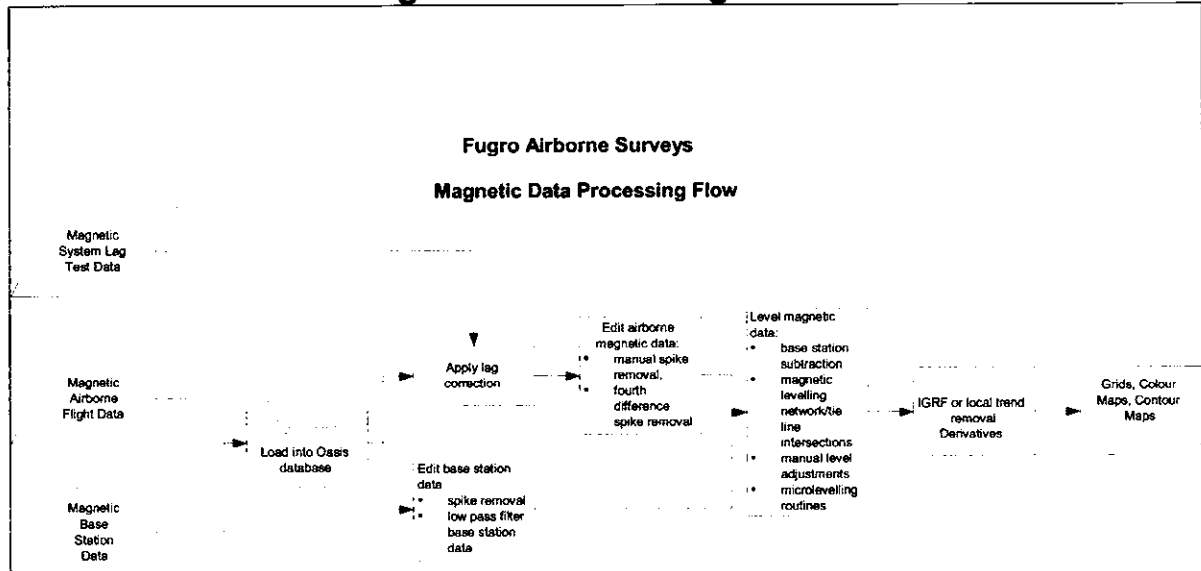
**DATA PROCESSING
FLOWCHARTS**

APPENDIX F

Processing Flow Chart - Electromagnetic Data



Processing Flow Chart - Magnetic Data



APPENDIX I

GLOSSARY

APPENDIX I

GLOSSARY OF AIRBORNE GEOPHYSICAL TERMS

Note: The definitions given in this glossary refer to the common terminology as used in airborne geophysics.

altitude attenuation: the absorption of gamma rays by the atmosphere between the earth and the detector. The number of gamma rays detected by a system decreases as the altitude increases.

apparent- : the *physical parameters* of the earth measured by a geophysical system are normally expressed as apparent, as in "apparent *resistivity*". This means that the measurement is limited by assumptions made about the geology in calculating the response measured by the geophysical system. Apparent resistivity calculated with *HEM*, for example, generally assumes that the earth is a *homogeneous half-space* – not layered.

amplitude: The strength of the total electromagnetic field. In *frequency domain* it is most often the sum of the squares of *in-phase* and *quadrature* components. In multi-component electromagnetic surveys it is generally the sum of the squares of all three directional components.

analytic signal: The total amplitude of all the directions of magnetic *gradient*. Calculated as the sum of the squares.

anisotropy: Having different *physical parameters* in different directions. This can be caused by layering or fabric in the geology. Note that a unit can be anisotropic, but still *homogeneous*.

anomaly: A localized change in the geophysical data characteristic of a discrete source, such as a conductive or magnetic body. Something locally different from the **background**.

B-field: In time-domain *electromagnetic* surveys, the magnetic field component of the (electromagnetic) *field*. This can be measured directly, although more commonly it is calculated by integrating the time rate of change of the magnetic field dB/dt , as measured with a receiver coil.

background: The "normal" response in the geophysical data – that response observed over most of the survey area. **Anomalies** are usually measured relative to the background. In airborne gamma-ray spectrometric surveys the term defines the *cosmic*, radon, and aircraft responses in the absence of a signal from the ground.

base-level: The measured values in a geophysical system in the absence of any outside signal. All geophysical data are measured relative to the system base level.

- Appendix I.2 -

base frequency: The frequency of the pulse repetition for a *time-domain electromagnetic* system. Measured between subsequent positive pulses.

bird: A common name for the pod towed beneath or behind an aircraft, carrying the geophysical sensor array.

calibration coil: A wire coil of known size and dipole moment, which is used to generate a field of known *amplitude* and *phase* in the receiver, for system calibration. Calibration coils can be external, or internal to the system. Internal coils may be called Q-coils.

coaxial coils: [CX] Coaxial coils are in the vertical plane, with their axes horizontal and collinear in the flight direction. These are most sensitive to vertical conductive objects in the ground, such as thin, steeply dipping conductors perpendicular to the flight direction. Coaxial coils generally give the sharpest anomalies over localized conductors. (See also *coplanar coils*)

coil: A multi-turn wire loop used to transmit or detect electromagnetic fields. Time varying *electromagnetic* fields through a coil induce a voltage proportional to the strength of the field and the rate of change over time.

compensation: Correction of airborne geophysical data for the changing effect of the aircraft. This process is generally used to correct data in *fixed-wing time-domain electromagnetic* surveys (where the transmitter is on the aircraft and the receiver is moving), and magnetic surveys (where the sensor is on the aircraft, turning in the earth's magnetic field).

component: In *frequency domain electromagnetic* surveys this is one of the two *phase* measurements – *in-phase or quadrature*. In “multi-component” electromagnetic surveys it is also used to define the measurement in one geometric direction (vertical, horizontal in-line and horizontal transverse – the Z, X and Y components).

Compton scattering: gamma ray photons will bounce off the nuclei of atoms they pass through (earth and atmosphere), reducing their energy and then being detected by *radiometric* sensors at lower energy levels. See also *stripping*.

conductance: See *conductivity thickness*

conductivity: [σ] The facility with which the earth or a geological formation conducts electricity. Conductivity is usually measured in milli-Siemens per metre (mS/m). It is the reciprocal of *resistivity*.

conductivity-depth imaging: see *conductivity-depth transform*.

conductivity-depth transform: A process for converting electromagnetic measurements to an approximation of the conductivity distribution vertically in the earth,

- Appendix I.3 -

assuming a **layered earth**. (Macnae and Lamontagne, 1987; Wolfgram and Karlik, 1995)

conductivity thickness: [σt] The product of the **conductivity**, and thickness of a large, tabular body. (It is also called the "conductivity-thickness product") In electromagnetic geophysics, the response of a thin plate-like conductor is proportional to the conductivity multiplied by thickness. For example a 10 metre thickness of 20 Siemens/m mineralization will be equivalent to 5 metres of 40 S/m; both have 200 S conductivity thickness. Sometimes referred to as conductance.

conductor: Used to describe anything in the ground more conductive than the surrounding geology. Conductors are most often clays or graphite, or hopefully some type of mineralization, but may also be man-made objects, such as fences or pipelines.

coplanar coils: [CP] The coplanar coils lie in the horizontal plane with their axes vertical, and parallel. These coils are most sensitive to massive conductive bodies, horizontal layers, and the **halfspace**.

cosmic ray: High energy sub-atomic particles from outer space that collide with the earth's atmosphere to produce a shower of gamma rays (and other particles) at high energies.

counts (per second): The number of **gamma-rays** detected by a gamma-ray **spectrometer**. The rate depends on the geology, but also on the size and sensitivity of the detector.

culture: A term commonly used to denote any man-made object that creates a geophysical anomaly. Includes, but not limited to, power lines, pipelines, fences, and buildings.

current gathering: The tendency of electrical currents in the ground to channel into a conductive formation. This is particularly noticeable at higher frequencies or early time channels when the formation is long and parallel to the direction of current flow. This tends to enhance anomalies relative to inductive currents (see also **induction**). Also known as current channelling.

current channelling: See current gathering.

daughter products: The radioactive natural sources of gamma-rays decay from the original element (commonly potassium, uranium, and thorium) to one or more lower-energy elements. Some of these lower energy elements are also radioactive and decay further. **Gamma-ray spectrometry** surveys may measure the gamma rays given off by the original element or by the decay of the daughter products.

- Appendix I.4 -

dB/dt : As the **secondary electromagnetic field** changes with time, the magnetic field [**B**] component induces a voltage in the receiving **coil**, which is proportional to the rate of change of the magnetic field over time.

decay: In **time-domain electromagnetic** theory, the weakening over time of the **eddy currents** in the ground, and hence the **secondary field** after the **primary field** electromagnetic pulse is turned off. In **gamma-ray spectrometry**, the radioactive breakdown of an element, generally potassium, uranium, thorium, or one of their **daughter** products.

decay series: In **gamma-ray spectrometry**, a series of progressively lower energy **daughter products** produced by the radioactive breakdown of uranium or thorium.

decay constant: see time constant.

depth of exploration: The maximum depth at which the geophysical system can detect the target. The depth of exploration depends very strongly on the type and size of the target, the contrast of the target with the surrounding geology, the homogeneity of the surrounding geology, and the type of geophysical system. One measure of the maximum depth of exploration for an electromagnetic system is the depth at which it can detect the strongest conductive target – generally a highly conductive horizontal layer.

differential resistivity: A process of transforming **apparent resistivity** to an approximation of layer resistivity at each depth. The method uses multi-frequency HEM data and approximates the effect of shallow layer **conductance** determined from higher frequencies to estimate the deeper conductivities (Huang and Fraser, 1996)

dipole moment: [NIA] For a transmitter, the product of the area of a **coil**, the number of turns of wire, and the current flowing in the coil. At a distance significantly larger than the size of the coil, the magnetic field from a coil will be the same if the dipole moment product is the same. For a receiver coil, this is the product of the area and the number of turns. The sensitivity to a magnetic field (assuming the source is far away) will be the same if the dipole moment is the same.

diurnal: The daily variation in a natural field, normally used to describe the natural fluctuations (over hours and days) of the earth's magnetic field.

dielectric permittivity: [ϵ] The capacity of a material to store electrical charge, this is most often measured as the relative permittivity [ϵ_r], or ratio of the material dielectric to that of free space. The effect of high permittivity may be seen in HEM data at high frequencies over highly resistive geology as a reduced or negative **in-phase**, and higher **quadrature** data.

drift: Long-time variations in the base-level or calibration of an instrument.

- Appendix I.5 -

eddy currents: The electrical currents induced in the ground, or other conductors, by a time-varying *electromagnetic field* (usually the *primary field*). Eddy currents are also induced in the aircraft's metal frame and skin; a source of *noise* in EM surveys.

electromagnetic: [EM] Comprised of a time-varying electrical and magnetic field. Radio waves are common electromagnetic fields. In geophysics, an electromagnetic system is one which transmits a time-varying *primary field* to induce *eddy currents* in the ground, and then measures the *secondary field* emitted by those eddy currents.

energy window: A broad spectrum of *gamma-ray* energies measured by a spectrometric survey. The energy of each gamma-ray is measured and divided up into numerous discrete energy levels, called windows.

equivalent (thorium or uranium): The amount of radioelement calculated to be present, based on the gamma-rays measured from a *daughter* element. This assumes that the *decay series* is in equilibrium – progressing normally.

fiducial, or fid: Timing mark on a survey record. Originally these were timing marks on a profile or film; now the term is generally used to describe 1-second interval timing records in digital data, and on maps or profiles.

fixed-wing: Aircraft with wings, as opposed to “rotary wing” helicopters.

footprint: This is a measure of the area of sensitivity under the aircraft of an airborne geophysical system. The footprint of an *electromagnetic* system is dependent on the altitude of the system, the orientation of the transmitter and receiver and the separation between the receiver and transmitter, and the conductivity of the ground. The footprint of a *gamma-ray spectrometer* depends mostly on the altitude. For all geophysical systems, the footprint also depends on the strength of the contrasting *anomaly*.

frequency domain: An *electromagnetic* system which transmits a *primary field* that oscillates smoothly over time (sinusoidal), inducing a similarly varying electrical current in the ground. These systems generally measure the changes in the *amplitude* and *phase* of the *secondary field* from the ground at different frequencies by measuring the *in-phase* and *quadrature* phase components. See also *time-domain*.

full-stream data: Data collected and recorded continuously at the highest possible sampling rate. Normal data are stacked (see *stacking*) over some time interval before recording.

gamma-ray: A very high-energy photon, emitted from the nucleus of an atom as it undergoes a change in energy levels.

gamma-ray spectrometry: Measurement of the number and energy of natural (and sometimes man-made) gamma-rays across a range of photon energies.

- Appendix I.6 -

gradient: In magnetic surveys, the gradient is the change of the magnetic field over a distance, either vertically or horizontally in either of two directions. Gradient data is often measured, or calculated from the total magnetic field data because it changes more quickly over distance than the **total magnetic field**, and so may provide a more precise measure of the location of a source. See also **analytic signal**.

ground effect: The response from the earth. A common calibration procedure in many geophysical surveys is to fly to altitude high enough to be beyond any measurable response from the ground, and there establish **base levels** or **backgrounds**.

half-space: A mathematical model used to describe the earth – as infinite in width, length, and depth below the surface. The most common halfspace models are **homogeneous** and **layered earth**.

heading error: A slight change in the magnetic field measured when flying in opposite directions.

HEM: Helicopter ElectroMagnetic, This designation is most commonly used to helicopter-borne, **frequency-domain** electromagnetic systems. At present, the transmitter and receivers are normally mounted in a **bird** carried on a sling line beneath the helicopter.

herringbone pattern: a pattern created in geophysical data by an asymmetric system, where the **anomaly** may be extended to either side of the source, in the direction of flight. Appears like fish bones, or like the teeth of a comb, extending either side of centre, each tooth an alternate flight line.

homogeneous: This is a geological unit that has the same **physical parameters** throughout its volume. This unit will create the same response to an HEM system anywhere, and the HEM system will measure the same apparent **resistivity** anywhere. The response may change with system direction (see **anisotropy**).

in-phase: the component of the measured **secondary field** that has the same phase as the transmitter and the **primary field**. The in-phase component is stronger than the **quadrature** phase over relatively higher **conductivity**.

induction: Any time-varying electromagnetic field will induce (cause) electrical currents to flow in any object with non-zero **conductivity**. (see **eddy currents**)

infinite: In geophysical terms, an "infinite" dimension is one much greater than the **footprint** of the system, so that the system does not detect changes at the edges of the object.

International Geomagnetic Reference Field: [IGRF] An approximation of the smooth magnetic field of the earth, in the absence of variations due to local geology. Once the IGRF is subtracted from the measured magnetic total field data, any remaining variations

- Appendix I.7 -

are assumed to be due to local geology. The IGRF also predicts the slow changes of the field up to five years in the future.

inversion, or inverse modeling: A process of converting geophysical data to an earth model, which compares theoretical models of the response of the earth to the data measured, and refines the model until the response closely fits the measured data (Huang and Palacky, 1991)

layered earth: A common geophysical model which assumes that the earth is horizontally layered – the **physical parameters** are constant to **infinite** distance horizontally, but change vertically.

magnetic permeability: [μ] This is defined as the ratio of magnetic induction to the inducing magnetic field. The relative magnetic permeability [μ_r] is often quoted, which is the ratio of the rock permeability to the permeability of free space. In geology and geophysics, the **magnetic susceptibility** is more commonly used to describe rocks.

magnetic susceptibility: [k] A measure of the degree to which a body is magnetized. In SI units this is related to relative **magnetic permeability** by $k = \mu_r - 1$, and is a dimensionless unit. For most geological material, susceptibility is influenced primarily by the percentage of magnetite. It is most often quoted in units of 10^{-6} . In HEM data this is most often apparent as a negative **in-phase** component over high susceptibility, high **resistivity** geology such as diabase dikes.

noise: That part of a geophysical measurement that the user does not want. Typically this includes electronic interference from the system, the atmosphere (**sferics**), and man-made sources. This can be a subjective judgment, as it may include the response from geology other than the target of interest. Commonly the term is used to refer to high frequency (short period) interference. See also **drift**.

Occam's inversion: an **inversion** process that matches the measured **electromagnetic** data to a theoretical model of many, thin layers with constant thickness and varying resistivity (Constable et al, 1987).

off-time: In a **time-domain electromagnetic** survey, the time after the end of the **primary field pulse**, and before the start of the next pulse.

on-time: In a **time-domain electromagnetic** survey, the time during the **primary field pulse**.

phase: The angular difference in time between a measured sinusoidal electromagnetic field and a reference – normally the primary field. The phase is calculated from $\tan^{-1}(\text{in-phase} / \text{quadrature})$.

physical parameters: These are the characteristics of a geological unit. For electromagnetic surveys, the important parameters for electromagnetic surveys are

conductivity, magnetic permeability (or **susceptibility**) and **dielectric permittivity**; for magnetic surveys the parameter is magnetic susceptibility, and for gamma ray spectrometric surveys it is the concentration of the major radioactive elements: potassium, uranium, and thorium.

permittivity: see **dielectric permittivity**.

permeability: see **magnetic permeability**.

primary field: the EM field emitted by a transmitter. This field induces **eddy currents** in (energizes) the conductors in the ground, which then create their own **secondary fields**.

pulse: In time-domain EM surveys, the short period of intense **primary** field transmission. Most measurements (the **off-time**) are measured after the pulse.

quadrature: that component of the measured **secondary field** that is phase-shifted 90° from the **primary field**. The quadrature component tends to be stronger than the **in-phase** over relatively weaker **conductivity**.

Q-coils: see **calibration coil**.

radiometric: Commonly used to refer to **gamma ray** spectrometry.

radon: A radioactive daughter product of uranium and thorium, radon is a gas which can leak into the atmosphere, adding to the non-geological background of a gamma-ray spectrometric survey.

resistivity: [ρ] The strength with which the earth or a geological formation resists the flow of electricity, typically the flow induced by the **primary field** of the electromagnetic transmitter. Normally expressed in ohm-metres, it is the reciprocal of **conductivity**.

resistivity-depth transforms: similar to **conductivity depth transforms**, but the calculated **conductivity** has been converted to **resistivity**.

resistivity section: an approximate vertical section of the resistivity of the layers in the earth. The resistivities can be derived from the **apparent resistivity**, the **differential resistivities**, **resistivity-depth transforms**, or **inversions**.

secondary field: The field created by conductors in the ground, as a result of electrical currents induced by the **primary field** from the **electromagnetic** transmitter. Airborne **electromagnetic** systems are designed to create, and measure a secondary field.

Sengpiel section: a **resistivity section** derived using the **apparent resistivity** and an approximation of the depth of maximum sensitivity for each frequency.

- Appendix I.9 -

sferic: Lightning, or the **electromagnetic** signal from lightning, it is an abbreviation of "atmospheric discharge". These appear to magnetic and electromagnetic sensors as sharp "spikes" in the data. Under some conditions lightning storms can be detected from hundreds of kilometres away. (see **noise**)

signal: That component of a measurement that the user wants to see – the response from the targets, from the earth, etc. (See also **noise**)

skin depth: A measure of the depth of penetration of an electromagnetic field into a material. It is defined as the depth at which the primary field decreases to 1/e of the field at the surface. It is calculated by approximately $503 \times \sqrt{(\text{resistivity}/\text{frequency})}$. Note that depth of penetration is greater at higher **resistivity** and/or lower **frequency**.

spectrometry: Measurement across a range of energies, where **amplitude** and energy are defined for each measurement. In gamma-ray spectrometry, the number of gamma rays are measured for each energy **window**, to define the **spectrum**.

spectrum: In **gamma ray spectrometry**, the continuous range of energy over which gamma rays are measured. In **time-domain electromagnetic** surveys, the spectrum is the energy of the **pulse** distributed across an equivalent, continuous range of frequencies.

spheric: see **sferic**.

stacking: Summing repeat measurements over time to enhance the repeating **signal**, and minimize the random **noise**.

stripping: Estimation and correction for the gamma ray photons of higher and lower energy that are observed in a particular **energy window**. See also **Compton scattering**.

susceptibility: See **magnetic susceptibility**.

tau: [τ] Often used as a name for the **time constant**.

TDEM: **time domain electromagnetic**.

thin sheet: A standard model for electromagnetic geophysical theory. It is usually defined as thin, flat-lying, and **infinite** in both horizontal directions. (see also **vertical plate**)

tie-line: A survey line flown across most of the **traverse lines**, generally perpendicular to them, to assist in measuring **drift** and **diurnal** variation. In the short time required to fly a tie-line it is assumed that the drift and/or diurnal will be minimal, or at least changing at a constant rate.

- Appendix I.10 -

time constant: The time required for an *electromagnetic* field to decay to a value of $1/e$ of the original value. In *time-domain* electromagnetic data, the time constant is proportional to the size and *conductance* of a tabular conductive body. Also called the decay constant.

Time channel: In *time-domain electromagnetic* surveys the decaying *secondary field* is measured over a period of time, and the divided up into a series of consecutive discrete measurements over that time.

time-domain: *Electromagnetic* system which transmits a pulsed, or stepped *electromagnetic* field. These systems induce an electrical current (*eddy current*) in the ground that persists after the *primary field* is turned off, and measure the change over time of the *secondary field* created as the currents *decay*. See also *frequency-domain*.

total energy envelope: The sum of the squares of the three *components* of the *time-domain electromagnetic secondary field*. Equivalent to the *amplitude* of the secondary field.

transient: Time-varying. Usually used to describe a very short period pulse of *electromagnetic* field.

traverse line: A normal geophysical survey line. Normally parallel traverse lines are flown across the property in spacing of 50 m to 500 m, and generally perpendicular to the target geology.

vertical plate: A standard model for electromagnetic geophysical theory. It is usually defined as thin, and *infinite* in horizontal dimension and depth extent. (see also *thin sheet*)

waveform: The shape of the *electromagnetic pulse* from a *time-domain* electromagnetic transmitter.

window: A discrete portion of a *gamma-ray spectrum* or *time-domain electromagnetic decay*. The continuous energy spectrum or *full-stream* data are grouped into windows to reduce the number of samples, and reduce *noise*.

Version 1.1, March 10, 2003
Greg Hodges,
Chief Geophysicist
Fugro Airborne Surveys, Toronto

Common Symbols and Acronyms

k	Magnetic susceptibility
ϵ	Dielectric permittivity
μ, μ_r	Magnetic permeability, apparent permeability
ρ, ρ_a	Resistivity, apparent resistivity
σ, σ_a	Conductivity, apparent conductivity
σt	Conductivity thickness
τ	Tau, or time constant
$\Omega.m$	Ohm-metres, units of resistivity
AGS	Airborne gamma ray spectrometry.
CDT	Conductivity-depth transform, conductivity-depth imaging (Macnae and Lamontagne, 1987; Wolfgram and Karlik, 1995)
CPI, CPQ	Coplanar in-phase, quadrature
CPS	Counts per second
CTP	Conductivity thickness product
CXI, CXQ	Coaxial, in-phase, quadrature
fT	femtoteslas, normal unit for measurement of B-Field
EM	Electromagnetic
keV	kilo electron volts – a measure of gamma-ray energy
MeV	mega electron volts – a measure of gamma-ray energy 1MeV = 1000keV
NIA	dipole moment: turns x current x Area
nT	nano-Tesla, a measure of the strength of a magnetic field
ppm	parts per million – a measure of secondary field or noise relative to the primary.
pT/s	picoTeslas per second: Units of decay of secondary field, dB/dt
S	Siemens – a unit of conductance
x:	the horizontal component of an EM field parallel to the direction of flight.
y:	the horizontal component of an EM field perpendicular to the direction of flight.
z:	the vertical component of an EM field.

References:

Constable, S.C., Parker, R.L., And Constable, C.G., 1987, Occam's inversion: a practical algorithm for generating smooth models from electromagnetic sounding data: *Geophysics*, 52, 289-300

Huang, H. and Fraser, D.C, 1996. The differential parameter method for multifrequency airborne resistivity mapping. *Geophysics*, 55, 1327-1337

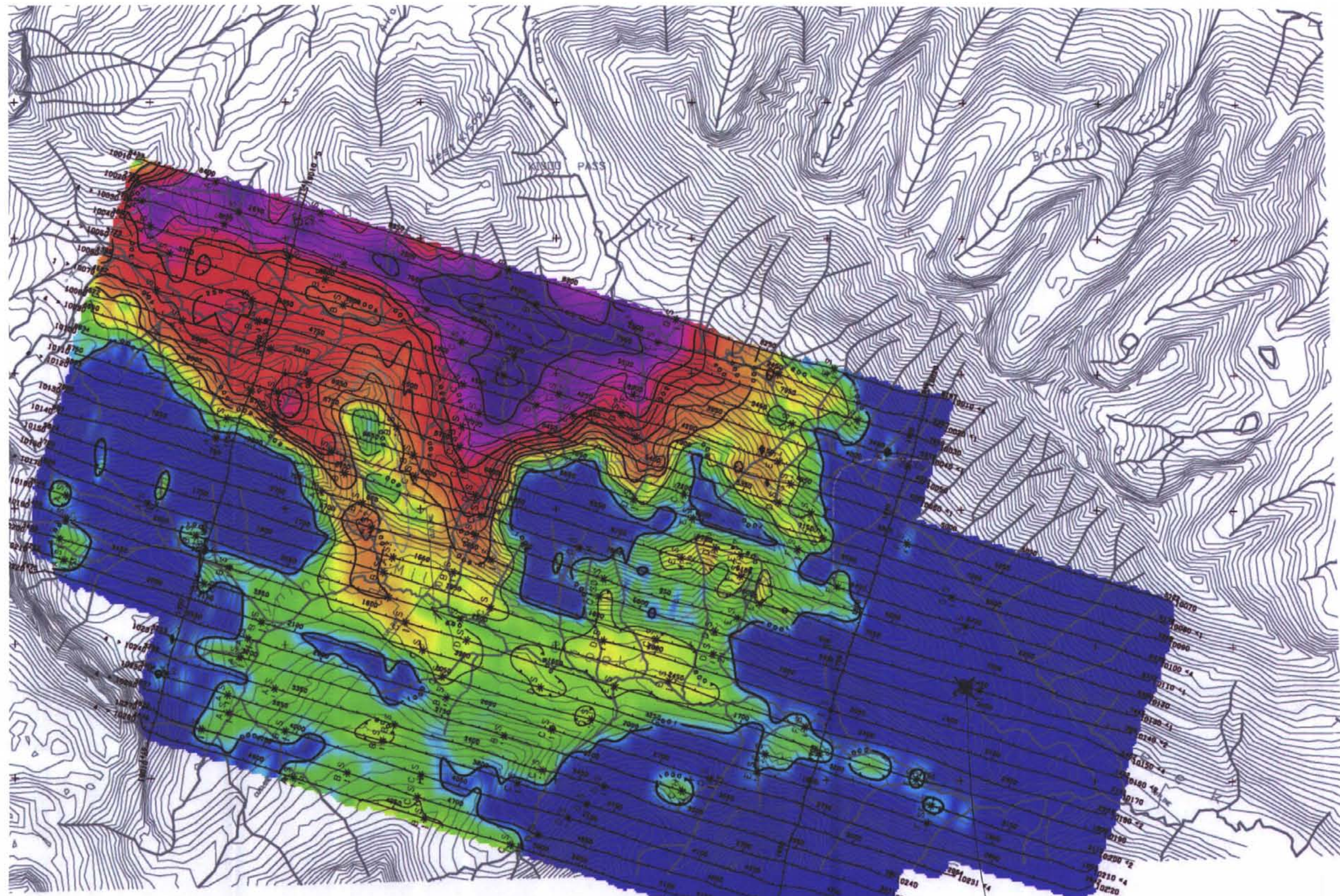
Huang, H. and Palacky, G.J., 1991, Damped least-squares inversion of time-domain airborne EM data based on singular value decomposition: *Geophysical Prospecting*, v.39, 827-844

Macnae, J. and Lamontagne, Y., 1987, Imaging quasi-layered conductive structures by simple processing of transient electromagnetic data: *Geophysics*, v52, 4, 545-554.

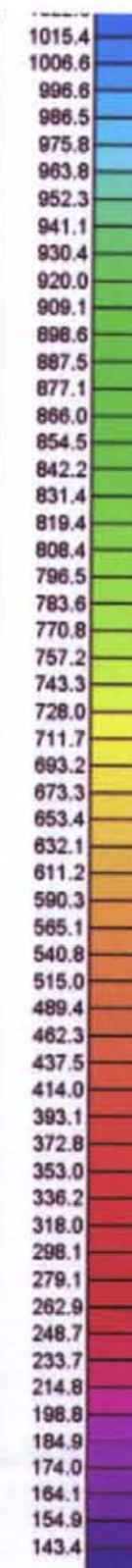
Sengpiel, K-P. 1988, Approximate inversion of airborne EM data from a multi-layered ground. *Geophysical Prospecting*, 36, 446-459

Wolfgram, P. and Karlik, G., 1995, Conductivity-depth transform of GEOTEM data: *Exploration Geophysics*, 26, 179-185.

Yin, C. and Fraser, D.C. (2002), The effect of the electrical anisotropy on the responses of helicopter-borne frequency domain electromagnetic systems, Submitted to *Geophysical Prospecting*

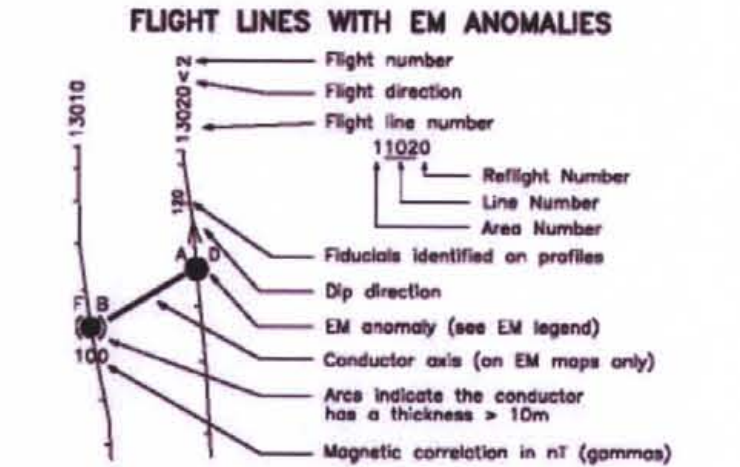


Y500 DS6E



Urose	Anomaly	Conductance
7	●	>100 siemens
6	●	50-100 siemens
5	●	20-50 siemens
4	●	10-20 siemens
3	●	5-10 siemens
2	●	<1 siemens
1	●	<1 siemens
-	*	Questionable anomaly

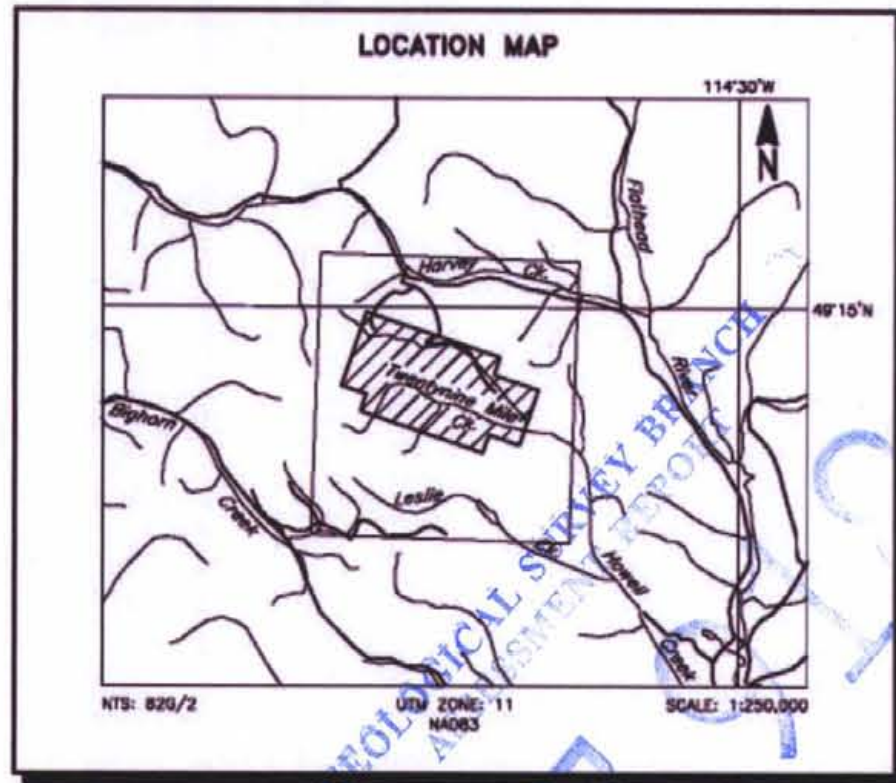
Interpretive symbol	Conductor ("mode")
B	Bedrock conductor
D	Narrow bedrock conductor ("thin dia")
S	Conductive cover ("horizontal thin sheet")
H	Broad conductive rock unit, deep conductive weathering, thick conductive cover ("half space")
E	Edge of broad conductor ("edge of half space")
L	Culture, e.g. power line, metal building or fence



RESISTIVITY CONTOURS

1000
800
600
500
400
300
250
200
150
125
100

Contours in ohm-m at 10 intervals per decade. Apparent resistivity calculated using a pseudo-layer half-space model (Fraser 1978).

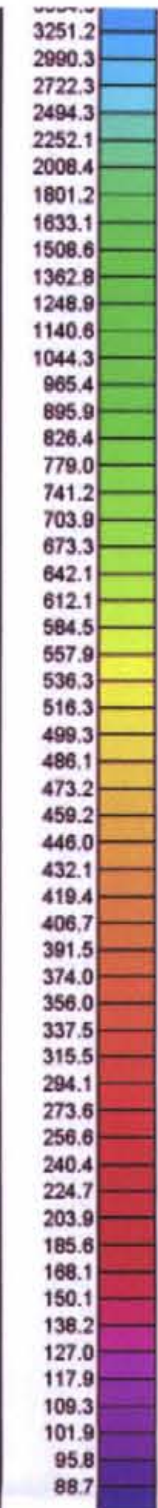
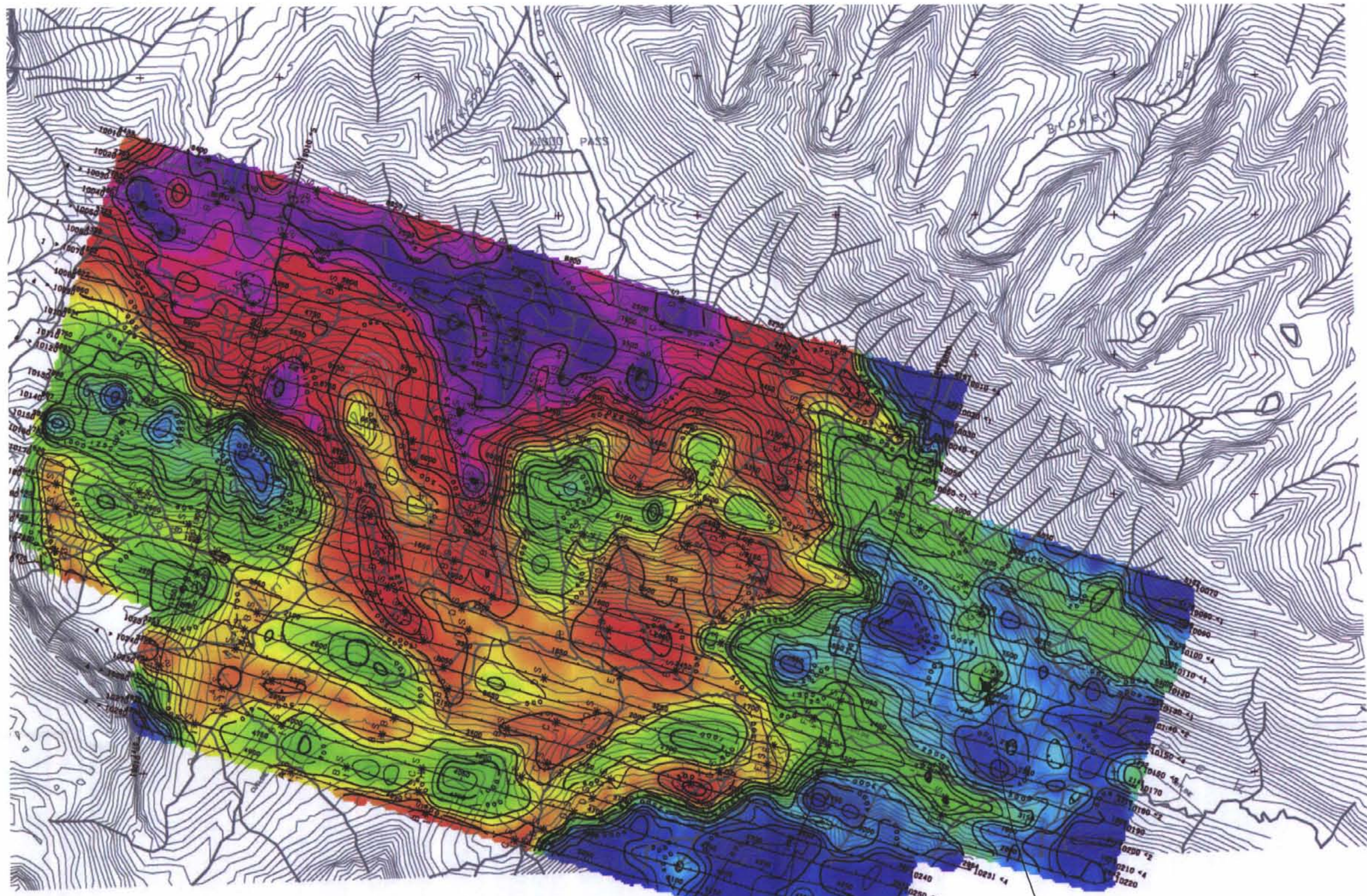


LA QUINTA RESOURCE CORP.
HOWELL PROPERTY SURVEY, B.C.

APPARENT RESISTIVITY
900 Hz COPLANAR

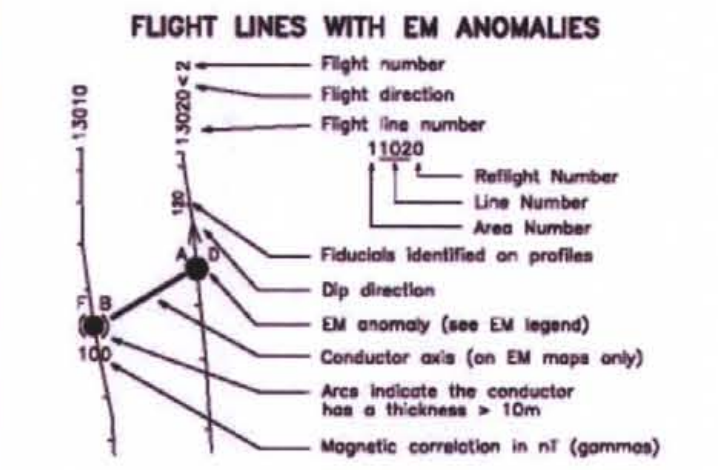
FLUGRO DIGHEM* SURVEY	NTS: 820/2	GEOPHYSICIST:
DATE: OCTOBER, 2004	JOB: 04086	SHEET: 1

Fugro Airborne Surveys

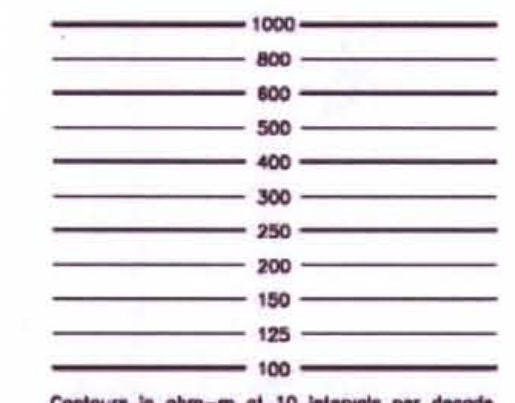


0	100-100 siemens
1	20-50 siemens
2	10-20 siemens
3	5-10 siemens
4	1-5 siemens
5	< 1 siemens
6	Questionable anomaly

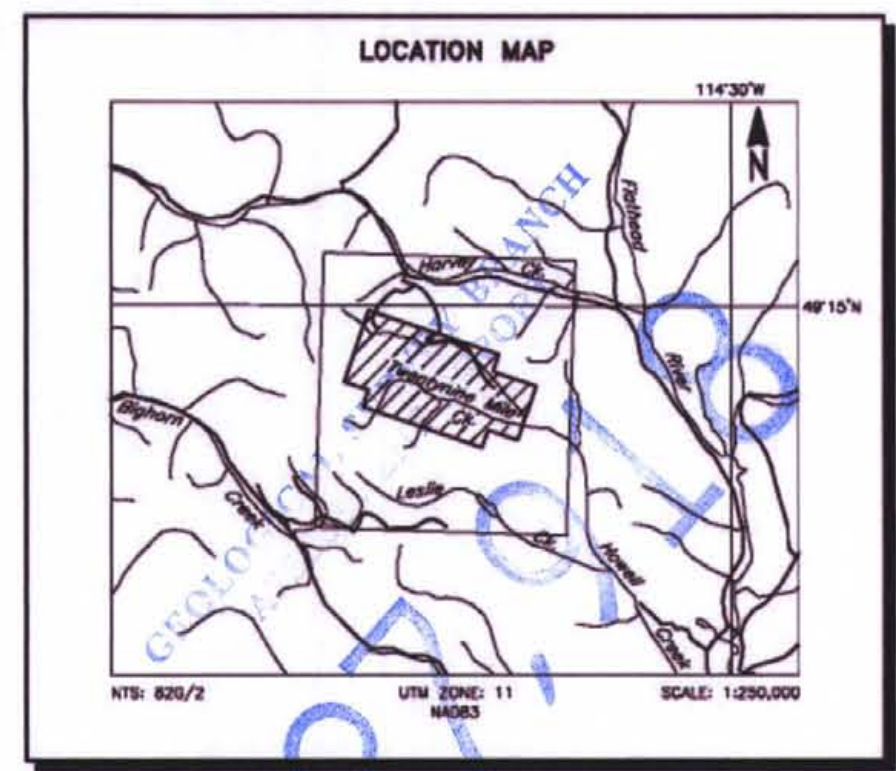
Interpretive symbol	Conductor ("model")
B	Bedrock conductor
D	Narrow bedrock conductor ("thin dike")
S	Conductive cover ("horizontal thin sheet")
H	Broad conductive rock unit, deep conductive weathering, thick conductive cover ("half space")
E	Edge of broad conductor ("edge of half space")
L	Culture, e.g. power line, metal building or fence



RESISTIVITY CONTOURS



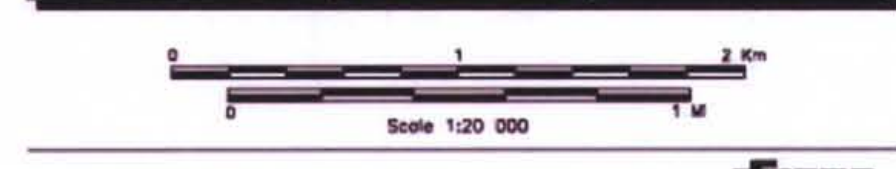
Contours in ohm-m at 10 intervals per decade. Apparent resistivity calculated using a pseudo-layer half-space model (Fraser 1978).

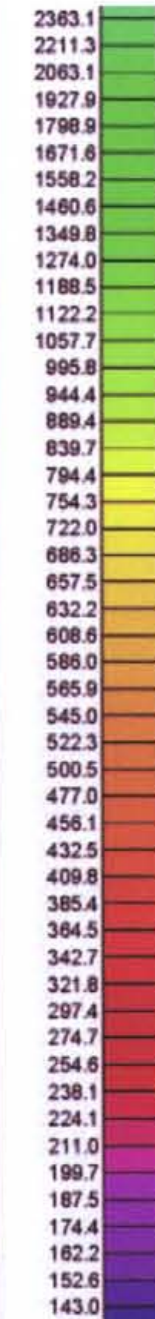
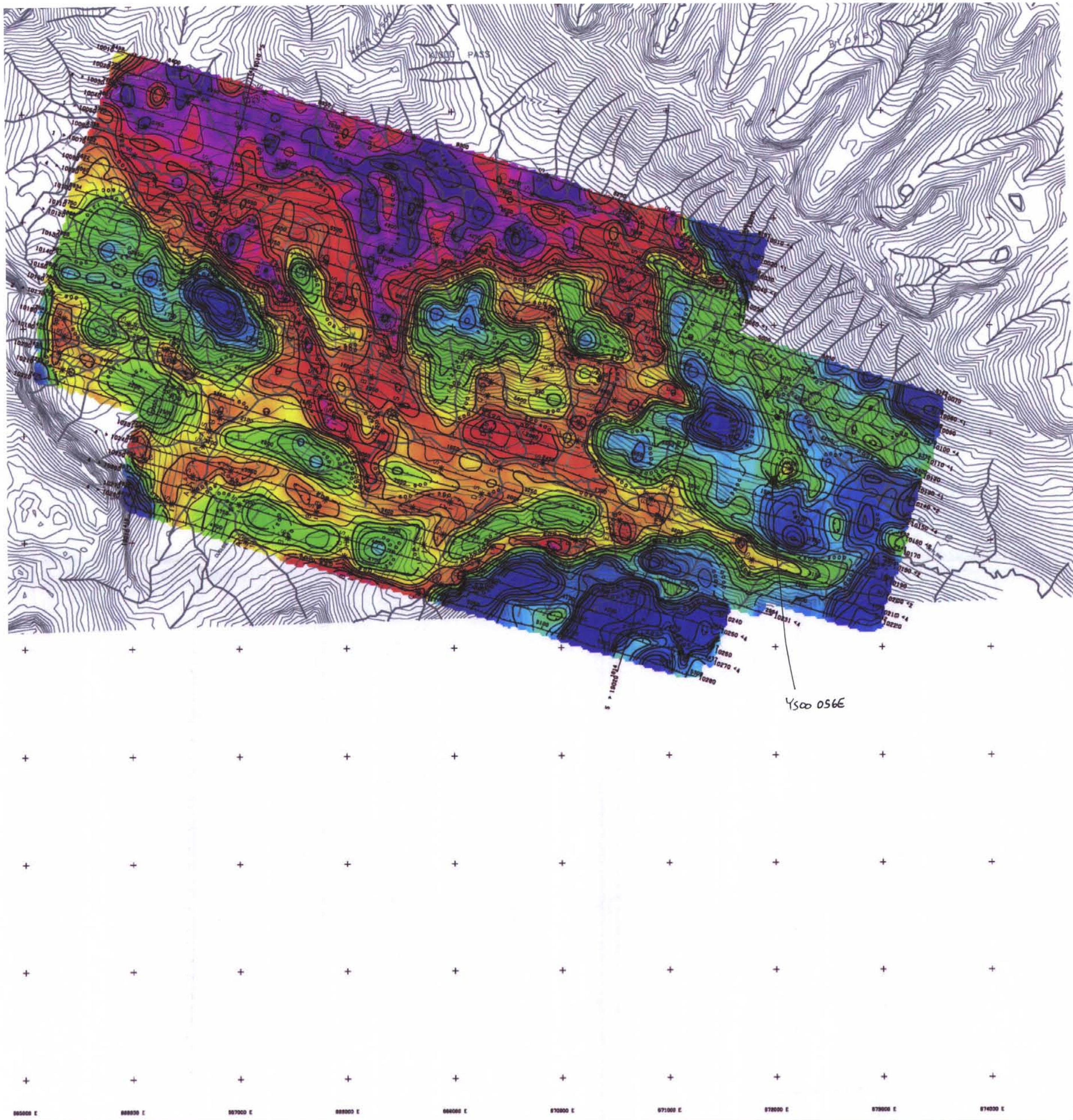


LA QUINTA RESOURCE CORP.
HOWELL PROPERTY SURVEY, B.C.

APPARENT RESISTIVITY
7200 Hz COPLANAR

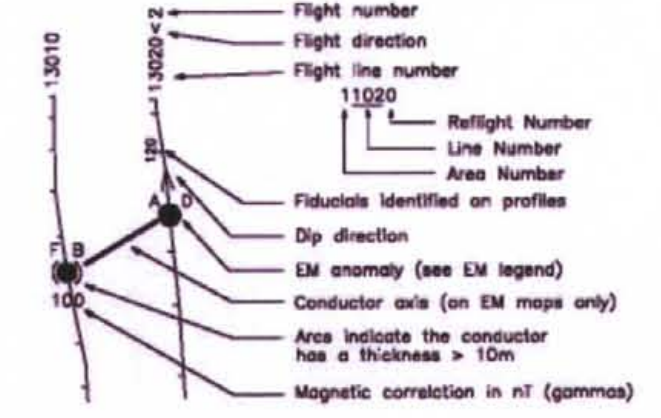
FUGRO DIGHEM [®] SURVEY	NTS: 820/2	GEOPHYSICIST:
DATE: OCTOBER, 2004	JOB: 04086	SHEET: 1



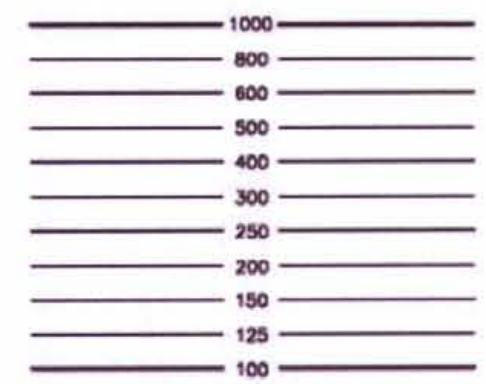


Questionable anomaly	Interpretive symbol	Conductor ("model")
*	B	Bedrock conductor
	D	Narrow bedrock conductor ("thin dike")
	S	Conductive cover (horizontal thin sheet)
	H	Broad conductive rock unit, deep conductive weathering, thick conductive cover ("half space")
	E	Edge of broad conductor ("edge of half space")
	L	Cultural, e.g. power line, metal building or fence

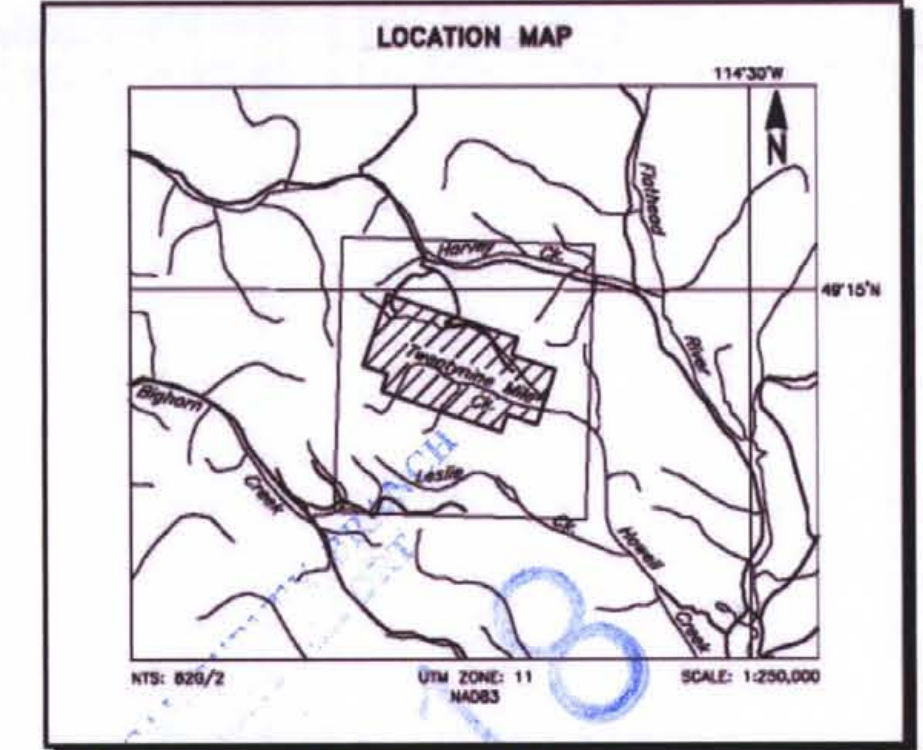
FLIGHT LINES WITH EM ANOMALIES



RESISTIVITY CONTOURS



Contours in ohm-m at 10 intervals per decade. Apparent resistivity calculated using a pseudo-layer half-space model (Frasser 1976).

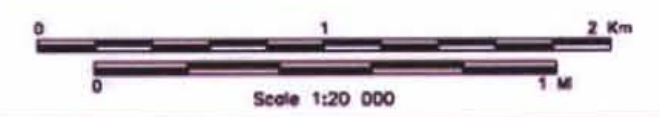


LA QUINTA RESOURCE CORP.
HOWELL PROPERTY SURVEY, B.C.

APPARENT RESISTIVITY
56,000 Hz COPLANAR

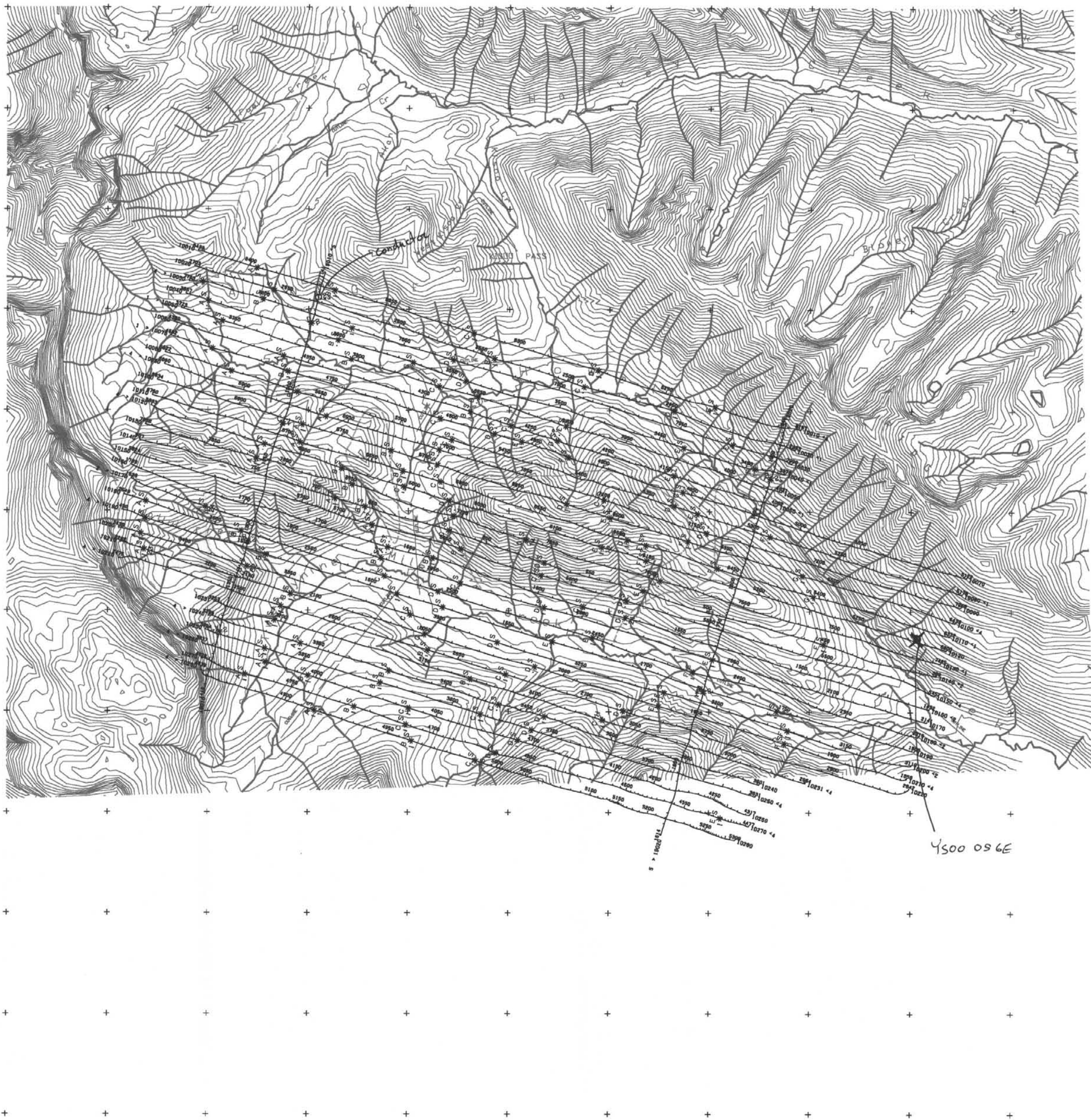
FUGRO DIGHEM* SURVEY	NTS: 820/2	GEOPHYSICIST:
DATE: OCTOBER, 2004	JOB: 04088	SHEET: 1

Fugro Airborne Surveys



FUGRO AIRBORNE SURVEYS





Terrain clearance Helicopter 57 m
 Electromagnetic sensor 30 m
 Magnetometer 30 m
 Data sampling interval 0.1 second
 Magnetometer / sensitivity Casium / 0.01 nT
 Electromagnetic system DIGHEM[®]

Frequency	Sensitivity	Coil Orientation
1000 Hz	.06 ppm	Vertical coaxial
5500 Hz	.12 ppm	Vertical coaxial
900 Hz	.12 ppm	Horizontal coplanar
2200 Hz	.24 ppm	Horizontal coplanar
58000 Hz	.60 ppm	Horizontal coplanar

ELECTROMAGNETIC ANOMALIES

Grade	Anomaly	Conductance
7	●	>100 siemens
6	⊙	50-100 siemens
5	⊖	20-50 siemens
4	⊕	10-20 siemens
3	⊗	5-10 siemens
2	○	1-5 siemens
1	○	<1 siemens
-	*	Questionable anomaly

Interpretive symbol

Interpretive symbol	Conductor ("model")
B	Bedrock conductor
D	Narrow bedrock conductor ("thin dikes")
S	Conductive cover ("horizontal thin sheet")
H	Broad conductive rock unit, deep conductive weathering, thick conductive cover ("half space")
E	Edge of broad conductor ("edge of half space")
L	Culture, e.g. power line, metal building or fence

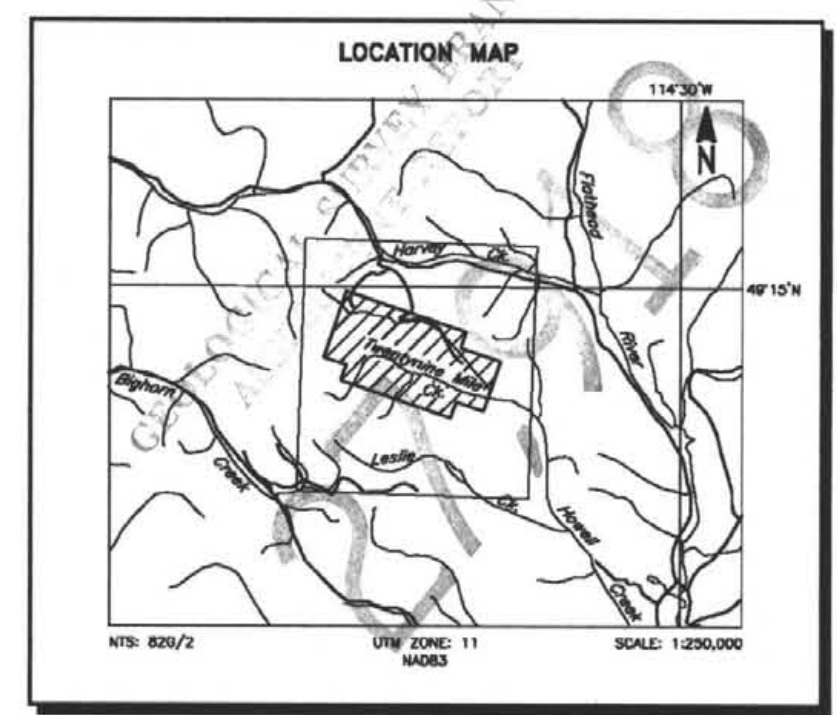
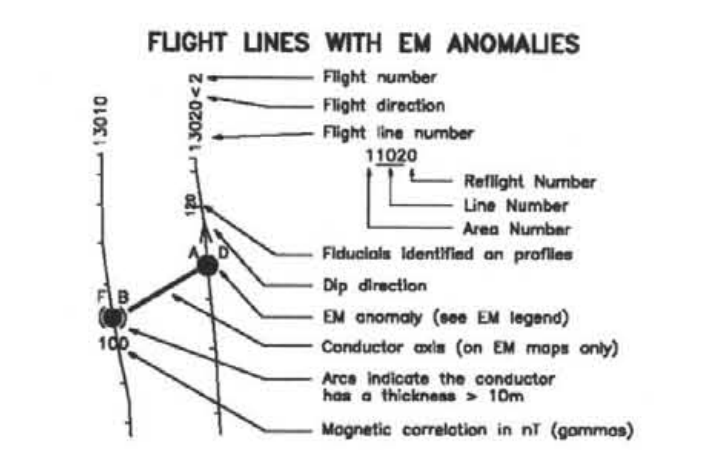
Anomaly Identifier

Depth is greater than

- 15 m
- 30 m
- 45 m
- 60 m

Interphase and Quadrature of coaxial coil is greater than

- 5 ppm
- 10 ppm
- 15 ppm
- 20 ppm

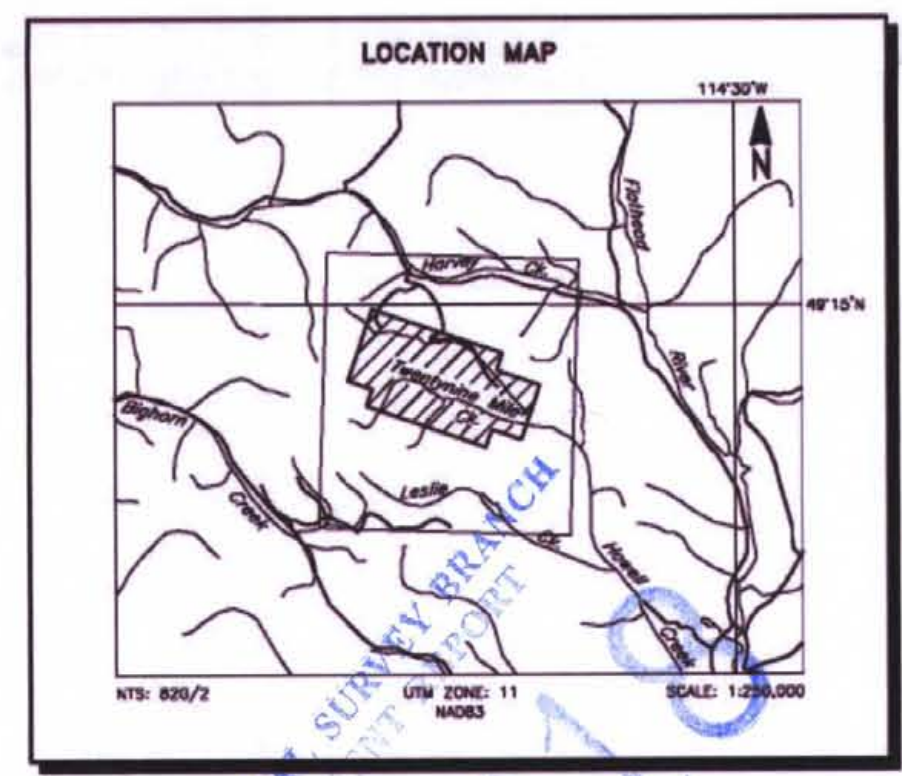
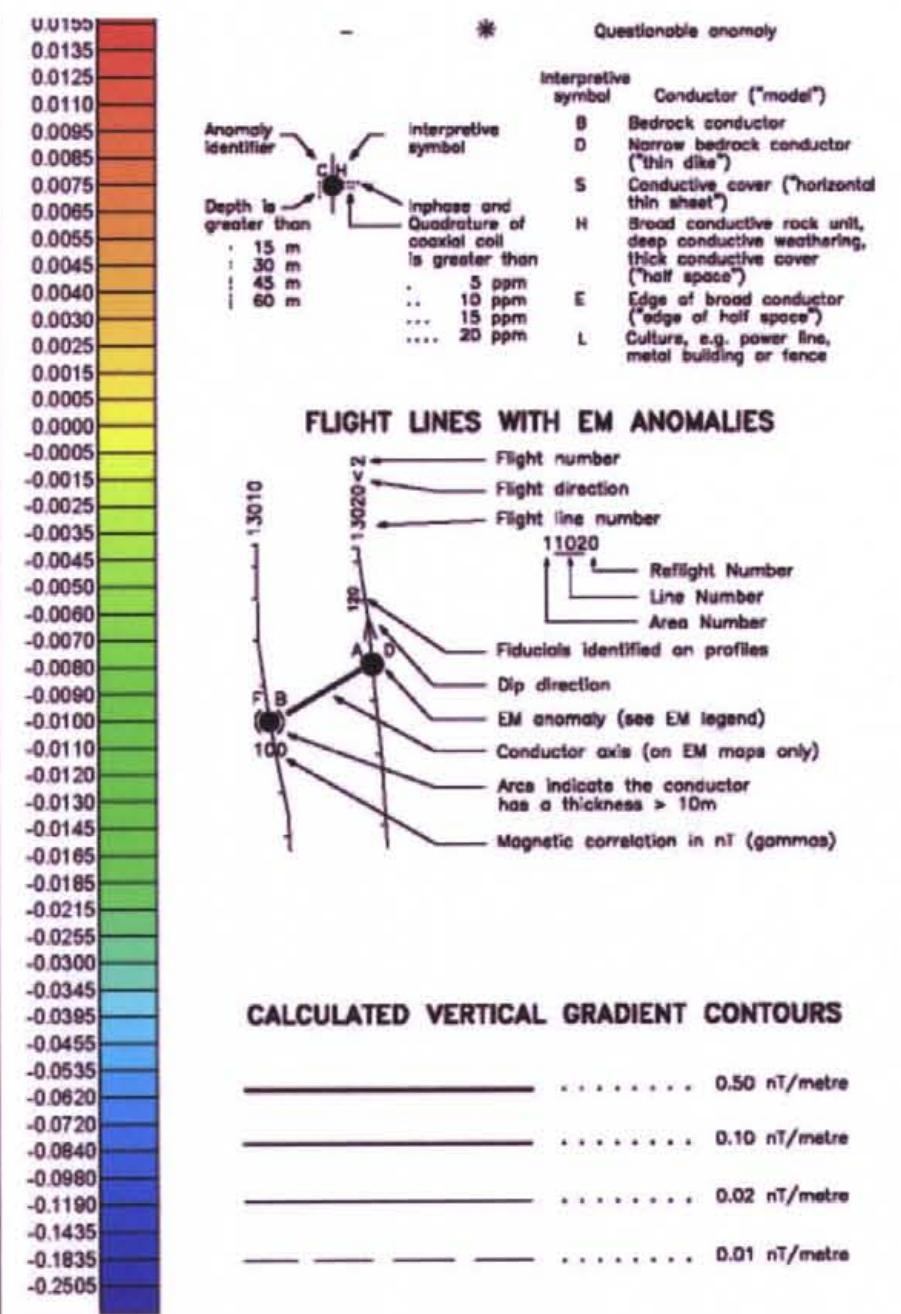
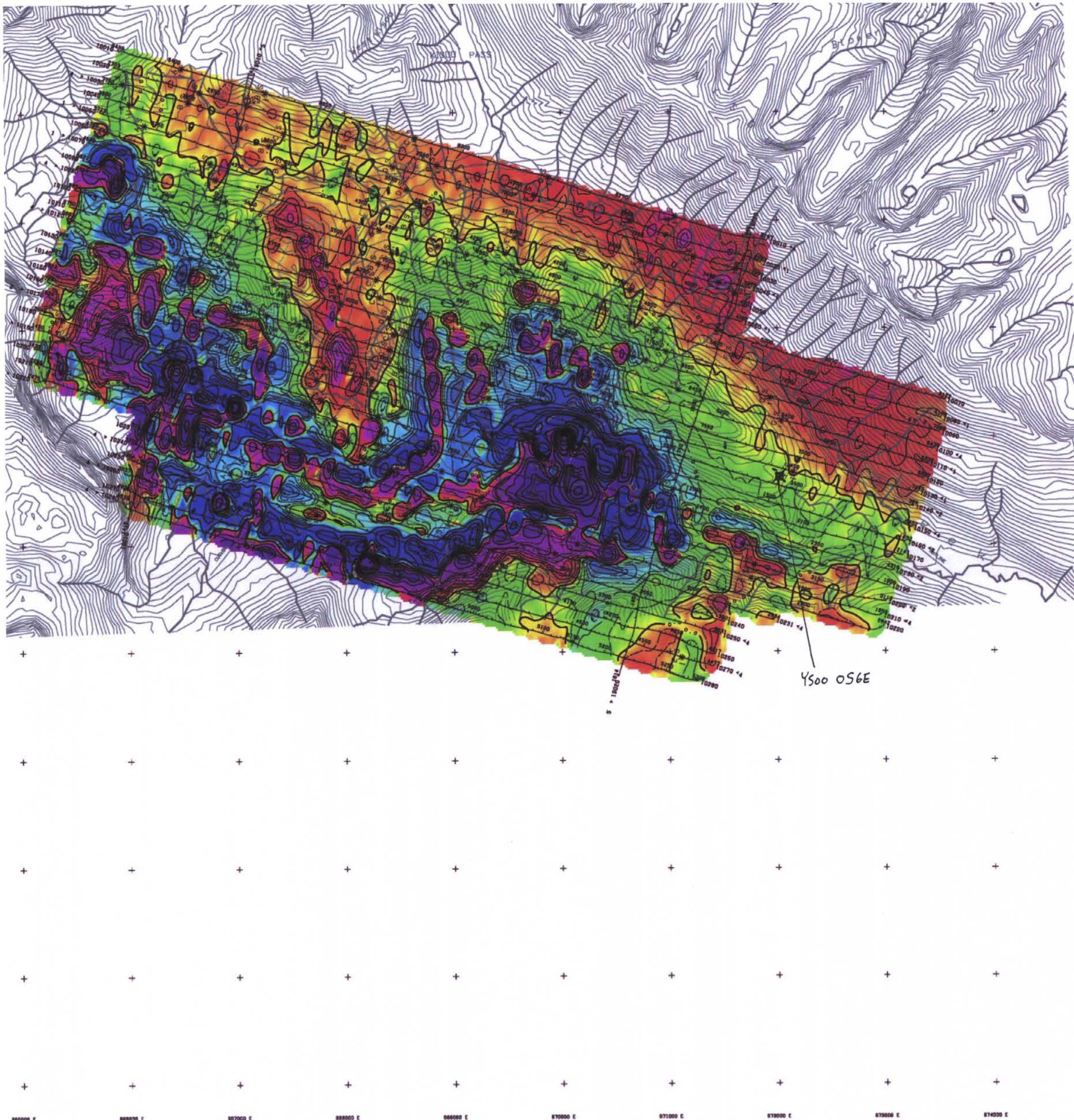


LA QUINTA RESOURCE CORP.
HOWELL PROPERTY SURVEY, B.C.

ELECTROMAGNETIC ANOMALIES

FUGRO DIGHEM [®] SURVEY	NTS: 820/2	GEOPHYSICIST:
DATE: OCTOBER, 2004	JOB: 04086	SHEET: 1

Fugro Airborne Surveys

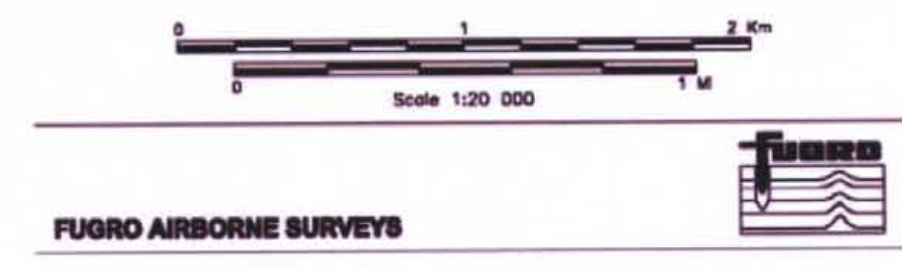


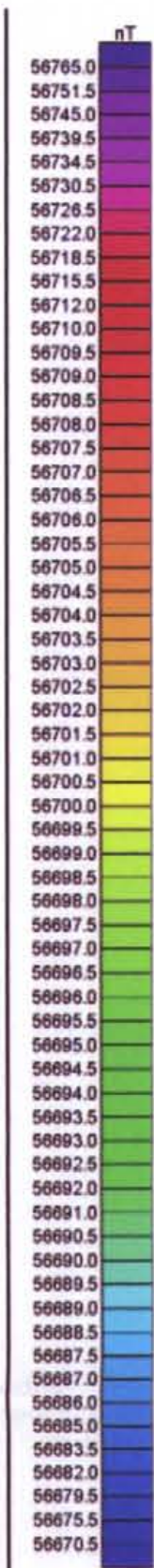
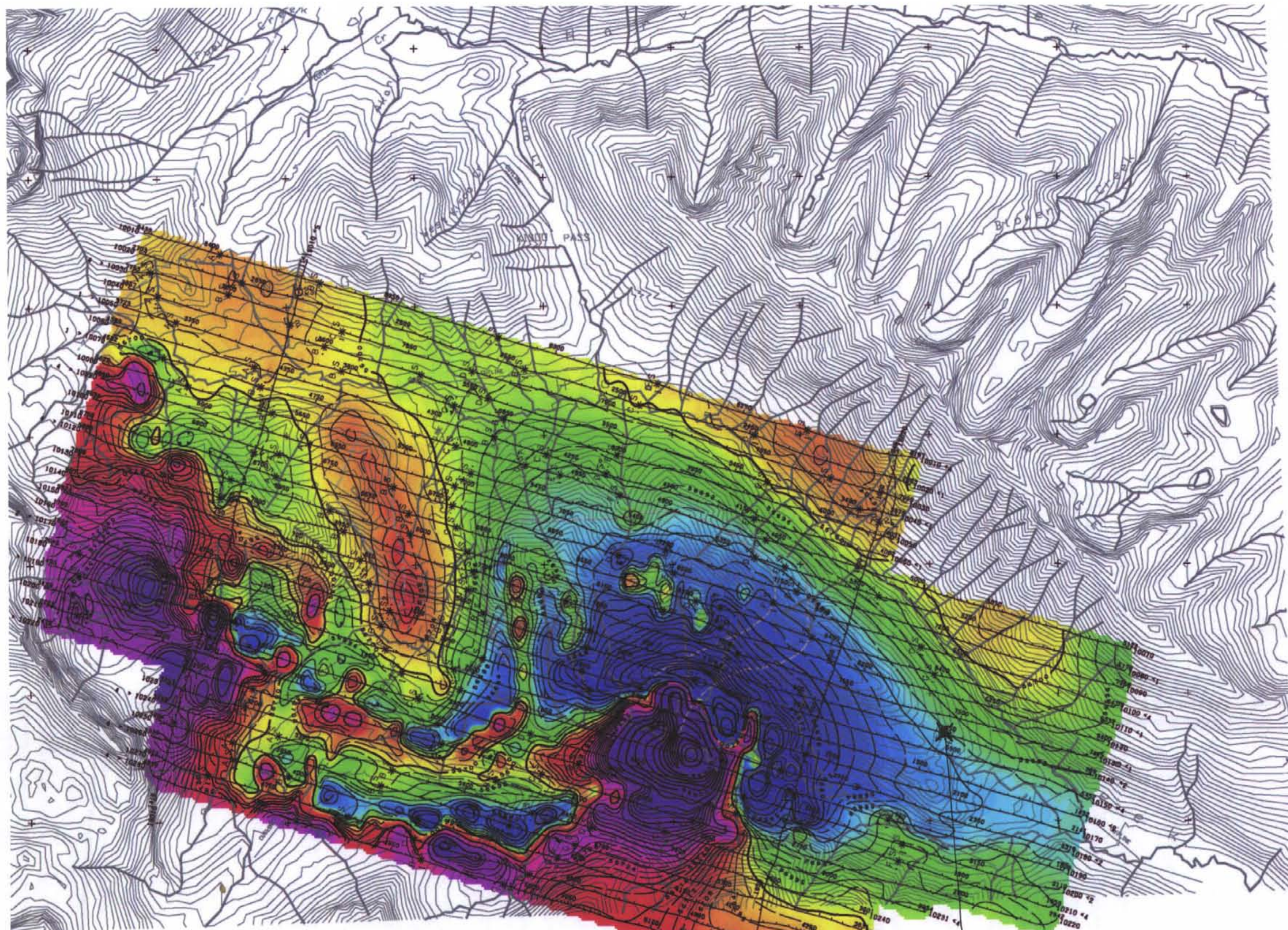
LA QUINTA RESOURCE CORP.
HOWELL PROPERTY SURVEY, B.C.

CALCULATED VERTICAL MAGNETIC GRADIENT

FUGRO DIG-EM [®] SURVEY	NTS: 820/2	GEOPHYSICIST:
DATE: OCTOBER, 2004	JOB: 04085	SHEET: 1

Fugro Airborne Surveys





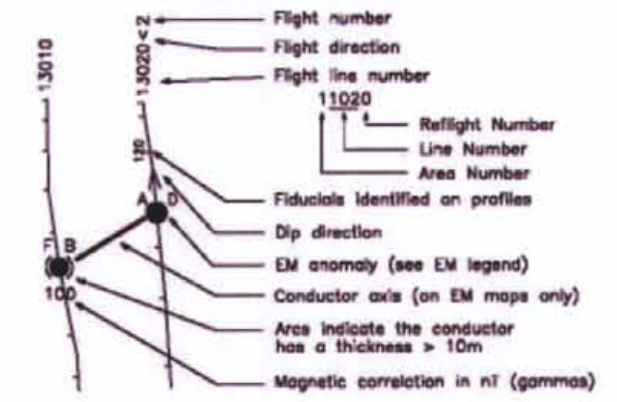
5500 Hz	.12 ppm	Vertical coplaner
900 Hz	.12 ppm	Horizontal coplaner
7200 Hz	.24 ppm	Horizontal coplaner
56000 Hz	.60 ppm	Horizontal coplaner

ELECTROMAGNETIC ANOMALIES

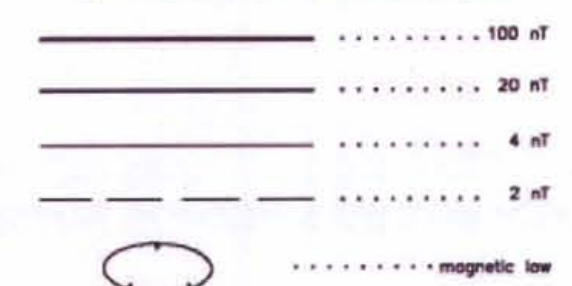
Grade	Anomaly	Conductance
7	●	>100 siemens
6	●	50-100 siemens
5	●	20-50 siemens
4	●	10-20 siemens
3	●	5-10 siemens
2	●	1-5 siemens
1	●	< 1 siemens
-	●	Questionable anomaly

Anomaly Identifier	Interpretive symbol	Conductor ("mode")
B	○	Bedrock conductor
D	○	Narrow bedrock conductor ("thin dikes")
S	○	Conductive cover ("horizontal thin sheet")
H	○	Broad conductive rock unit, deep conductive weathering, thick conductive cover ("half space")
E	○	Edge of broad conductor ("edge of half space")
L	○	Culture, s.g. power lines, metal building or fence

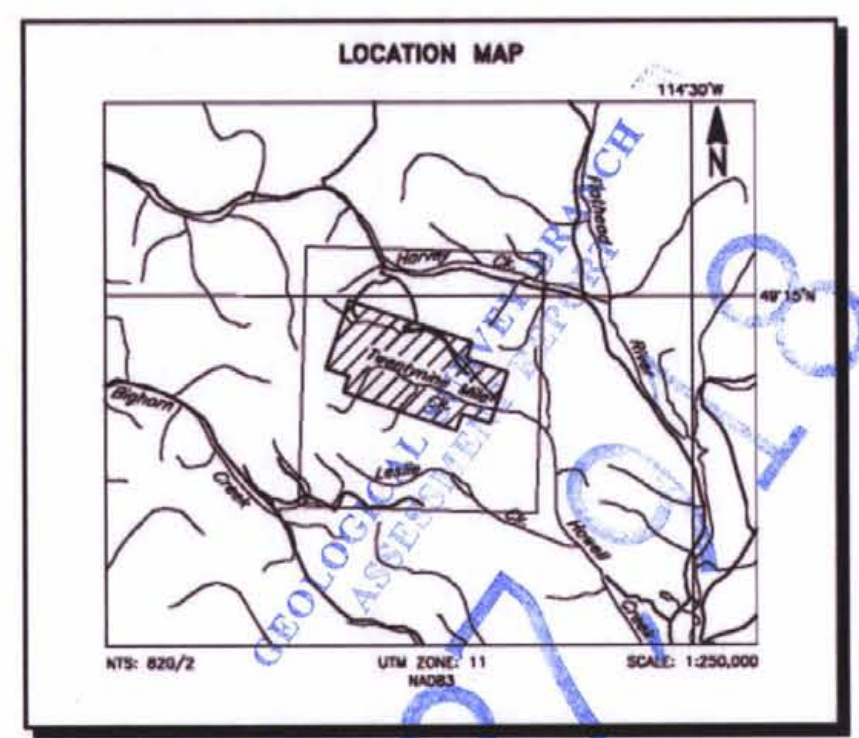
FLIGHT LINES WITH EM ANOMALIES



TOTAL MAGNETIC FIELD CONTOURS



Magnetic inclination within the survey area: 72 degrees N
 Magnetic declination within the survey area: 17 degrees E



LA QUINTA RESOURCE CORP.
HOWELL PROPERTY SURVEY, B.C.

TOTAL MAGNETIC FIELD

FUGRO DIG-EM* SURVEY	NTS: 820/2	GEOPHYSICIST:
DATE: OCTOBER, 2004	JOB: 04088	SHEET: 1

Fugro Airborne Surveys

